

**University of Alberta**

*Fundamental Cryobiology of Cells  
from a Bioengineered Human Corneal Equivalent*

By

*Stacey Lee Ebertz*



A thesis submitted to the Faculty of Graduate Studies and Research in partial  
fulfillment of the requirements for the degree of Doctor of Philosophy

in

Medical Sciences – Laboratory Medicine and Pathology

Edmonton, Alberta

*Fall 2002*



National Library  
of Canada

Acquisitions and  
Bibliographic Services

395 Wellington Street  
Ottawa ON K1A 0N4  
Canada

Bibliothèque nationale  
du Canada

Acquisitions et  
services bibliographiques

395, rue Wellington  
Ottawa ON K1A 0N4  
Canada

*Your file Votre référence*

*Our file Notre référence*

The author has granted a non-exclusive licence allowing the National Library of Canada to reproduce, loan, distribute or sell copies of this thesis in microform, paper or electronic formats.

The author retains ownership of the copyright in this thesis. Neither the thesis nor substantial extracts from it may be printed or otherwise reproduced without the author's permission.

L'auteur a accordé une licence non exclusive permettant à la Bibliothèque nationale du Canada de reproduire, prêter, distribuer ou vendre des copies de cette thèse sous la forme de microfiche/film, de reproduction sur papier ou sur format électronique.

L'auteur conserve la propriété du droit d'auteur qui protège cette thèse. Ni la thèse ni des extraits substantiels de celle-ci ne doivent être imprimés ou autrement reproduits sans son autorisation.

0-612-81185-9

**Canada**

**University of Alberta**

**Library Release Form**

**Name of Author:** Stacey Lee Ebertz

**Title of Thesis:** Fundamental Cryobiology of Cells from a Bioengineered Human Corneal Equivalent

**Degree:** Doctor of Philosophy

**Year this Degree Granted:** 2002

Permission is hereby granted to the University of Alberta Library to reproduce single copies of this thesis and to lend or sell such copies for private, scholarly or scientific research purposes only.

The author reserves all other publication and other rights in association with the copyright in the thesis, and except as herein before provided, neither the thesis nor any substantial portion thereof may be printed or otherwise reproduced in any material form whatever without the author's prior written permission.

  
Stacey Lee Ebertz

*55 Foxhaven Crescent  
Sherwood Park, Alberta  
T8A 6B8*

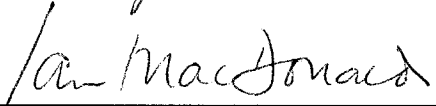
Aug 29/02

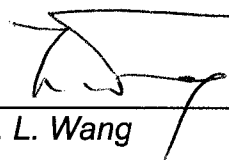
University of Alberta

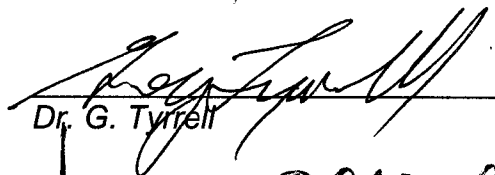
Faculty of Graduate Studies and Research

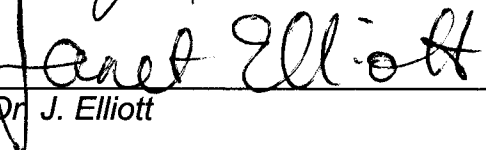
The undersigned certify that they have read, and recommend to the Faculty of Graduate Studies and Research for acceptance, a thesis entitled **Fundamental Cryobiology of a Bioengineered Human Corneal Equivalent** submitted by **Stacey Lee Ebertz** in partial fulfillment of the requirements for the degree of **Doctor of Philosophy in Medical Sciences – Laboratory Medicine and Pathology**.

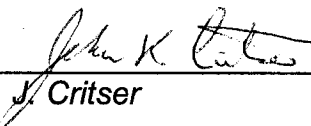
  
\_\_\_\_\_  
Dr. L.E. McGann

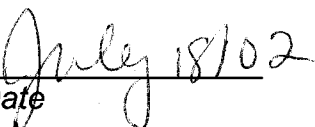
  
\_\_\_\_\_  
Dr. I. MacDonald

  
\_\_\_\_\_  
Dr. L. Wang

  
\_\_\_\_\_  
Dr. G. Tyrrell

  
\_\_\_\_\_  
Dr. J. Elliott

  
\_\_\_\_\_  
Dr. J. Critser

  
\_\_\_\_\_  
Date

## ABSTRACT

Technological advances in the bioengineering of human corneal equivalents establish the need for successful intermediate-term storage to facilitate their availability and use.

Successful cryopreservation of corneas has proven to be difficult, with much of the research based on empirical experimentation. It now seems that the ability to cryopreserve tissues, requires a more methodical approach that addresses the individual components of the tissue separately and subsequently bringing this knowledge together and applying it to the entire tissue. This thesis describes such an approach and provides a rational, scientific method for developing a cryopreservation protocol for a bioengineered human corneal equivalent.

Graded freezing studies of the human corneal endothelial monolayers showed that solution effects damage is not a significant cause of injury, but rapid cooling to  $-196^{\circ}\text{C}$  is detrimental. Improved recovery and decreased detachment was seen after rapid cooling and storage at  $-80^{\circ}\text{C}$ , indicating the need to re-evaluate the final storage conditions for long-term preservation of corneas.

Osmotic (membrane hydraulic conductivity;  $L_p$ , osmotically-inactive fraction, Arrhenius activation energy of  $L_p$ ) and permeability parameters (membrane hydraulic conductivity, membrane cryoprotectant permeability;  $P_s$ , reflection coefficient, and Arrhenius activation of  $L_p$  and  $P_s$ ) of human corneal endothelial, keratocyte, and epithelial cells were determined. The osmotic and permeability values obtained for the constituent cells of the corneal equivalent show

significant differences in their osmotic and low temperature responses, which has physiological consequences during freezing and thawing and makes clear the challenge of optimizing a cryopreservation strategy.

Knowledge of these parameters also allows theoretical prediction of addition and removal of cryoprotectants, response of cells to cooling at varying rates in different cryoprotectants and combinations of cryoprotectants. These simulations of the low temperature responses of the cells of the corneal equivalent, led to conclusions of mechanisms of cryoinjury, such as increased likelihood of intracellular ice formation during rapid cooling from the predictions of degree of supercooling, and cryoprotection, where low temperature simulations in the presence of cryoprotectants show a decrease in deleterious solute concentrations.

Combining knowledge from experimentation and mathematical modeling establishes a scientific and theoretical basis for the development of tissue cryopreservation protocols.

## **Acknowledgements**

To Dr. Locksley McGann, my supervisor, teacher and friend. Your encouragement, support and guidance have been inspiring and helped me grow as a researcher and a person.

To members of my supervisory committee, Dr. Ian MacDonald and Dr. Larry Wang, thank you for your time and insightful comments.

To Dr. Janet Elliott, my external examiner, thank you for your enthusiasm, which has been contagious, and introducing me to the world of thermodynamics.

To Dr. John Critser, my external examiner, for your encouragement and support.

To the members of my lab, for our much deserved coffee breaks and scientific conversations.

To my parents, Gord and Linda, and my sister Keri, for their continued love and support during all my scholastic endeavours.

Finally, to my husband, Derek, your endless love, patience and belief in me, have enabled me to reach the goals I have set in my life. I love you.

## Table of Contents

<b>Chapter 1: Introduction</b>	<b>1</b>
1.1 The Cornea	1
1.2 Corneal Transplantation	2
1.3 Biosynthetic Human Corneal Equivalent	4
1.4 History of Corneal Preservation	5
1.5 Cryobiology of Cells	7
1.6 Cryobiology of Tissues	10
1.7 Cryoprotection in Tissue Systems	11
1.8 Status of Corneal Cryopreservation	12
1.9 Objectives	16
1.10 References	19
<b>Chapter 2: A Human Corneal Endothelial Monolayer as an In Vitro Model for Corneal Cryoinjury</b>	
2.1 Introduction	25
2.2 Materials and Methods	27
Human Corneal Endothelial Cell Culture	27
Assessment of Monolayer Recovery	28
Experimental Solutions	29
Graded Freezing Experiments	29
Cooling and Warming Conditions Between $-80^{\circ}\text{C}$ and $-196^{\circ}\text{C}$	30
Cryoprotectant Solutions	30
1M DMSO and 5% pluronic F68 as a cryoprotectant	31
2.3 Results	31
Graded Freezing	31
Effect of Varying Cooling and Warming Conditions Between $-80^{\circ}\text{C}$ and $-196^{\circ}\text{C}$	33
Effect of Varying Cryoprotectant Solutions	33
2.4 Discussion	34
2.5 References	38

### **Chapter 3: Osmotic Parameters for Cells from a Bioengineered Human Corneal Equivalent and Consequences for Cryopreservation**

3.1	Introduction	48
3.2	Materials and Methods	49
	Human Corneal Cell Culture	49
	Experimental Solutions	50
	Osmotic Responses of Human Corneal Cells	50
	Determination of Osmotic Parameters	51
	Statistical Analysis	52
	Simulations of Low Temperature Responses	52
3.3	Results	53
	Osmotic Parameters	53
	Activation Energies for $L_p$	53
	Boyle van't Hoff Plot	54
	Simulations of Low Temperature Responses	54
3.4	Discussion	55
3.5	References	58

### **Chapter 4: Determination of Cryoprotectant Permeability for Cells from a Bioengineered Human Corneal Equivalent and Applications for Cryopreservation**

4.1	Introduction	74
4.2	Material and Methods	75
	Human Corneal Cell Culture	75
	Experimental Solutions	76
	Permeability Measurements of Human Corneal Cells	76
	Determination of Permeability Parameters	77
	Statistical Analysis	78
	Simulation of Low Temperature Responses	78
4.3	Results	79
	Permeability Parameters	79
	Activation Energies for $L_p$ and $P_s$	79
	Simulations of Low Temperature Responses	80
4.4	Discussion	81
4.5	References	89

## **Chapter 5: Simulations of Cellular Low Temperature Responses of Cells from a Bioengineered Human Corneal Equivalent**

5.1	Introduction	113
5.2	Methods	114
5.3	Results	115
5.4	Discussion	116
5.5	References	124

## **Chapter 6: Thesis Conclusions** 135

## **Appendix A: Low Temperature Responses of Human Corneal Stroma and Epithelial Cells**

A.1	Introduction	140
A.2	Materials and Methods	142
	Human Corneal Cell Culture	142
	Assessment of Monolayer Recovery	142
	Experimental Solutions	143
	Graded Freezing Experiments	143
A.3	Results/Discussion	144
	Control Monolayers	144
	Graded Freezing of Human Corneal Keratocyte Monolayers	144
	Graded Freezing of Human Corneal Epithelial Cell Monolayers	146
A.4	References	148

## **Appendix B: Measure of Central Tendency**

B.1	Introduction	151
B.2	Materials and Methods	151
	Human Corneal Cell Culture	151
	Measurement of Isotonic Volume Distribution	152
	Simulating Volume Responses	152
	Determination of Osmotic Parameters	153
B.3	Results/Discussion	153
B.4	References	155

## List of Tables

		Page
<b>Chapter 3:</b>	1A. $L_p$ for human corneal endothelial cells.	67
	1B. $L_p$ for human corneal keratocytes.	67
	1C. $L_p$ for human corneal epithelial cells	67
	1D. Pooled $L_p$ for human corneal cells in hypertonic solutions	67
	2A. $V_b$ for human corneal endothelial cells.	68
	2B. $V_b$ for human corneal keratocytes.	68
	2C. $V_b$ for human corneal epithelial cells	68
	2D. Pooled $V_b$ for human corneal cells in hypertonic solutions	68
	3. Summary of osmotic parameters for human corneal cells.	71
	<b>Chapter 4:</b>	1A. $L_p$ for human corneal endothelial cells in DMSO and PG.
1B. $L_p$ for human corneal keratocytes in DMSO and PG.		95
1C. $L_p$ for human corneal epithelial cells in DMSO and PG		95
1D. Pooled $L_p$ for human corneal cells in DMSO and PG.		95
2A. $P_s$ for human corneal endothelial cells.		96
2B. $P_s$ for human corneal keratocytes.		96
2C. $P_s$ for human corneal epithelial cells		96
2D. Pooled $P_s$ for human corneal cells in DMSO and PG.		96
3A. $\sigma$ for human corneal endothelial cells.		97
3B. $\sigma$ for human corneal keratocytes.		97
3C. $\sigma$ for human corneal epithelial cells		97

	3D. Pooled $\sigma$ for human corneal cells in DMSO and PG.	97
	4A. Summary of osmotic parameters for human corneal cells.	100
	4B. Summary of osmotic parameters for human corneal cells in the presence of DMSO.	101
	4C. Summary of osmotic parameters for human corneal cells in the presence of PG.	101
<b>Appendix B:</b>	1. 10 000 cell simulations for determining $L_p$ and $V_b$ and their errors.	161
	2. 500 000 cell simulations for determining $L_p$ and $V_b$ and their errors.	161

## List of Figures

		Page
<b>Chapter 1:</b>	1. Capella and Kaufman method for corneal cryopreservation.	24
<b>Chapter 2:</b>	1. Representative pictures to depict the subjective measurement of detachment.	42
	2. Schematic representation of the graded freezing procedure.	43
	3. Schematic representation of protocol to vary cooling and warming rates between $-80^{\circ}\text{C}$ and $-196^{\circ}\text{C}$ .	44
	4. Comparison of membrane integrity and detachment of HCEC monolayers after graded freezing.	45
	5. The effect of varying cooling and warming conditions between $-80^{\circ}\text{C}$ and $-196^{\circ}\text{C}$ on membrane integrity and detachment of HCEC monolayers.	46
	6. The effect of varying cryoprotectant solutions on membrane integrity and detachment of HCEC monolayers.	47
<b>Chapter 3:</b>	1. Schematic of CryoSim4 program	65
	2. Volume versus time plot for human corneal endothelial, keratocyte, and epithelial cells exposed to 862mosm/kg PBS.	66
	3. Arrhenius plot for $L_p$ of human corneal endothelial, keratocyte, and epithelial cells.	69
	4. Boyle van't Hoff plot of human corneal endothelial, keratocyte, and epithelial cells.	70
	5. Simulated volume response of human corneal endothelial cells during freezing at varying cooling rates using the measured osmotic parameters.	72
	6. Maximum supercooling for human corneal endothelial, keratocytes, and epithelial cells at varying cooling rates.	73

<b>Chapter 4:</b>	1. Volume versus time plot for human corneal endothelial, keratocyte, and epithelial cells exposed to 1M DMSO at 22°C.	94
	2. Arrhenius plot for $L_p$ of human corneal endothelial, keratocyte, and epithelial cells.	98
	3. Arrhenius plot for $P_s$ of human corneal endothelial, keratocyte, and epithelial cells	99
	4. Simulated addition and removal of DMSO of human corneal endothelial, keratocyte, and epithelial cells.	102
	5. Simulated addition and removal of PG of human corneal endothelial, keratocyte, and epithelial cells.	103
	6. Simulation of sucrose dilution of 2M DMSO and PG for human corneal endothelial, keratocyte, and epithelial cells.	104
	7. Predicted responses of human corneal endothelial cells in DMSO cooled at varying cooling rates.	105
	8. Predicted responses of human corneal keratocytes in DMSO cooled at varying cooling rates.	106
	9. Predicted responses of human corneal epithelial cells in DMSO cooled at varying cooling rates.	107
	10. Predicted responses of human corneal endothelial cells in PG cooled at varying cooling rates.	108
	11. Predicted responses of human corneal keratocytes in PG cooled at varying cooling rates.	109
	12. Predicted responses of human corneal epithelial cells in PG cooled at varying cooling rates.	110
	13. Maximum supercooling, intracellular electrolyte concentration, and intracellular DMSO concentration predicted at varying cooling rates for human corneal endothelial, keratocyte, and epithelial cells.	111
	14. Maximum supercooling, intracellular electrolyte concentration, and intracellular PG concentration predicted at varying cooling rates for human corneal endothelial, keratocyte, and epithelial cells.	112

<b>Chapter 5:</b>	1. Simulated responses of human corneal endothelial cells in DMSO using the graded freezing conditions from chapter 2.	127
	2. Simulated responses of human corneal endothelial cells in PG using the graded freezing conditions from chapter 2.	128
	3. Simulation of intracellular cryoprotectant concentrations of human corneal endothelial cells using the graded freezing conditions in chapter 2.	129
	4. Simulated volume response of human corneal endothelial, keratocyte, and epithelial cells cooled at varying cooling rates with no cryoprotectant, 1M DMSO and 1M DMSO + 0.3M sucrose.	130
	5. Simulated volume response of human corneal endothelial, keratocyte, and epithelial cells cooled at varying cooling rates with no cryoprotectant, 1M PG and 1M PG + 0.3M sucrose.	131
	6. Maximum supercooling at varying cooling rates for human corneal endothelial, keratocyte, and epithelial cells.	132
	7. Maximum intracellular electrolyte concentration at varying cooling rates for human corneal endothelial, keratocyte, and epithelial cells.	133
	8. Maximum intracellular cryoprotectant concentration at varying cooling rates for human corneal endothelial, keratocyte, and epithelial cells.	134
<b>Appendix A:</b>	1. Membrane integrity and detachment of human corneal keratocyte monolayers after graded freezing.	149
	2. Membrane integrity and detachment of human corneal epithelial cell monolayers after graded freezing.	150
<b>Appendix B:</b>	1. Raw data, smoothed raw data, and log normal isotonic volume distributions of human corneal endothelial cells.	156
	2. Schematic of the distribution program.	157
	3. Schematic of the cell size analyzer utility program.	157

4. Volume versus time plot predicted by the distributions program from the raw population of human corneal endothelial cells.	158
5. Volume versus time plot predicted by the distributions program from the smoothed raw population of human corneal endothelial cells.	159
6. Volume versus time plot predicted by the distributions program from the log normal population of human corneal endothelial cells.	160

## List of Abbreviations and Symbols

### Abbreviations

PK	penetrating keratoplasty
IIF	intracellular ice formation
DMSO	dimethyl sulfoxide
PG	propylene glycol
HCEC	human corneal endothelial cells
EB	ethidium bromide
PBS	phosphate buffered saline
NaCl	sodium chloride
KCl	potassium chloride
H <sub>2</sub> O	water
CPA	cryoprotective agent

### Symbols

$V_{iso}$	isotonic volume
$V_b$	osmotically-inactive fraction
$\pi$	osmolality
$L_p$	membrane hydraulic conductivity
$A$	cell surface area
$R$	universal gas constant
$T$	absolute temperature
$E_a$	activation energy
$\Delta f_p$	freezing point depression

osm	osmolality
K	constant
$P_s$	cryoprotectant permeability
$\Delta C_s$	difference between extracellular and intracellular solute concentration
$\sigma$	reflection coefficient

### **Subscripts and Superscripts**

o	isotonic
e	extracellular
i	intracellular
n	nonpermeating solute
s	permeating solute

# Chapter 1: Introduction

## 1.1 The Cornea

The cornea is the clear transparent structure of the outer tunic of the eye, which is continuous with the white sclera. The cornea consists of five layers, the epithelium, Bowman's layer, stroma, Descemet's membrane, and the endothelium (16). The function of the cornea is to provide a clear refractive interface that facilitates vision, provide tensile strength and protect the eye from environmental factors (16). Viability of the corneal endothelium and preservation of the intercellular and stromal structure are essential for maintenance of optical quality in the cornea. The stroma consists of an extracellular matrix of proteoglycans and collagen fibres that are arranged uniformly and run parallel to the corneal surface, and the main cellular component is the keratocytes (16). The proteoglycans in the stroma bring water into the stroma from the aqueous humor as they have a natural tendency to bind water (16), which is important to get nutrients into the cornea. If this water is not removed from the stroma, the cornea swells, the arrangement of the collagen is disturbed and transparency is lost (16). Under normal in vivo conditions the cornea does not swell, because of the barrier and pump functions of the endothelial cells. Normal corneal hydration is a balance between the leak of water through the endothelium into the stroma and the exclusion of ions and water by the endothelial pump, which consists of a  $\text{Na}^+/\text{K}^+$  ATPase, a sodium-hydrogen exchanger and a bicarbonate transporter (16,36). The current model explains ion transport and osmotic flow of water as follows. The sodium-hydrogen exchanger acidifies the extracellular fluid,

increasing the amount of carbon dioxide that diffuses into the endothelial cell (16). Carbonic anhydrase converts carbon dioxide to bicarbonate and a hydrogen ion, which is transported out of the cell by the basolateral sodium-hydrogen exchanger and the apical bicarbonate transport, respectively (16). The entire system is dependent on the sodium pump, which maintains the sodium gradient required for sodium-hydrogen exchange and promotes bicarbonate production (16). Essential to this model is the existence of an osmotic gradient that favours higher concentration of osmotically active sodium in the aqueous humor than in the stroma that draws water out of the stroma down the electrochemical gradient. Loss of integrity of the endothelium leads to a loss of function of the metabolic ion pump, which controls corneal hydration, resulting in edema, which increases spacing between collagen fibrils in the stroma, causes loss of transparency of the cornea, and loss of function for vision. Initial attempts at corneal cryopreservation have identified the endothelium being particularly sensitive to damage.

## **1.2 Corneal Transplantation**

Transplantation of human corneal grafts is used to restore vision in about 250 patients per year in Alberta, all of which were performed as emergency procedures. The first successful corneal transplant (penetrating keratoplasty; PK) was done in 1906 (38). The past three to four decades have seen major advances in PK, which has become the most frequently performed transplant procedure.

There are a number of reasons a patient may require a corneal graft including, allograft rejection, Fuch's dystrophy, keratoconus, cornea scarring,

intraocular surgical damage of the endothelium. Allograft rejection is characterized by edema and lymphocyte precipitate. Rejection rates are substantial in recipients with vascularization of their own cornea. Fuch's dystrophy presents clinically with decreased vision upon awakening that improves over the day as evaporation from the epithelial surface compensates for decreased function of the endothelial cell pump and is characterized microscopically by corneal guttae. Upon examination, signs include epithelial and stromal edema, and Descemet's folds. The condition worsens until there is complete decompensation of endothelial cell function, resulting in loss of transparency of the cornea. Keratoconus is when the cornea assumes a conical shape because of thinning and protrusion of the tissue, and the condition progresses with a worsening of the astigmatism and thinning of the cornea, which gradually stabilizes. The end stage of keratoconus can range from very mild astigmatism to severe thinning, protrusion and scarring requiring PK. Corneal scarring is usually caused by trauma or chemical burns, and if the scar is over the visual axis, requires PK. Damage to the endothelium during cataract surgery (intraocular lens implantation), by touching the surgical instruments to the endothelial surface. If enough endothelial cells are damaged, the remaining cells may not have a high enough pump activity to maintain transparency of the cornea, indicating the need for PK.

Although the current demand for corneas exceeds the supply, there is a need for long term storage of corneas for conditions such as a cornea perforation that without emergency treatment would result in permanent loss of vision. Low

temperature banking of corneas would be beneficial for the small percentage of patients with multiple rejection episodes that require specific HLA-matched tissue. In addition, the successful cryopreservation of corneas would allow the transplants to be performed as a scheduled procedure, permit time for complete microbiological, infectious disease and immunological testing, and eliminate wastage of tissue. The mechanisms and protocols for successful low temperature long-term banking of corneas do not currently exist and hypothermic preservation and organ culture are the only methods for storing corneas prior to transplantation.

### **1.3 Biosynthetic Human Corneal Equivalent**

The development and use of bioengineered human corneas is rapidly becoming a reality (11,12,33). Researchers have demonstrated the feasibility of bioengineering corneas and have met with significant success (33), and these engineered human corneal equivalents have immediate applications in replacing animals for evaluating irritancy of new chemicals and drugs (12), and are also a valuable tool in biomedical research, to study wound healing, cell-matrix interactions, gene expression (11,12), and can also be used to better understand complications and improve techniques for refractive surgeries, such as LASIK and PRK (11). Along with the research applications, biosynthetic human corneal equivalents have clinical applications in transplantation by replacing the use of human grafts, that have the risk of transmitting disease and the supply of human tissue cannot meet current demands. With the development of engineered human corneas and the immediate applicability of these bioengineered products,

comes the need for maintaining large stocks, to ensure availability, marketability, and ease of transportation, which necessitates the development of long-term storage protocols, such as cryopreservation, for these biomedical products (15).

#### **1.4 History of Corneal Preservation**

Up to about 20 years ago moist chamber storage was used to preserve corneas for transplantation (36,38). The whole globe was enucleated, rinsed with antibiotics, and then stored in a sealed jar at 4°C for 24-48 hours. This method is very simple and requires little expertise, but there are serious limitations, such as the limited storage time, which does not allow time for infectious disease testing (HIV, hepatitis B, and hepatitis C), HLA typing, or preparing recipients for surgery. Even with short storage times endothelial cells exhibit disruption of the plasma membranes (36,38).

In 1974, McCarey Kaufman medium was introduced; and corneas were excised from the globe and stored in tissue culture medium at 4°C. It was made up of TC-199 medium, dextran and antibiotics. MK medium can preserve corneas for two to four days. Storage of excised corneas in tissue culture medium at 4°C is still the preferred method of corneal preservation in North America, and storage solutions have continued to evolve, to extend hypothermic storage times of corneas and improve tissue quality. Today Optisol®, which contains chondroitin sulfate, is the most widely used cornea preservation medium, and can preserve corneas for up to 20 days.

Organ culture preservation of corneas is widely used in European eye banks. Corneoscleral segments are put into tissue culture media at 34°C. The

initial procedure introduced for organ culture preservation, required the media to be changed three times a week, introducing the problem of bacterial contamination. Over the past 15 years, a closed system for the organ culture of corneas was developed, and no media changes are required, reducing the risk of bacterial contamination. Chondroitin sulfate was added to the closed system to inhibit thickening of the cornea in storage to facilitate ease of handling during transplant surgery. Organ culture can preserve corneas for up to 35 days (38). Normal endothelial morphology is maintained and central endothelial damage shows evidence of repair making organ culture an appealing method for preserving corneas. Technical complexity and the need for specialized equipment limit the usability of this storage method.

Cryopreservation has the theoretical advantage of indefinite storage of corneas. There are two methods of cryopreservation: classic cryopreservation and vitrification. Classic cryopreservation involves the addition of a cryoprotectant and subsequent freezing of the tissue at a controlled optimal cooling rate which is slow enough to avoid damaging intracellular ice formation, and high enough to avoid exposure to damaging osmotic stresses and toxicity caused by increasing intracellular and extracellular solute concentrations (23). Vitrification is the solidification of a liquid without crystallization, by an extreme elevation in viscosity during cooling (i.e. the solution becomes a glass) (8). Cryopreservation of corneas is difficult to assess. Changes noted with different viability assessments may be reversible with time and latent injury undetected soon after thawing may manifest with time (38). Corneas have been

cryopreserved (gold standard is the method developed by Capella et al. (7); see Fig. 1) and transplanted successfully (3). Recently, Brunette et al. conducted a retrospective study of 124 cases of corneal transplants performed with tissue cryopreserved by the Capella-Kaufman method, by a single surgeon between March 1978 and April 1991 (4). They concluded the use of cryopreserved corneas results in an increase in primary failure and higher initial endothelial cell loss, but that cryopreserved corneas are viable (4). They recommend cryopreserved grafts should only be used in emergency situations, when fresh corneas are not available. Although, current methods may be adequate for cryopreserving corneas for emergency situations, this would not be an acceptable outcome for cryopreservation of a bioengineered human corneal construct, where virtually 100% recovery of the construct will be required for use in the research and clinical applications mentioned previously. Therefore, it is necessary to understand the low temperature responses of these bioengineered corneas to proceed to the development of a cryopreservation protocol.

### **1.5 Cryobiology of Cells**

Cryopreservation studies on cells in suspension have contributed to understanding the events that occur in response to low temperatures, including the physical and biological responses of cells and causes of cryoinjury. As cells are slowly cooled to temperatures below their freezing point, ice forms extracellularly, while intracellular water remains unfrozen. As water is removed from the extracellular solution in the form of ice, solutes are excluded, resulting in an increase in extracellular solute concentration in the unfrozen water. The

solute in the intracellular water have a lower osmolality than the solutes in the extracellular water and water will flow out of the cell by ex-osmosis, provided that the cooling rate is sufficiently slow, allowing the cell to maintain osmotic equilibrium with the external environment by becoming increasingly dehydrated with continued cooling, which helps to avoid intracellular ice formation.

Cooling cells rapidly results in supercooling of the cytoplasm and formation of intracellular ice, as the rate of cooling is too rapid for the cells to lose water in response to the increasing external osmotic pressure.

Mazur, Leibo, and Chu proposed the two-factor hypothesis of freezing injury to explain cellular cryoinjury (23). Cells cooled rapidly are damaged by the formation of intracellular ice during cooling and its recrystallization upon warming, and cells cooled slowly are damaged by solution effects injury, which result from the increasing intracellular and extracellular solute concentrations as a result of extracellular ice formation (23). This study also determined that an optimal cooling rate exists that is slow enough to avoid intracellular ice formation and rapid enough to avoid damaging exposure to high concentrations of solutes, and this optimal cooling rate is dependent on the cell type.

There have been a number of other mechanisms proposed to explain slow cooling injury. Lovelock proposed that, damage to cells also increases as solute concentrations increase and times of exposure to these solutes is lengthened (17). Meryman proposed the "minimum cell volume" theory, which describes the existence of a critical minimum volume, where cell shrinkage below this volume causes irreversible damage (26). Steponkus et al. showed that portions of the

membrane are lost as a cell shrinks due to osmotic movement of water. Damage occurs during rehydration if there is not enough membrane material remaining for the cell to return to isotonic volume (34).

Intracellular ice formation (IIF) during rapid cooling is the other factor identified as a cause of cryoinjury and it is thought that the cell membrane itself prevents ice propagation (20). Therefore other mechanisms of intracellular ice nucleation must be involved and three main hypothetical mechanisms have been proposed.

The pore theory states that when the tip of a growing ice crystal is the same size of the aqueous pores in the plasma membrane, the extracellular ice propagates through these pores and nucleates the intracellular water (23).

Another hypothesis promotes membrane failure as the cause of IIF, assuming that intracellular ice forms as a result of mechanical breakdown of the plasma membrane, thus exposing the cytoplasm to external ice. One theory proposes that electrical transients, reaching a critical level ruptures the plasma membrane and allows intracellular ice nucleation (35). Finally, the osmotic rupture hypothesis states that membrane damage is due to some critical gradient in osmotic pressure, specifically; membrane rupture is due to osmotic water efflux (27).

Surface-catalyzed nucleation of IIF assumes that the membrane acts as a nucleator of intracellular ice, when acted upon by extracellular ice (37).

Knowledge is limited about the exact mechanisms of IIF and the damage to the cells following IIF, but it has been suggested that injury caused by IIF may

be due to mechanical forces from the ice on plasma and intracellular organelle membranes (3a).

Recrystallization of intracellular ice during warming may actually be more damaging than the formation of intracellular ice alone, as there is evidence that some cells that form intracellular ice survive if warmed very rapidly to avoid recrystallization (21,22,23). Ice crystals that form during rapid cooling are usually very small and are less thermodynamically stable compared to larger crystals, and have a tendency to form large crystals upon slow warming (21,22,23). If warmed rapidly enough, intracellular ice crystals will melt before recrystallization can occur and damage the cells.

For every cell type there is an optimal cooling rate that avoids both slow and fast cooling injury that results in maximum survival. Understanding the mechanisms and causes of damage during cryopreservation will aid in the development of cryopreservation protocols.

## **1.6 Cryobiology of Tissues**

Although many cells can be cryopreserved with high recovery of viability and function, this is not true for most tissues and biosynthetic constructs. A limiting factor is the ability to predict and modify low temperature responses in tissues. It is generally accepted that osmotic stresses due to the effects of high concentrations of cryoprotectants and other solutes, during addition and removal of cryoprotectants and during cooling and warming of the tissue, and the formation of interstitial and intracellular ice are the causes of injury during cryopreservation. The two-factor hypothesis of freezing injury still applies to cells

in tissues, but there are important differences between cells in suspension and cells in tissues that account for the difficulties of cryopreserving tissues. These include: 1) different cell types with different cryobiological and biological properties (permeability to water and solutes, sensitivity to osmotic pressures) within the tissue, 2) high cell densities, 3) the 3-dimensional nature and arrangement of tissues, 4) cell-cell and cell-matrix interactions, and 5) problems related to heat and mass transfer in tissues, such as cryoprotectant addition and removal, redistribution of water during freezing and thawing, diffusion and large thermal gradients which lead to non-uniform cooling and warming rates (15,28,29).

### **1.7 Cryoprotection in Tissue Systems**

Cryoprotectants (permeating or non-permeating) are used to avoid injury during cryopreservation by eliminating or minimizing intracellular ice formation and decreasing damage to cells from solution effects during cooling (15,24,25). Permeating and non-permeating cryoprotectants act colligatively, reducing cell water content and increasing viscosity of the extra- and intracellular solutions, thus decreasing the amount of ice formed during cooling (15,24,25). Permeating cryoprotectants also dilute the deleterious increase in concentration of electrolytes as water precipitates as ice, thereby decreasing damage by osmotic stress and intolerable changes in cell volume (15). Although cryoprotective agents protect against damage they can be the source of damage, by their direct toxicity on the cells or by the excessive volume excursions that can destroy the cell membrane as cryoprotectants and water are exchanged across the plasma

membrane. In addition, uneven distribution of cryoprotectants due to mass transport limitations in the tissue can result in areas that are not protected or areas that are injured by prolonged exposure to the cryoprotectant (15).

### **1.8 Status of Corneal Cryopreservation**

Many studies have made attempts at corneal cryopreservation, but these have been met with limited success mainly due to the inability to preserve the viability of the endothelial cells and the detachment of the endothelial monolayer after thawing.

Fong et al. compared the transplantation outcomes of cryopreservation of rabbit corneas in 2M DMSO frozen in air or liquid to the Capella-Kaufman method (9). After thawing all groups showed considerable endothelial detachment from Descemet's membrane, but the least was observed when corneas were frozen in air. The stroma was thickened and the epithelium was irregular and many cells were vacuolated. Upon thawing the corneas swelled rapidly, which made surgical manipulation and wound closure difficult during the transplant procedure. All corneas that had been frozen in media become opaque and 2/5 frozen in air became opaque, although the endothelial cell number was significantly decreased and poorly adhered to Descemet's membrane. They concluded that freezing corneas in air is superior to freezing in media, and that extracellular ice is important in causing damage (9). Other studies support this conclusion (10,18). Fong et al. did not support using cryopreserved corneas for clinical transplantation (9).

Madden et al. also recognized detachment of the endothelial cells as a significant result of cryoinjury (19). However, they found that rapid cooling resulted in an intact endothelial cell layer with normal morphology, and with decreasing cooling rates the cellular adhesion was reduced.

Other studies have looked at the effects of non-permeating cryoprotectants on porcine corneas after cryopreservation. They were able to get 75% recovery of structural integrity of the porcine endothelial cell monolayers in the presence of chondroitin sulfate (13) or dextran (14).

Wusteman et al. have developed a strategy to add and remove DMSO in rabbit corneas, to maintain the osmotically induced changes in endothelial cell volume within tolerable limits without damaging the corneal endothelial cells (39). They determined that sufficient endothelial cells were preserved intact after cryopreservation to restrict stromal swelling, but the endothelial cell layer was clearly more fragile and more easily detached than non-osmotically challenged, non-cryopreserved corneas.

In a subsequent paper, Wusteman et al. went on to evaluate the applicability of the above procedure to different species by testing its ability to successfully cryopreserve porcine corneas (40). They found significant differences between the response of porcine corneas to cryoprotectant exposure and freezing as compared to the results with rabbit corneas, in that porcine corneas were more susceptible to injury. This study showed the importance of species variation when studying cryopreservation.

Bourne et al. compared the recovery of human corneas after cryopreservation by 3 different procedures that use DMSO: 1). Capella-Kaufman method (gold standard), 2). Wusteman et al. method, and 3). Bourne et al. method (3). The Capella-Kaufman method resulted in the lowest recovery of human corneas after thawing with very abnormal endothelial monolayer morphology and scattered dead cell remnants. The corneas cryopreserved with the method by Wusteman et al. showed fewer changes in endothelial morphology than the corneas cryopreserved with the Capella-Kaufman method, but dead cell remnants were apparent. The method described by Bourne et al. resulted in the least changes in endothelial morphology, however there were still remnants of dead cells. This study reinforced the need to use human corneas as shown by the large discrepancy in the recovery of rabbit versus human corneas cryopreserved by the method of Wusteman et al. Although, this study showed improved results in human corneal endothelial cell presentation following cryopreservation, the recovery was not high enough to use cryopreservation routinely for storing corneas for transplantation.

Another study looking at cryopreservation of human corneas found that cooling at 1°C/min in 7% DMSO was optimal, but still only resulted in 60% of the corneas cryopreserved meeting acceptable criteria for transplantation (6). Because of the high variability of recovery after cryopreservation, cryopreservation cannot be used for routine preservation of corneas for transplant (6).

Canals et al. optimized a cryopreservation method for rabbit corneas and attempted to apply this method to human corneas (5). Unfortunately, the human corneas had a significant loss of endothelial cell viability and number following cryopreservation, again demonstrating the inability of methods developed for animal corneas to successfully cryopreserve human corneas.

In these reviewed studies, extracellular ice formation was thought to be the cause of injury, and this led to investigations of corneal vitrification.

Vitrification is the solidification of a liquid by an extreme increase in viscosity and without crystallization of ice during the cooling process (8). Vitrification provides cryoprotection by avoiding intracellular and extracellular ice formation during cooling and warming, by the formation of glass instead of ice (8). One of the major obstacles of vitrification is that high concentrations of CPA are typically required to achieve vitrification at practical cooling and warming rates, and these CPA concentrations have been found to be toxic to the cornea endothelium (1,2,30,31,32). Bourne and Nelson (1), Bourne et al. (2), and Rich and Armitage (30,31,32) studied the tolerance of corneal endothelial cells to high concentrations of different cryoprotectants and combinations of cryoprotectants. Rich and Armitage (30,31,32) were able to achieve vitrification of corneas during cooling; however, during warming, devitrification (ice formation) could not be avoided, thus destroying the endothelium. To avoid devitrification using tolerable concentrations of cryoprotectants, faster warming rates would have to be used, which has been difficult to achieve. Rich and Armitage concluded that the tolerance of the corneal endothelium to cryoprotectants may be improved by

modifying the addition and dilution protocols, or changing the ratio or combinations of cryoprotectants; no specific conclusions concerning protocol modifications were made (31).

Bourne et al. showed that corneas could be successfully vitrified without ice formation on rewarming, but this was only achieved after prolonged exposure to cryoprotectants which resulted in extensive damage to the endothelium (2). They concluded that successful vitrification would require a safe method for obtaining corneal equilibration with cryoprotectant (2).

## **1.9 Objectives**

Much of the previous work on the cryopreservation of corneas has used a trial and error approach and has used animal tissue as a model for cryopreservation of human corneas. Recent reports have questioned the applicability of the results from animal model systems to human corneas (3,5). Therefore it is important to proceed with studies using human tissue, engineered human constructs, or human derived in vitro cellular model systems to further study cryopreservation of human corneas and biosynthetic corneas. Successful cryopreservation of human corneas and newly developed bioengineered human corneal equivalents will also depend on proceeding with a more scientific approach by first understanding the basic responses of the human corneal endothelial, keratocyte, and epithelial cells to low temperatures, slow and rapid cooling injury, osmotic and permeability parameters. Defining and understanding the osmotic and physiological responses of corneal cells to cooling and warming and to osmotic stresses in the presence and absence of cryoprotectants are the

main objectives of this thesis. The studies in this thesis use primary human corneal endothelial, keratocyte, and epithelial cell lines that are the constituent cells of the bioengineered human corneal construct that we are trying to cryopreserve, and are morphologically, biochemically, and electrophysiologically similar to freshly-isolated human corneal cells (12). The results from this thesis can eventually be used to develop a scientifically derived cryopreservation protocol that can be verified experimentally. The objectives more specifically are as follows.

- 1. Low temperature responses of the human corneal equivalent.** A unique experimental protocol, graded freezing, designed to differentiate between slow cooling and rapid cooling injury is used to examine low temperature responses and determine mechanisms of cryoinjury in a cellular human corneal model system. These experiments use human corneal cells cultured as confluent monolayers on collagen coated coverslips to mimic the native tissue structure *in vitro*.
- 2. Osmotic responses.** Determine osmotic parameters (membrane hydraulic conductivity, osmotically-inactive fraction, and Arrhenius activation energy) for cultured human corneal endothelial, keratocyte, and epithelial cells in suspension and use these values to mathematically model low temperature responses of the bioengineered human corneal construct.
- 3. Permeability parameters.** Determine membrane permeability to DMSO and PG, membrane hydraulic conductivity in the presence of these cryoprotectants, and the Arrhenius activation energies for membrane

cryoprotectant permeability and hydraulic conductivity for human corneal endothelial, keratocyte, and epithelial cells. These values will be applied to mathematically model the addition and removal of cryoprotectants and low temperature responses of the constituent cells of the corneal construct during cooling at varying cooling rates and the implications for cryopreservation will be discussed.

- 4. Simulations of low temperature responses of the bioengineered human corneal construct.** Use the osmotic and permeability parameters determined to simulate the conditions of the graded freezing procedure used for human corneal endothelial monolayers and relate the simulated results to the experimental results obtained. Also, simulate the low temperature responses of human corneal endothelial, keratocyte, and epithelial cells in the presence of permeating and non-permeating cryoprotectants and discuss the applications to cryopreservation and how these simulations can be used in the development of cryopreservation procedures. Mathematical models are powerful tools for developing and predicting osmotic responses of tissues, and are useful in reducing the scope of empirical experimentation required.

## 1.10 References

1. Bourne, W.M., and Nelson, L.R. Human corneal studies with a vitrification solution containing dimethyl sulfoxide, formamide, and 1,2-propanediol. *Cryobiology*. **31**, 522-530 (1994).
2. Bourne, W.M., Shearer, D.R., and Nelson, L.R. Human corneal endothelial tolerance to glycerol, dimethyl sulfoxide, 1,2-propanediol, and 2,3-butanediol. *Cryobiology*. **31**, 1-9 (1994).
3. Bourne, W.M., Nelson, L.R., and Hodge, D.O. Comparison of three methods for human corneal cryopreservation that utilize dimethyl sulfoxide. *Cryobiology*. **39**, 47-57 (1999).
4. Brunette, I., Le Francois, M., Tremblay, M., and Guertin, M.C. Corneal transplant tolerance to cryopreservation. *Cornea*. **20**, 590-596 (2001).
5. Canals, M., Costa, J., Potau, J.M., Dalmases, C., Costa-Vila, J., and Miralles, A. Optimization of a method for the cryopreservation of rabbit corneas: Attempted application to human corneas. *Cell and Tissue Banking*. **1**, 271-278 (2000).
6. Canals, M., Costa, J., Potau, M.D., Merindano, D., Pita, D., and Ruano, D. Long-term cryopreservation of human donor corneas. *Eur J Ophthalmol*. **6**, 234-241 (1996).
7. Capella, J.A., Kaufman, H.E., and Robbins, J.E. Preservation of viable corneal tissue. *Arch Ophthalmol*. **74**, 669-673 (1965).
8. Fahy, G.M., MacFarlane, D.R., Angell, C.A., and Meryman, H.T. Vitrification as an approach to cryopreservation. *Cryobiology*. **21**, 407-426 (1984).

9. Fong, L.P., Hunt, C.J., Taylor, M.J., and Pegg, D.E. Cryopreservation of rabbit corneas: assessment by microscopy and transplantation. *Br J Ophthalmol.* **70**, 751-760 (1986).
10. Fong, L.P., Hunt, C.J., and Pegg, D.E. Cryopreservation of the rabbit cornea: freezing with dimethyl sulfoxide in air or in medium. *Curr Eye Res.* **6**, 569-577 (1987).
11. Germain, L., Carrier, P., Auger, F.A., Salessé, C., and Guerin, S.L. Can we produce a human corneal equivalent by tissue engineering? *Progress in Retinal and Eye Research.* **19**, 497-527 (2000).
12. Griffith, M., Osborne, R., Munger R., Xiong, X., Doillon, C.J., Laycock, N.L.C., Hakim, M., Song, Y., and Watsky, M.A. Functional human corneal equivalents constructed from cell lines. *Science.* **286**, 2169-2172 (1999).
13. Hagenah, M., and Bohnke, M. Corneal cryopreservation with chondroitin sulfate. *Cryobiology.* **30**, 396-406 (1993).
14. Halberstadt, S., Athmann, S., and Hagenah, M. Corneal cryopreservation with dextran. *Cryobiology.* **43**, 71-80 (2001).
15. Karlsson, J.O., and Toner, M. Long-term storage of tissues by cryopreservation: critical issues. *Biomaterials.* **17**, 243-256 (1996).
16. Klyce, S.D., and Beuerman, R.W. Structure and Function of the Cornea. In "The Cornea" (H.E. Kaufman, B.A. Baron, M.B. McDonald, and S.R. Waltman, Ed.), pp. 3-54. Churchill Livingstone, New York, 1988.
17. Lovelock, J.E. The haemolysis of human red blood cells by freezing and thawing. *Biochim Biophys Acta.* **10**, 414-426 (1953).

18. Madden, P.W., and Easty, D.L. An investigation of damage during corneal cryopreservation II. With temperature reduction to  $-196^{\circ}\text{C}$ . *Cryo-letters*. **7**, 162-169 (1986).
19. Madden, P.W., Taylor, M.J., Hunt, C.J., and Pegg, D.E. The effect of polyvinylpyrrolidone and the cooling rate during corneal cryopreservation. *Cryobiology*. **30**, 135-157 (1993).
20. Mazur, P. The role of cell membranes in the freezing of yeast and other single cells. *Ann NY Acad Sci*. **125**, 658-676 (1965).
21. Mazur, P. The role of intracellular freezing in the death of cells cooled at supraoptimal rates. *Cryobiology*. **14**, 251-272 (1977)
22. Mazur, P. Freezing of living cells: mechanisms and implications. *Am J Physiol*. **247**, 125-142 (1984)
23. Mazur, P., Leibo, S.B., and Chu, E.H.Y. A Two-Factor hypothesis of freezing injury. *Exper Cell Res*. **71**, 345-355 (1972).
24. McGann, L.E. Differing actions of penetrating and nonpenetrating cryoprotective agents. *Cryobiology*. **15**, 382-390 (1978).
25. Meryman, H.T. Cryoprotective agents. *Cryobiology*. **8**, 173-183 (1971).
26. Meryman, H. Freezing injury and its prevention in living cells. *Annu Rev Biophys*. **3**, 341-363 (1974).
27. Muldrew, K., and McGann, L. Mechanisms of intracellular ice formation. *Biophys J*. **57**, 525-532 (1990).
28. Pegg, D.E. The current status of tissue cryopreservation. *Cryo-letters*. **22**, 105-114 (2001).

29. Pegg, D.E., Rubinsky, B., Diaper, M.P., and Lee, C.Y. Analysis of the introduction and removal of glycerol in rabbit kidneys using a Krogh cylinder model. *Cryobiology*. **23**, 150-160 (1986).
30. Rich, S.J., and Armitage, W.J. Corneal tolerance of vitrifiable concentrations of propane-1,2-diol. *Cryobiology*, **28**, 159-170 (1991).
31. Rich, S.J., and Armitage, W.J. Corneal tolerance of vitrifiable concentrations of glycerol. *Cryobiology*, **29**, 153-194 (1992).
32. Rich, S.J., and Armitage, W.J. The potential of an equimolar combination of propane-1,2-diol and glycerol as a vitrification solution for corneas. *Cryobiology*. **28**, 314-326 (1991).
33. Schwab, I.R., Reyes, M., and Isseroff, R.R. Successful transplantation of bioengineered tissue replacements in patients with ocular surface disease. *Cornea*. **19**, 421-426 (2000).
34. Steponkus, P., and Wiest, S. Plasma membrane alterations following cold acclimation and freezing. In "Plant cold hardiness and freezing stress: mechanisms and crop implications" (P. Li and A. Sakai, Eds.), pp. 75-91, Academic Press, New York, 1978.
35. Steponkus, P., Stout, D., Wolfe, J., and Lovelace, R. Freeze-induced electrical transients and cryoinjury. *Cryo-letters*. **5**, 343-348 (1984).
36. Taylor, M.J. Clinical cryobiology of tissues: preservation of corneas. *Cryobiology*. **23**, 237-259 (1986).

37. Toner, M., Cravahlo, E., and Karel, M. Thermodynamics and kinetics of intracellular ice formation during freezing of biological cells. *J Appl Phys.* **67**, 1582-1593 (1990).
38. Wilson, S.E., and Bourne, W.M. Corneal preservation. *Surv Ophthalmol.* **33**, 237-259 (1989).
39. Wusteman, M.C., Boylan, S., and Pegg, D.E. Cryopreservation of rabbit corneas in dimethyl sulfoxide. *Invest Ophthalmol Vis Sci.* **38**, 1934-1943 (1997).
40. Wusteman, M.C., Armitage, J.W., Wang, L.H., Busza, A.L., and Pegg, D.E. Cryopreservation studies with porcine corneas. *Curr Eye Res.* **19**, 228-233 (1999).

Solutions	I	II	III	IV
% DMSO	2	4	5	7.5
% Sucrose	2.5	5	7.5	10

In serum (animals) or 25% albumin (humans)

The corneal scleral segment is placed in 1 ml of solution at 4°C, using the following addition protocol.

sol I (10 min) → sol II (10 min) → sol III (10 min) → sol IV (10 min) → at 4°C

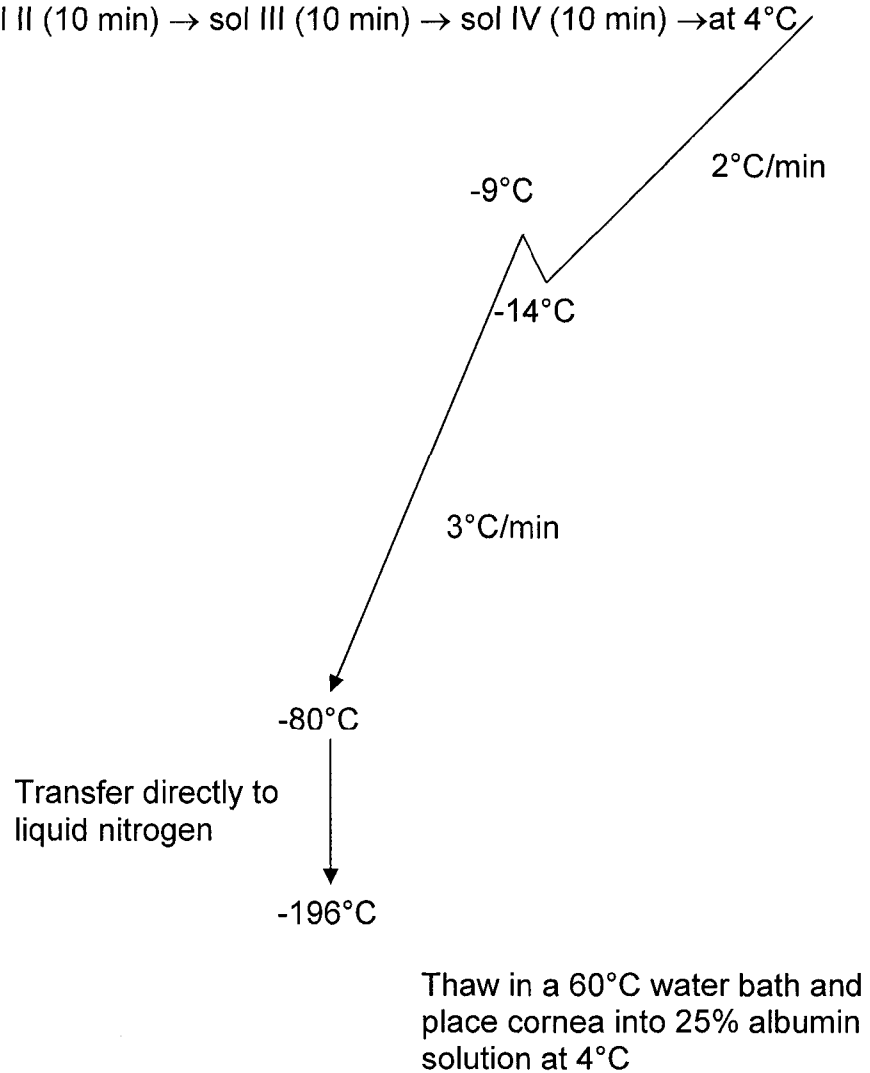


Fig. 1. Capella and Kaufman method for corneal cryopreservation (7).

## **\*Chapter 2: A Human Corneal Endothelial Monolayer as an In Vitro Model for Corneal Cryoinjury**

### **2.1 Introduction**

The development and usage of biosynthetic human corneas is rapidly becoming a reality (7). With these technological advances in tissue engineering resulting in products coming to the marketplace, their success and availability require intermediate-term storage. Cryopreservation has proven to be an effective method to maintain viability and function in a wide variety of tissues for transplant (3,19,24,25).

Studies on the cryobiology of cells in suspension have contributed to understanding the events that occur in response to low temperature exposures, including the physical and biological responses of cells and the causes of cryoinjury. When cells are slowly cooled to temperatures below the freezing point of the suspending solution, ice initially forms extracellularly while the intracellular water remains unfrozen, resulting in an increase in extracellular solute concentration in the residual liquid and water efflux from the cells by passive osmotic transport. At low cooling rates, the cells become increasingly dehydrated to maintain osmotic equilibrium with the extracellular environment (14,16). At high cooling rates, there is increased supercooling of the cytoplasm and an increased likelihood of intracellular ice formation (14,16). These observations led Mazur to propose the two-factor hypothesis of freezing injury, where cells cooled rapidly are damaged by formation of intracellular ice during cooling and its

---

\* This chapter with minor modifications has been submitted to *Investigative Ophthalmology and Visual Sciences* as: S.L. Ebertz and L.E. McGann, "A Human Corneal Endothelial Monolayer as an In Vitro Model for Corneal Cryoinjury"

recrystallization on slow warming. Cells cooled slowly are damaged by increasing osmotic pressures and increasing solute concentrations as extracellular ice forms (13). Successful cryopreservation of cell suspensions therefore necessitates the avoidance of cryoinjury described by the two-factor hypothesis by using cryoprotective compounds.

Cryoprotectants act colligatively, reducing the amount of ice formed, thereby reducing electrolyte concentrations during cooling. Cryoprotectants can, however, contribute to damage by direct toxicity as the concentrations increase in the presence of ice, or by osmotic stresses during addition and removal.

While many cells can be cryopreserved with high recovery of viability and function, this is not true for most tissues and biosynthetic constructs. The two-factor hypothesis of freezing injury still applies to cells in tissues, but there are important differences between cells in suspension and cells in tissues that account for the difficulties of cryopreserving tissues (9,10). These include, different cell types with different properties (permeability to water and solutes, sensitivity to osmotic stresses), high cell densities, the 3-dimensional nature and arrangement of tissues, cell-cell and cell-matrix interactions, and problems related to heat and mass transfer, such as cryoprotectant addition and removal, redistribution of water during freezing and thawing, diffusion and large thermal gradients which lead to non-uniform cooling and warming rates (8). Developing successful cryopreservation strategies for tissues such as cornea has proven to be more difficult than anticipated (20).

Purely empirical approaches to the development of procedures for corneal cryopreservation have not resulted in successful or practical methods for cryopreservation of human corneas, and have not contributed significantly to understanding the mechanisms of injury or the responses of human corneas and their constituent cells during freezing and thawing (1,2,4,5,6,8,11,12,23,27). Most of these investigations have used porcine or rabbit corneas due to the unavailability of human corneas for research, but recent reports have questioned the applicability of the results of these animal model systems to human corneas (25,26).

This study uses a primary human corneal endothelial cell line, that is morphologically, biochemically, and electrophysiologically similar to freshly-isolated human corneal cells (7), in a unique experimental protocol to examine low temperature responses and mechanisms of cryoinjury in a human corneal model. The objective of the study is to extend our understanding of the basic cryobiological properties and mechanisms of cryoinjury in isolated human corneal endothelial cells cultured as confluent monolayers to model the native tissue structure.

## **2.2 Materials and Methods**

### *Human Corneal Endothelial Cell Culture*

Human corneal endothelial cells (HCEC; a gift from Dr. May Griffiths, University of Ottawa) were incubated at 37°C in 5% carbon dioxide in Medium 199 with 10% v/v fetal bovine serum (GIBCO BRL, Burlington, Canada), and supplemented with 1% v/v insulin transferrin selenium (Sigma, Mississauga,

Canada). Cells were grown in 75cm<sup>2</sup> Falcon tissue culture flasks (VWR, Edmonton, Canada) and harvested by exposure to 0.05% trypsin-EDTA (GIBCO BRL) solution at 37°C for 2-3 minutes. The HCEC were re-suspended in supplemented M199 to obtain cell suspensions, and plated on sterilized coverslips (12mm circle, Fisher Brand; Fisher Scientific, Edmonton, Canada) precoated with bovine collagen type I (Sigma). The cells were allowed to grow to a confluent monolayer on the coverslips for use in the freezing experiments.

#### *Assessment of Monolayer Recovery*

A dual fluorescent stain, SYTO 13 (SYTO; Molecular Probes, Eugene, OR) and ethidium bromide (EB; Sigma) was used to assess membrane integrity of the HCEC monolayers. SYTO enters cells and stains nucleic acids green. EB enters cells that have lost membrane integrity and stains nucleic acids red. The final staining solution contained 12.5µM SYTO and 25µM EB in phosphate buffered saline (PBS; Gibco BRL). Cell monolayers were stained with 20µl of SYTO/EB solution for 5 min at 22°C and examined with a Zeiss fluorescent microscope. Representative images were captured with a Polaroid DMCIe camera and counted with in-house software. Cell recovery is expressed as the percentage of cells with intact membranes in the monolayer after treatment.

The monolayers were also subjectively rated for cell detachment from the glass coverslips. Subjective measurements were assigned as 0 for no detachment, 1 for mild, 2 for moderate, 3 for severe and 4 for complete detachment, as shown in Fig. 1.

### *Experimental Solutions*

The experimental solutions used in the freezing experiments were 2M dimethyl sulfoxide (DMSO; Sigma), 2M propylene glycol (PG; Sigma) or isotonic PBS. The final concentrations of cryoprotectants were 1M DMSO and 1M PG in the experimental samples.

### *Graded Freezing Experiments*

Coverslips with HCEC monolayers were placed in 10ml glass vials (Kimble; Fisher Scientific) containing 100 $\mu$ l of isotonic PBS with the monolayers facing up, then 100 $\mu$ l of experimental solution was added. Monolayers were equilibrated with the experimental solution for 5 min at 22°C, and then immersed into ice water for 5 min. Three control samples were held in ice water until the completion of the graded freezing experiment, and assessed for membrane integrity and detachment after exposure to experimental solutions. The non-control vials were then placed into a programmable rate freezer (FTS systems, Stoneridge, NY) at -5°C and held for 5 min for temperature equilibration. Ice was nucleated in the experimental solution using a cooled copper probe and the temperature maintained for 1 min to allow release of the latent heat of fusion. The vials were cooled at 1°C/min to various subzero temperatures (-5, -10, -15, -20, -30, -40°C) and either thawed directly at 480°C/min in a 37°C water bath or cooled at 325°C/min to -196°C or at 235°C/min to -80°C for storage before thawing. The graded freezing procedure is shown schematically in Fig. 2. Monolayers were assessed immediately after thawing for membrane integrity and

detachment. Triplicate samples were used for each experimental condition, and experiments were repeated 3 times.

#### *Cooling and Warming Conditions Between -80°C and -196°C*

The final cooling and warming conditions between -80°C and -196°C were varied to determine the effect on membrane integrity and detachment of the HCEC monolayers. Samples were cooled as described above to either -15°C or -40°C, then subjected to one of three procedures: 1) cool at 235°C/min to -80°C, cool to -196°C, and thaw at 480°C/min, 2) cool at 325°C/min to -196°C, warm to -80°C, and thaw at 480°C/min, or 3) cool at 235°C/min to -80°C, cool to -196°C, warm to -80°C, and thaw at 480°C/min (shown schematically in Fig. 3.). Triplicate samples were used for each experimental condition, and experiments were repeated 3 times.

#### *Cryoprotectant Solutions*

Different cryoprotectant solutions were used to give final concentrations of 2M, 4M DMSO; 2M, 4M PG; and 5% pluronic F68 (Sigma). The addition of 4M DMSO and 4M PG was done in a step-wise procedure to avoid damaging volume changes. 100µl of isotonic PBS was added to the monolayers and 0.25µl of 8M DMSO or PG was added at 1min intervals in 4 steps until a final volume of 100µl of cryoprotectant solution had been added. The graded freezing procedure remained the same as described above, with experimental temperatures of -15°C and -40°C. The samples were cooled at 1°C/min to the experimental temperatures, then plunged into alcohol at -80°C, plunged into liquid nitrogen

(-196°C), or transferred to liquid nitrogen vapour (-165°C) for storage before thawing at 480°C/min. Triplicate samples were used for each experimental condition, and experiments were repeated twice.

#### *1M DMSO and 5% pluronic F68 as a cryoprotectant*

HCEC monolayers were frozen at 1°C/min to -40°C, followed by rapid cooling at 235°C/min to -80°C to test the effect of combining a permeating cryoprotectant with a non-permeating agent on recovery.

## **2.3 Results**

### *Graded Freezing*

The first obstacle to overcome in developing a cryopreservation protocol is to determine the causes of injury during freezing and thawing. Graded freezing has been shown to be an excellent technique to differentiate between the mechanisms of cryoinjury as defined by the two-factor hypothesis of freezing injury (18).

The control monolayers assessing the recovery of HCEC monolayers after exposure to experimental solutions, showed no loss of membrane integrity in all experimental solutions, no detachment in 1M DMSO, 1M PG, 2M DMSO, and 2M PG, and slight detachment in 5% pluronic F68, 4M DMSO and 4M PG.

Fig. 4A shows loss of membrane integrity and detachment of the HCEC monolayers after direct thaw from the experimental temperatures in three experimental solutions. Monolayers frozen to the experimental temperature without cryoprotectant showed a significant loss of membrane integrity below

-5°C and increased detachment at -20°C and lower. Monolayers frozen in 1M DMSO or 1M PG resulted in virtually 100% maintenance of membrane integrity and little detachment at all experimental temperatures. Human corneal endothelial cell monolayers tolerated increased solute concentrations and osmotic stresses during slow cooling at 1°C/min to -40°C. The results in Fig. 4A demonstrated that slow cooling injury is not a contributing factor to loss of viability of HCEC monolayers during freezing and thawing at the conditions tested.

Fig. 4B shows the results of rapid cooling to -196°C from the experimental temperatures. In the absence of cryoprotectant, cells lost membrane integrity and there was moderate to severe detachment at all experimental temperatures. 1M DMSO and 1M PG did not protect the endothelial cell monolayers from loss of membrane integrity and detachment when rapidly cooled and stored at -196°C.

Results when monolayers are rapidly cooled to -80°C from the experimental temperatures are shown in Fig. 4C. Monolayers frozen without cryoprotectant showed low recovery of membrane integrity and mild to moderate detachment and in comparison to storage at -196°C, storage at -80°C resulted in lower detachment, but no increase in membrane integrity. Monolayers frozen in 1M DMSO or 1M PG and stored at -80°C resulted in a significant increase in membrane integrity and decrease in detachment when compared to results after storage at -196°C. 1M DMSO and 1M PG offer protection to human corneal endothelial cells when monolayers were stored at -80°C, but not when stored at -196°C.

### *Effect of Varying Cooling and Warming Conditions Between -80°C and -196°C*

The above experimental results demonstrated that substantial cryoinjury occurred between -80°C and -196°C. Fig. 5A and B show the membrane integrity and detachment results respectively when the cooling and warming conditions were varied between -80°C and -196°C. None of the variations in cooling and warming protocols between -80°C and -196°C resulted in an improvement in membrane integrity or detachment. Storage at -80°C resulted in higher recovery of the HCEC monolayers and lower detachment than storage at -196°C.

### *Effect of Varying Cryoprotectant Solutions*

To test the hypothesis that the amount of ice formed contributed to the loss of membrane integrity and detachment below -80°C, higher concentrations of DMSO and PG were used to reduce the amount of ice at low temperatures. Fig. 6A and B show that increasing cryoprotectant concentrations had no beneficial effect on membrane integrity or detachment when the HCEC monolayers were cooled to -196°C from the experimental temperatures.

Cooling to -165°C (liquid nitrogen vapour) was added to the conditions in this set of experiments to test the hypothesis that the cooling rate to -196°C was causing excessive damage due to the thermo-mechanical effects on the glass coverslips, rather than damage to the endothelial cells themselves. Comparing Fig. 6C and D to the results in Fig. 6A and B, showed very little difference in the results between these two conditions. From these results cooling to and storage in liquid nitrogen vapour versus liquid nitrogen has no beneficial effects on recovery of HCEC monolayers.

Fig. 6E and F show the effects of increased concentration of cryoprotectants on recovery from rapid cooling and storage at  $-80^{\circ}\text{C}$ . Increasing the concentrations of DMSO and PG did not increase membrane integrity or decrease detachment after freezing and thawing the HCEC monolayers.

The presence of 5% pluronic F68 resulted in a decrease in detachment when HCEC monolayers were stored at  $-196^{\circ}\text{C}$ : the first report of a cryoprotectant to preserve cell adhesion. Pluronic F68 did not protect membrane integrity, implying different modes of cryoprotection.

Fig. 6A, C, and E show that increasing the concentration of either DMSO and PG results in a decrease in the membrane integrity, possibly the result of cryoprotectant toxicity or cooling at a suboptimal rate for these conditions.

## **2.4 Discussion**

Detachment of the corneal endothelium following cryopreservation has been recognized as a problem (12,27). This study identifies Pluronic F68 as a novel cryoprotectant for preserving cell adhesion during cryopreservation. Conclusive evidence from this study demonstrates that there are different mechanisms of cryoinjury to the corneal endothelium leading to detachment and loss of membrane integrity, suggesting that it is unlikely that a single, simple solution will overcome the problems of cryopreserving human corneas. Mazur suggested that the addition of high molecular weight compounds results in large freezing point depressions, decreasing crystallization (15), with the potential to alter the ice morphology. We hypothesize that pluronic polyols confer protection against cell detachment by altering the morphology of ice crystals.

Corneal cryoinjury has been hypothesized to result from ice in the extracellular solution (6,23). However, this study suggests that it is not the amount of ice that causes damage, as increasing cryoprotectant concentration, which decreases the amount of ice, does not decrease detachment or increase membrane integrity. This study indicates that, because of increased toxicity, increasing cryoprotectant concentrations is not a good strategy for improving cryopreservation outcomes, using the freezing conditions described.

Storage at  $-196^{\circ}\text{C}$  is detrimental to monolayers of human corneal endothelial cells. It is generally accepted that cryoinjury following rapid cooling is related to formation or recrystallization of intracellular ice (13). Intracellular ice formation is the likely cause of damage during rapid cooling to  $-80^{\circ}\text{C}$  and  $-196^{\circ}\text{C}$  from  $-40^{\circ}\text{C}$ , as there would still be intracellular water present that could be supercooled and nucleated. However, recrystallization of ice is not a likely cause of cryoinjury as shown by the lack of effects on monolayer recovery on varying the cooling and warming conditions between  $-80^{\circ}\text{C}$  and  $-196^{\circ}\text{C}$ . Between  $-80^{\circ}\text{C}$  and  $-196^{\circ}\text{C}$  additional damage is occurring as shown by the decrease in membrane recovery after thawing from these respective temperatures, and a hypothesis to explain this damage below  $-80^{\circ}\text{C}$  is as a result of a solution phase transition that is independent of the cooling and warming rates. Solutes and cryoprotectants are concentrated inside the cells as they are cooled slowly and intracellular water is lost. Upon subsequent rapid cooling the intracellular contents partially vitrify and, when warmed, may devitrify, resulting in cell damage. It has been shown that devitrification results in a non-viable cornea

(2,22,23) and this glass transition of cryoprotectant solutions occurs near  $-100^{\circ}\text{C}$  (21). To avoid membrane damage and monolayer detachment this study suggests that storage temperatures for human corneas should be re-evaluated, and storage at  $-80^{\circ}\text{C}$  considered. This storage temperature is acceptable from a practical perspective, allowing storage for up to 10 years (17).

This study demonstrates that cryopreservation of human corneas and biosynthetic human corneal equivalents will not be simple and a single cryoprotectant strategy that facilitates successful cryopreservation may not be feasible. Combining 1M DMSO and 5% pluronic F68 resulted in 78% membrane integrity and virtually no detachment when HCEC monolayers were frozen at  $1^{\circ}\text{C}/\text{min}$  to  $-40^{\circ}\text{C}$ , then rapidly cooled and stored at  $-80^{\circ}\text{C}$ . This is in comparison to 60% and 10% membrane integrity when frozen in 1M DMSO and 10% pluronic F68, respectively. Different mechanisms are responsible for membrane damage and cell detachment; therefore different strategies for developing a cryopreservation protocol are required. Classical cryopreservation has had limited success in past studies and vitrification strategies have difficulties in overcoming corneal toxicity of cryoprotectants and the avoidance of devitrification upon warming. Combined strategies for cryopreservation should be investigated, which include using a variety of cryoprotectants in a single solution, chosen for their ability to protect against specific mechanisms of damage identified during freezing and thawing.

This study shows that knowledge of the basic cryobiological responses and mechanisms of cryoinjury in the human corneal endothelium provide a

rational foundation for development of successful protocols for long-term preservation of human corneas and tissue-engineered human cornea equivalents. This is the first study to demonstrate when damage is occurring during freezing and thawing, and to identify potential mechanisms of cryoinjury for human corneal endothelial cells.

Future applications of this experimental protocol to human corneal epithelial cells and keratocytes, reported in Appendix A, will allow us to combine these results to model the low temperature responses of the bioengineered human corneal equivalent and optimize a cryopreservation protocol. The goal is to develop a successful cryopreservation protocol for human corneas and bioengineered human corneal equivalents by using experimental data determined from this *in vitro* model and theoretical simulations of low temperature responses.

Cryopreservation of tissues is a complex problem that needs to be addressed in smaller, manageable steps, rather than tackling the tissue as a whole, allowing us to demystify the mechanisms of cryoinjury and the low temperature responses of the individual components of the tissue of interest. Interpretation of results from a multi-cell, multi-component system is complex. Human *in vitro* model systems simplify the extrapolation of experimental findings to the complex real tissue, bringing us closer to developing successful cryopreservation protocols for tissue systems.

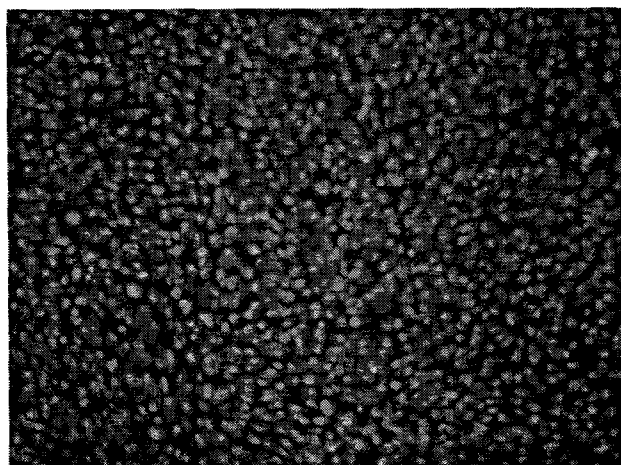
## 2.5 References

1. Bourne, W.M., Nelson, L.R., and Hodge, D.O. Comparison of Three Methods for Human Corneal Cryopreservation That Utilize Dimethyl Sulfoxide. *Cryobiology*. **39**, 47-57 (1999).
2. Bourne, W.M., and Nelson, L.R. Human Corneal Studies with a Vitrification Solution Containing Dimethyl Sulfoxide, Formamide, and 1,2-Propanediol. *Cryobiology*. **31**, 522-530 (1994).
3. Brunette, I., Le Francois, M., Tremblay, M.C., and Guertin, M.C. Corneal transplant tolerance of cryopreservation. *Cornea*. **20**, 590-596 (2001).
4. Canals, M., Costa, J., Potau, J.M., Merindano, M.D., Pita, D., and Ruano, D. Long-term cryopreservation of human donor corneas. *Eur J Ophthalmol*. **6**, 234-241 (1996).
5. Canals, M., Garcia, J., Potau, J.M., Dalmases, C., Costa-Vila, J., and Miralles, A. Optimization of a method for the cryopreservation of rabbit corneas: Attempted application to human corneas. *Cell and Tissue Banking*. **1**, 271-278 (2000).
6. Fong, L.P., Hunt, C.J., Taylor, M.J., and Pegg, D.E. Cryopreservation of Rabbit Corneas: assessment by microscopy and transplantation. *Br J Ophthalmol*. **70**, 751-760 (1986).
7. Griffith, M., Osborne, R., Munger, R., Xiong, X., Doillon, C.J., Laycock, N.L.C., Hakim, M., Song, Y., and Watsky, M.A. Functional Human Corneal Equivalents Constructed from Cell Lines. *Science*. **286**, 2169-2172 (1999).

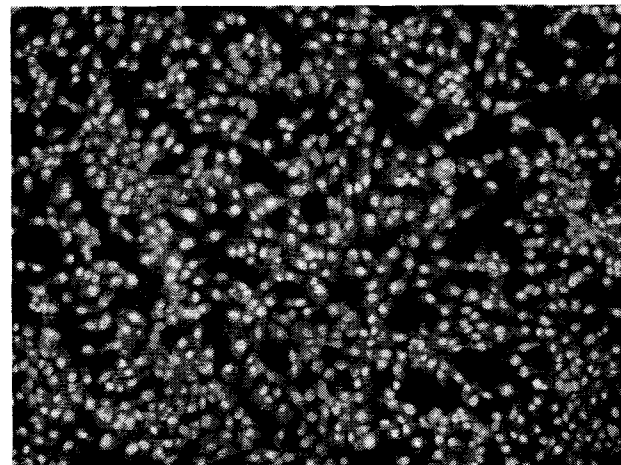
8. Hagenah, M., and Bohnke, M. Corneal Cryopreservation with Chondroitin Sulfate. *Cryobiology*. **30**, 396-406 (1993).
9. Jacobsen, I.A., and Pegg, D.E. Cryopreservation of Organs: A Review. *Cryobiology*. **21**, 377-384 (1984).
10. Karlsson, J.O.M., and Toner, M. Long-term Storage of Tissues by Cryopreservation: Critical Issues. *Biomaterials*. **17**, 243-256 (1996).
11. Madden, P.W., and Easty, D.L. An Investigation of Damage During Corneal Cryopreservation II. With temperature reduction to  $-196^{\circ}\text{C}$ . *Cryo-Letters*. **7**, 162-169 (1986).
12. Madden, P.W., Taylor, M.J., Hunt, C.J., and Pegg, D.E. The Effect of Polyvinylpyrrolidone and the Cooling Rate during Corneal Cryopreservation. *Cryobiology*. **30**, 135-157 (1993).
13. Mazur, P., Leibo, S.P., and Chu, E.H.Y. A Two-Factor Hypothesis of Freezing Injury. *Exp Cell Res*. **70**, 345-355 (1972).
14. Mazur, P. Cryobiology: The Freezing of Biological Systems. *Science*. **168**, 939-949 (1970).
15. Mazur, P. Fundamental Cryobiology and the preservation of organs by freezing. In "Organ Preservation for Transplantation" (A.M. Karow, D.E.Pegg Eds.) pp. 143-175. Decker, New York, 1981.
16. Mazur, P. Kinetics of water Loss from Cells at Subzero Temperatures and the Likelihood of Intracellular Freezing. *J Gen Physiol*. **47**, 347-369 (1963).

17. McGann, L.E., and Acker, J.P. Cryopreservation. *In* "Organ Procurement and Preservation for Transplantation Second Edition" (L.H. Toledo-Pereyra, Ed.) pp. 47-66. Landes Bioscience, Georgetown, TX, 1997.
18. McGann, L.E., Yang, H., and Walterson, M. Manifestations of Cell Damage after Freezing and Thawing. *Cryobiology*. **25**, 178-185 (1988).
19. McNally, R.T., and McCaa, C. Cryopreserved Tissues For Transplant. *In* "Low Temperature Biotechnology Emerging Applications and Engineering Contributions." (J.J McGrath, K.R. Diller Eds.) pp. 91-112. The American Society of Mechanical Engineers, New York, 1988.
20. Pegg, D.E. The Current Status of Tissue Cryopreservation. *Cryo-Letters*. **22**, 105-114 (2001).
21. Rabin, Y., Taylor, M.J., and Wolmark, N. Thermal expansion measurements of frozen biological tissues at cryogenic temperatures. *J Biomech Eng*. **120**, 259-266 (1998).
22. Rich, S.J., and Armitage, W.J. Corneal Tolerance of Vitrifiable Concentrations of Propane-1,2-diol. *Cryobiology*. **28**, 159-170 (1991).
23. Rich, S.J., and Armitage, W.J. The Potential of an Equimolar combination of Propane-1,2-Diol and Glycerol as a Vitrification Solution for Corneas. *Cryobiology*. **28**, 314-326 (1991).
24. Song, Y.C., Khirabadi, B.S., Lightfoot, F., Brockbank, K.G., and Taylor, M.J. Vitreous cryopreservation maintains function of vascular grafts. *Nat Biotechnol*. **18**, 296-299 (2000).

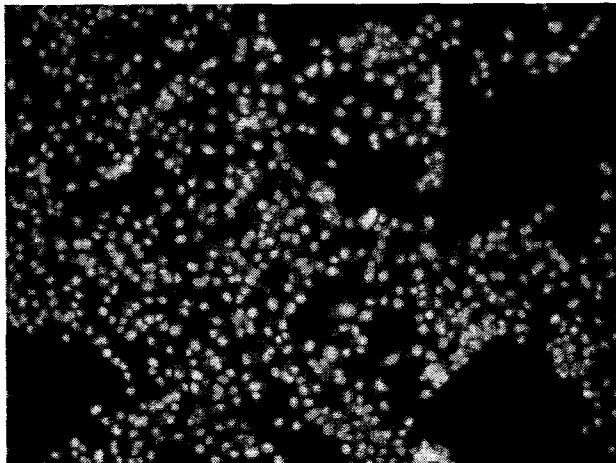
25. Song, Y.C., Lightfoot, F.G., Li, C.Y., et al. Successful Cryopreservation of Articular Cartilage by Vitrification. *Cryobiology*. **43**, 353 (2001).
26. Wusteman, M.C., Armitage, J.W., Wang, L.H., Busza, A.L., and Pegg, D.E. Cryopreservation studies with porcine corneas. *Curr Eye Res*. **19**, 228-233 (1999).
27. Wusteman, M.C., Boylan, S., and Pegg, D.E. Cryopreservation of Rabbit Corneas in Dimethyl Sulfoxide. *Invest Ophthalmol Vis Sci*. **38**, 1934-1943 (1997).



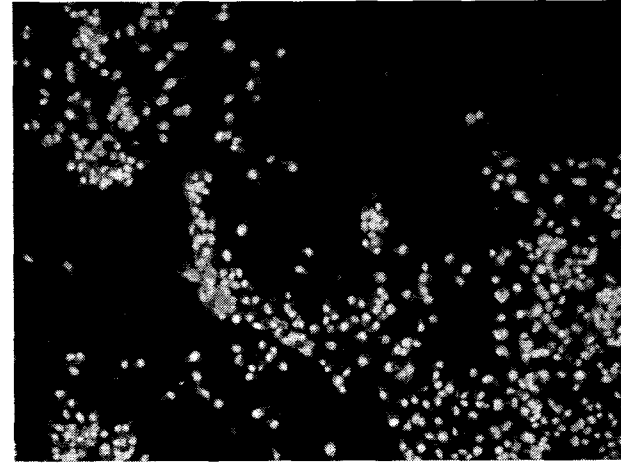
0 = no detachment



1 = mild detachment



2 = moderate detachment



3 = severe detachment

Fig. 1. Representative pictures to depict the subjective measurement of detachment used. 0-3 are shown, A rating of 4 is complete detachment with no cells present.

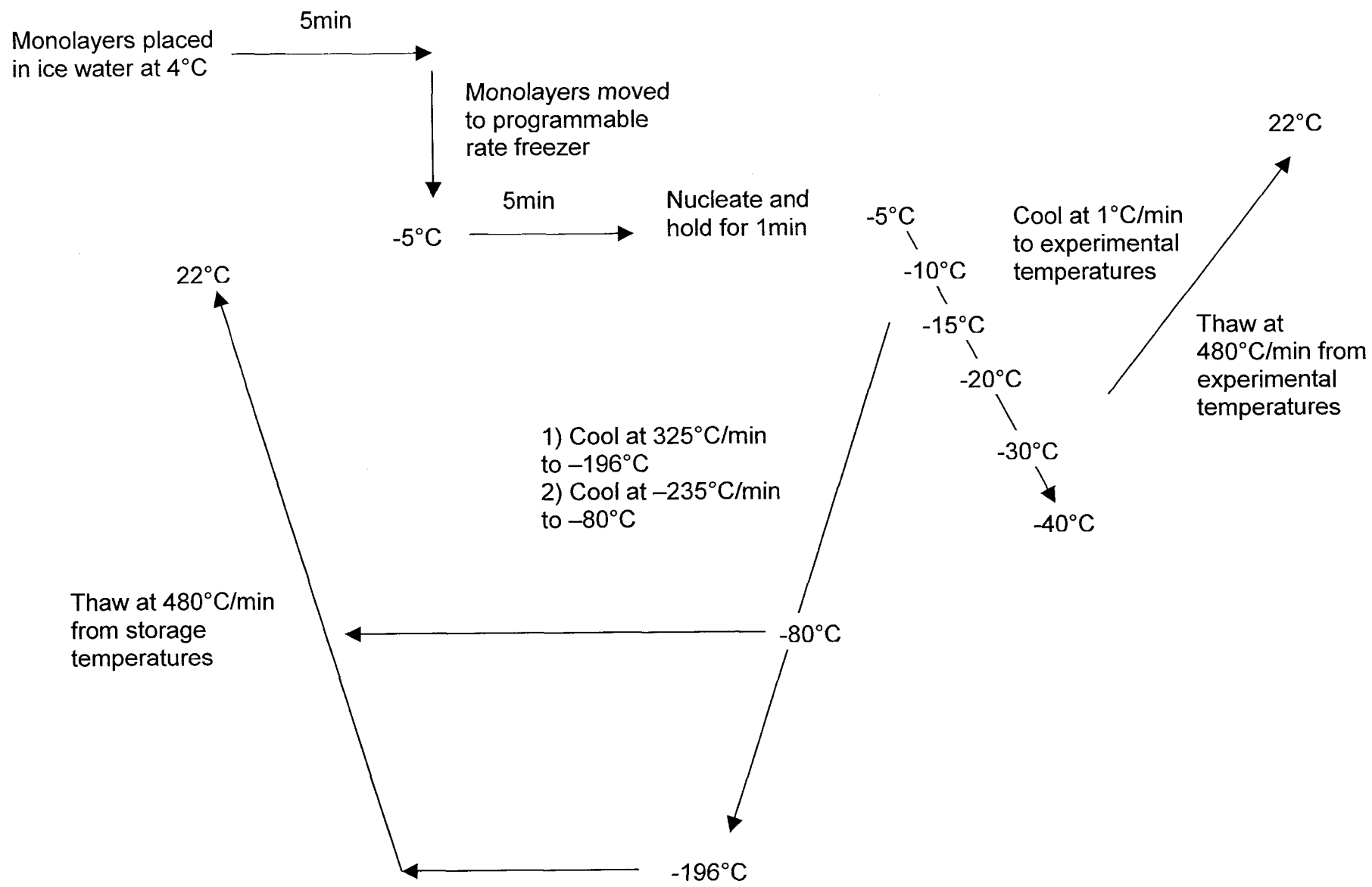


Fig. 2. Schematic representation of the graded freezing procedure

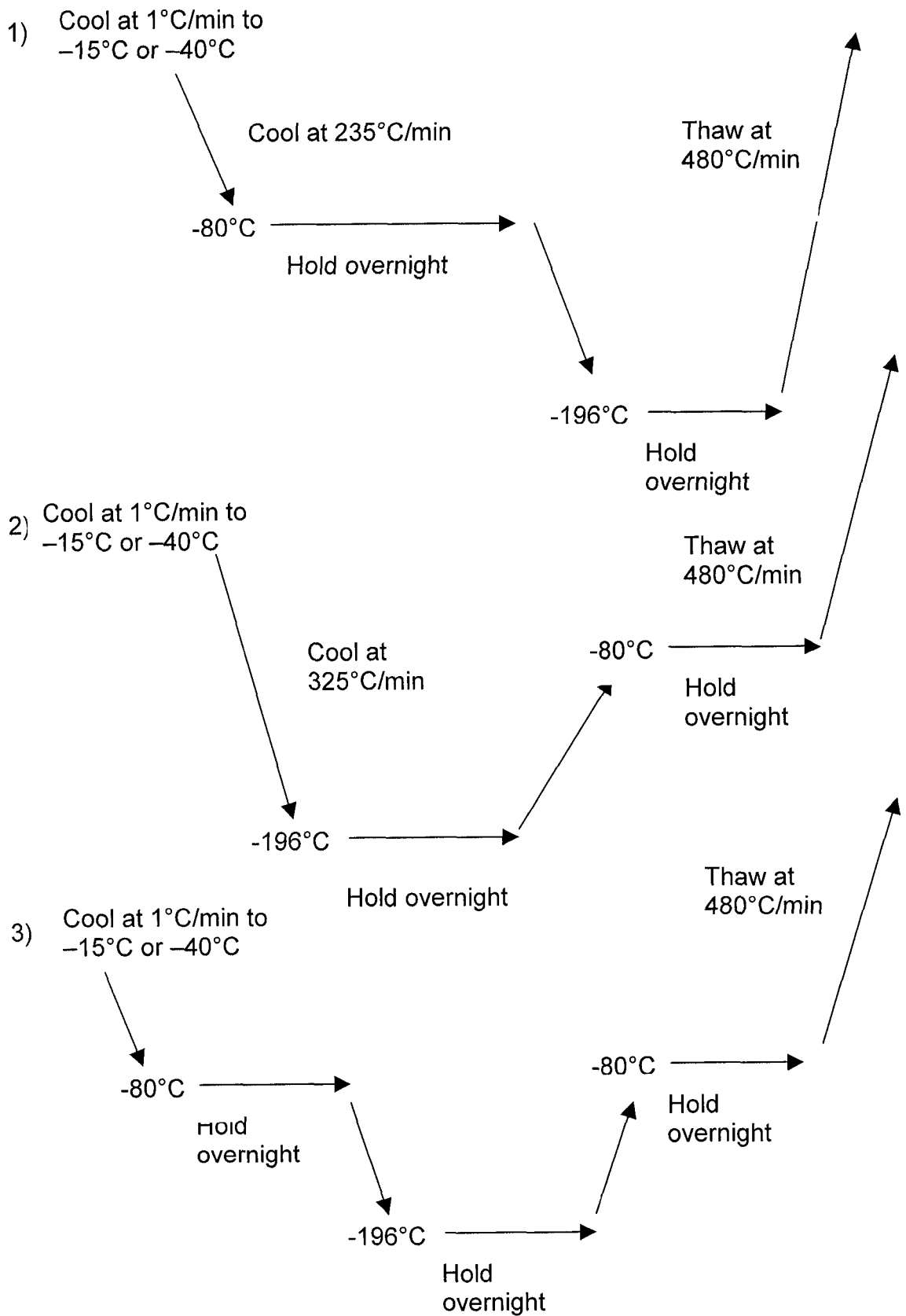


Fig. 3. Schematic representation of protocol to vary cooling and warming rates between -80°C and -196°C

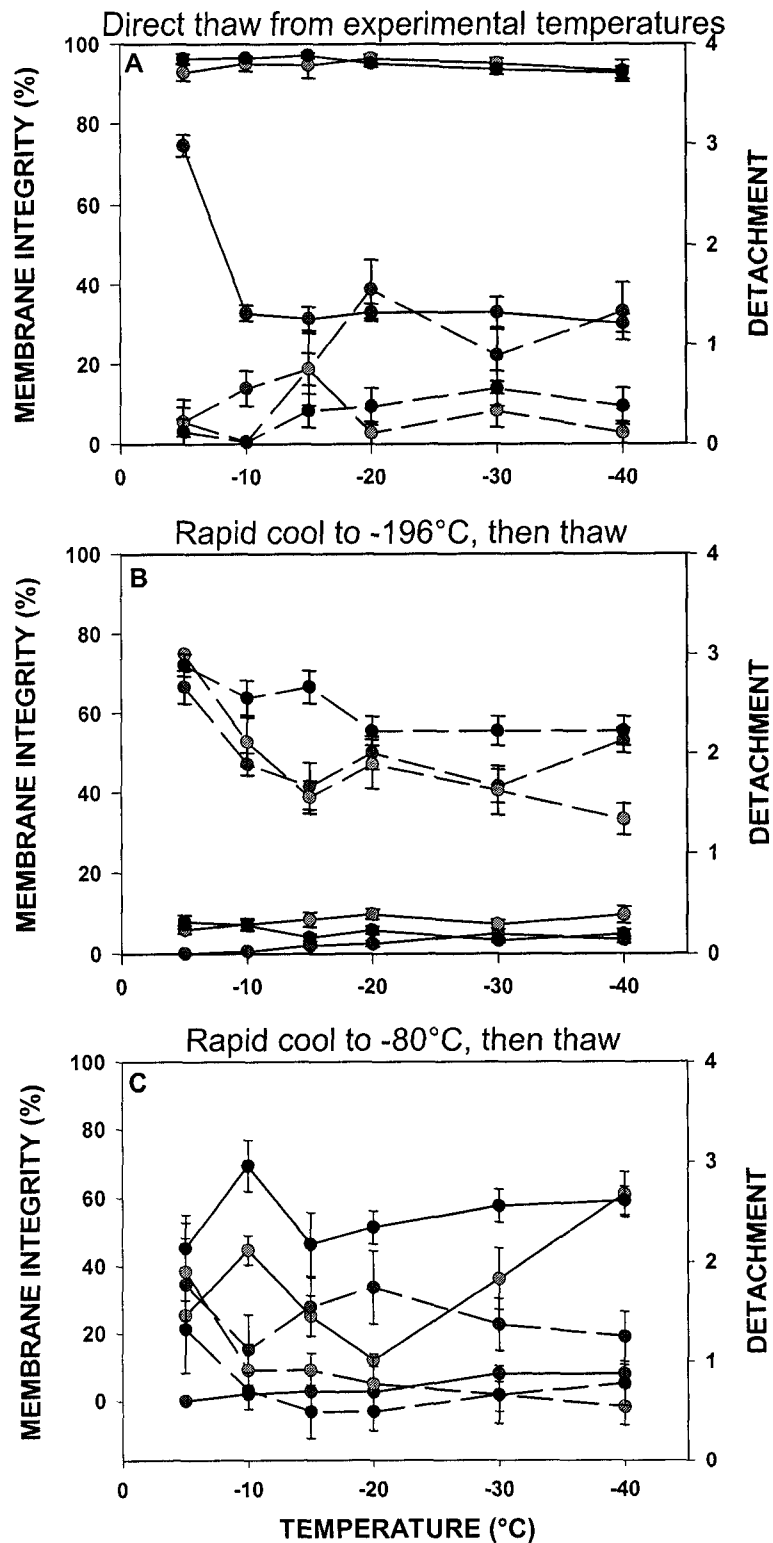


Fig. 4. Comparison of the membrane integrity (solid lines) and detachment (dashed lines) of human corneal endothelial cells frozen in isotonic PBS, 1M DMSO, or 1M PG following controlled cooling to experimental temperatures. Detachment: 0 = none, 1 = mild, 2 = moderate, 3 = severe, 4 = complete

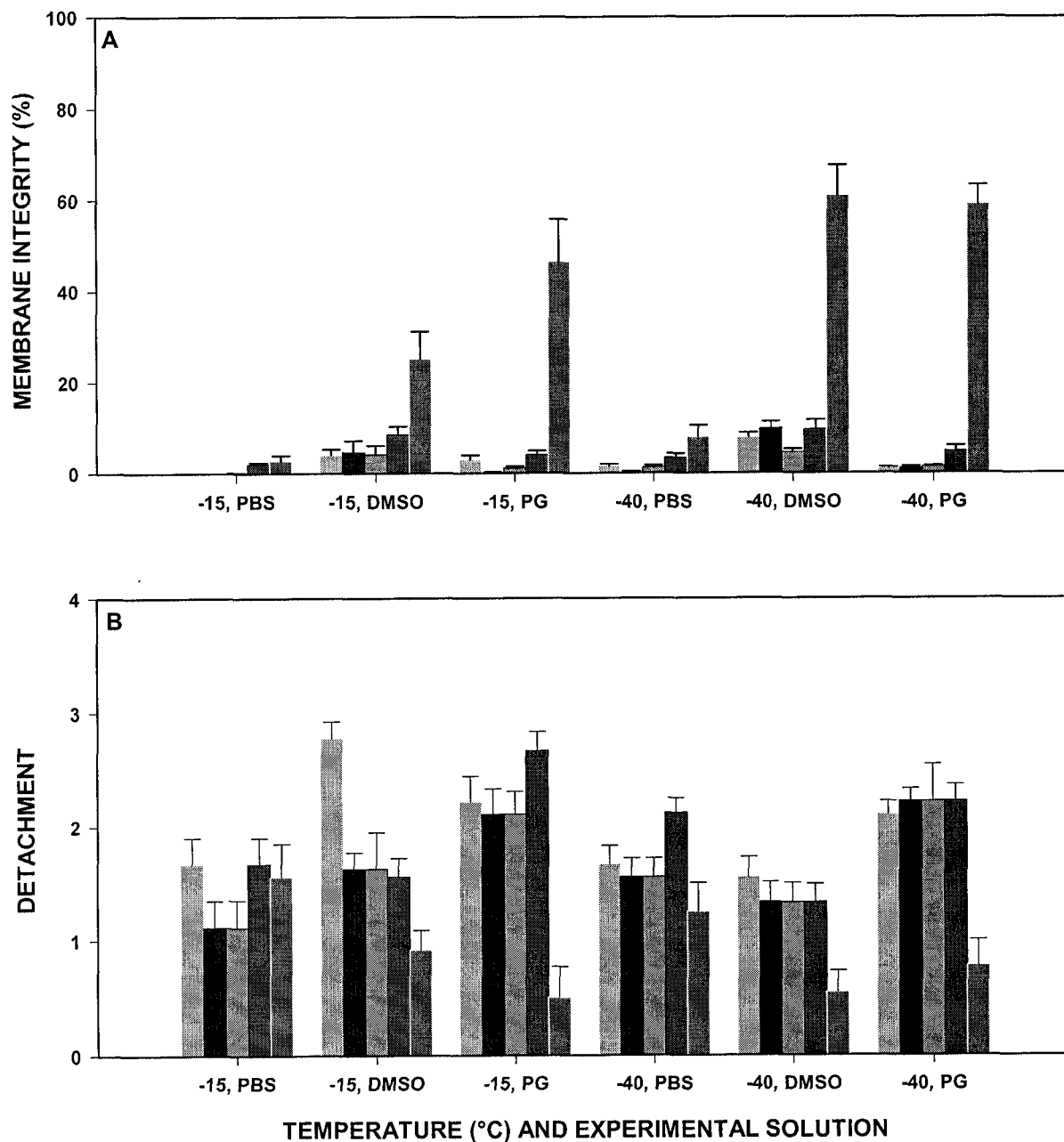


Fig. 5. The effect of varying the cooling and warming conditions (1. cool at 235°C/min to -80°C, cool to -196°C, thaw, 2. cool at 235°C/min to -80°C, cool to -196°C, warm to -80°C, thaw, 3. cool at 325°C/min to -196°C, warm to -80°C, thaw, 4. cool at 325°C/min to -196°C, thaw, and 5. cool at 235°C/min to -80°C, thaw) between -80°C and -196°C following controlled cooling to the experimental temperatures (-15°C and -40°C) on A) membrane integrity and B) detachment when frozen in PBS, 1M DMSO, or 1M PG. Detachment: 0 = none, 1 = mild, 2 = moderate, 3 = severe, 4 = complete

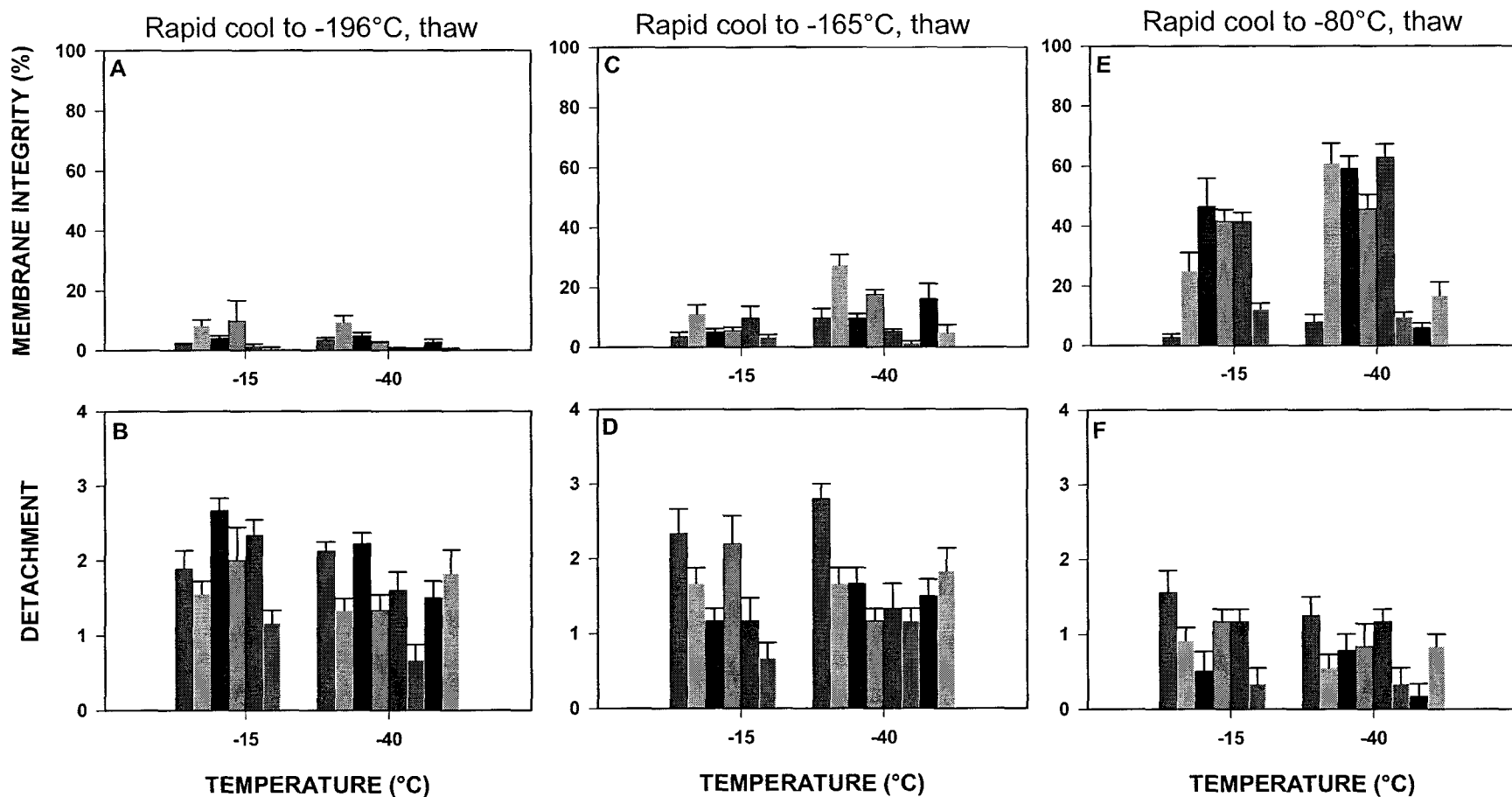


Fig. 6. The effect of varying cryoprotectant solutions (isotonic PBS, 1M DMSO, 1M PG, 2M DMSO, 2M PG, 5% pluronic F68, 4M DMSO, and 4M PG) on membrane integrity and detachment of HCEC monolayers following controlled cooling to -15°C or -40°C then rapidly cooled to -196°C (A,B), -165°C (C,D), or -80°C (E,F). Detachment: 0 = none, 1 = mild, 2 = moderate, 3 = severe, 4 = complete

## **\*Chapter 3: Osmotic Parameters for Cells from a Bioengineered Human Corneal Equivalent and Consequences for Cryopreservation**

### **3.1 Introduction**

A functional human corneal equivalent has been developed with applications for replacing animals in the evaluation of new chemicals and drugs for irritancy, and in biomedical research to study wound healing and cell-matrix interactions in the cornea (12). The ability to market and meet the demand for supply of these bioengineered human corneas depends on successful intermediate-term storage, and cryopreservation has proven to be a convenient and effective method to maintain viability and function in a wide variety of tissues (5,31,35).

Approaches to the development of corneal cryopreservation procedures have been largely unsuccessful (3,4,6,7,10,13,20,21,34,42), due in part to the empirical nature of these attempts and the lack of knowledge of the pertinent cellular parameters to effectively model low temperature responses. When cells are slowly cooled to temperatures below the freezing point of the suspending solution, ice initially forms extracellularly resulting in an increase in extracellular solute concentration in the residual liquid and water efflux from the cells by passive osmotic transport. At low cooling rates, the cells become increasingly dehydrated to maintain osmotic equilibrium with the extracellular environment, and at high cooling rates the cytoplasm becomes supercooled and the probability

---

\* This chapter with minor modifications has been submitted to Cryobiology as: S.L. Ebertz and L.E McGann, "Cellular Osmotic Parameters for a Bioengineered Human Corneal Equivalent and Consequences for Cryopreservation"

of intracellular ice formation increases (22,23,24,25,26). An optimal cooling rate exists that is high enough to avoid excessive exposure to damaging solute concentrations and low enough to allow intracellular water to leave the cell and decrease the degree of supercooling, avoiding damage by intracellular ice formation (23,24,25,26). The optimal cooling rate is therefore a function of cell membrane hydraulic conductivity to water and its Arrhenius activation energy (22,24).

This study uses primary human corneal endothelial, keratocyte, and epithelial cell lines that are the constituent cells in the bioengineered human corneal construct (12) that we are attempting to cryopreserve. The objective of this study is to determine the osmotic parameters (membrane hydraulic conductivity, osmotically-inactive fraction and Arrhenius activation energy) for cultured human corneal endothelial, keratocyte and epithelial cells and to use these values to simulate low temperature responses of the cells in this bioengineered corneal construct.

### **3.2 Materials and Methods**

#### *Human Corneal Cell Culture*

Human corneal endothelial, keratocyte, and epithelial cells (a gift from Dr. May Griffiths, University of Ottawa) were incubated at 37°C in 5% carbon dioxide in Medium 199 with 10% v/v fetal bovine serum (GIBCO BRL, Burlington, Canada), and supplemented with 1% v/v insulin transferrin selenium (Sigma, Mississauga, Canada). Cells were grown in 75cm<sup>2</sup> Falcon tissue culture flasks (VWR, Edmonton, Canada) and harvested by exposure to 0.05% trypsin-EDTA

(GIBCO BRL) solution at 37°C for 2-3 minutes. The corneal cells were re-suspended in supplemented M199 to obtain cell suspensions for use in osmotic determinations.

#### *Experimental Solutions*

Experimental solutions were prepared by diluting 10X PBS to final osmolalities of 150±4, 210±7, 300±10, 596±32, 862±18, 1152±30, and 1422±35 mosm/kg as measured with a freezing point depression osmometer (model 5004; Precision Systems Inc, Natick, MA).

#### *Osmotic Responses of Human Corneal Cells*

Electronic particle counters have been used extensively to determine osmotic parameters of cells in suspension (19,27,28,41). After rapid addition and mixing of cells with the test solution, the cells pass through a 100-120µm aperture that displaces a volume of the conducting fluid resulting in a voltage pulse proportional to the cell volume. A Coulter counter (model ZB1; Coulter Inc, Hialeah, FL) was connected to a personal computer via a pulse-height analyzer (The Great Canadian Computer Company, Spruce Grove, Canada), with the accompanying cell size analyzer software, which recorded the time and relative volume of each cell passing through the aperture (29). Experimental solutions were maintained within 0.1°C of the test temperatures (4, 13, 22 and 37°C) with a custom-made insulated jacket connected to a circulating water bath. Spherical latex beads (15µm diameter; Coulter Inc.) were used as calibrators to convert relative volumes to actual volumes. Isotonic cell volumes ( $V_{iso}$ ) were calculated by measuring the mean relative volume of the human corneal cells in isotonic

tissue culture medium and multiplying this average by the calibration factor obtained from the calibration beads. In-house software allowed kinetic analysis of mean cell volume as a function of time. Triplicate runs with each experimental solution were repeated with three different passages of cultured human corneal endothelial, keratocyte, and epithelial cells.

#### *Determination of Osmotic Parameters*

The Boyle van't Hoff relationship (Eq. 1) was used to calculate the osmotically-inactive fraction ( $V_b$ ) using the measured mean equilibrium cell volume after exposure to different anisotonic experimental solutions.

$$\frac{V}{V_{iso}} = \frac{\pi_o}{\pi} (1 - V_b) + V_b \quad (1)$$

Where  $V$  is the equilibrium cell volume,  $\pi$  is the experimental osmolality,  $\pi_o$  is the isotonic osmolality,  $V_{iso}$  is the isotonic cell volume and  $V_b$  is the osmotically-inactive fraction of the isotonic cell volume.

The hydraulic conductivity was calculated using the membrane mass transport model by Jacobs and Stewart (17), which describes the rate of volume change:

$$\frac{dV}{dt} = L_p A R T (\pi_i - \pi_e) \quad (2)$$

where  $L_p$  is the membrane hydraulic conductivity,  $A$  is the cell surface area,  $R$  is the universal gas constant,  $T$  is the absolute temperature,  $\pi_e$  is the extracellular osmolality, and  $\pi_i$  is the intracellular osmolality, which is calculated from Eq. 1.  $L_p$  was determined by fitting the experimental data to Eq. 1 and 2 using the least-square error method.

The Arrhenius activation energy (Eq. 3) was used to describe the temperature dependence of  $L_p$ . The activation energy was calculated from the slope of an Arrhenius plot of the natural logarithm of  $L_p$  as a function of inverse absolute temperature.

$$L_p = K * \exp\left(\frac{-E_a}{RT}\right) \quad (3)$$

Where  $L_p$  is the membrane hydraulic conductivity,  $K$  is a fitting constant,  $R$  is the universal gas constant,  $T$  is the reference temperature for  $L_p$ , and  $E_a$  is the activation energy.

#### *Statistical Analysis*

A one way ANOVA was used with a level of significance set at 5%.

#### *Simulation of Low Temperature Responses*

Simulations were performed using in-house software (CryoSim4; schematic shown in Fig. 1) designed by Dr. Locksley McGann. CryoSim4 performs simulations by calculating cellular osmotic responses to the concentration of solutes in the residual liquid in the presence of ice at low temperatures and assumes ice is nucleated in the extracellular solution at its freezing point. Phase diagrams were used to calculate concentrations in the liquid phase for NaCl-H<sub>2</sub>O (39) and KCl-H<sub>2</sub>O (39) for the intracellular compartment. Eq. 2 describing water transport across the plasma membrane, was used to calculate osmotic cellular responses to the changing extracellular conditions. The experimentally-determined Arrhenius activation energies were used to describe temperature dependencies of hydraulic conductivity, and the temperature as a function of time was calculated from the cooling rate.

### 3.3 Results

#### *Osmotic Parameters*

The size distributions of human corneal endothelial, keratocyte, and epithelial cells were similar, with the mean volumes of  $3307 \pm 292$ ,  $3186 \pm 297$ ,  $4134 \pm 169 \mu\text{m}^3$ , respectively. Changes in mean volume as a function of time after exposure to the experimental solution were used to calculate osmotic parameters for human corneal endothelial, keratocyte, and epithelial cells. The examples in Fig. 2 show typical experimental data, and values for the  $L_p$  and  $V_b$  for each cell type for all experimental solutions and temperatures tested are summarized in Tables 1 and 2, respectively. The  $L_p$  for the three human corneal cell types showed no concentration-dependence in hypertonic solutions (600-1500 mosm/kg) ( $p > 0.09$ ), so the  $L_p$  values were pooled for each experimental temperature and the values listed in Table 1D. Values for  $V_b$  were found to be independent of both concentration and temperature after exposure to hypertonic solutions ( $p > 0.07$ ), and the pooled values are listed in Table 2D.

#### *Activation Energies for $L_p$*

Fig 3 shows Arrhenius plots of  $L_p$  values at 4, 13, 22, and 37°C, resulting in activation energies of 14.8, 12.0, and 14.1 kcal/mol for human corneal endothelial, keratocyte, and epithelial cells respectively, indicating that water movement across the plasma membrane changes significantly with temperature, particularly for endothelial and epithelial cells.

### *Boyle van't Hoff Plot*

Fig. 4 shows the Boyle van't Hoff plot of equilibrium volume fraction of the human cornea cells as a function of inverse osmolality, linear in the hypertonic realm. As reported for other cell types (19,41),  $V_b$  diverges from the Boyle van't Hoff relation in hypotonic solutions, so values of  $V_b$  for the isotonic and hypertonic solutions were used in the linear regression shown in Fig. 4. Of the three human corneal cells studied, only the epithelial cells exhibited a linear response in the hypotonic solutions. The value of  $V_b$  from the y-intercept of the linear regression of the Boyle van't Hoff plot was the same as the  $V_b$  obtained from fitting the experimental data to Eqs. 1 and 2.

### *Simulations of Low Temperature Responses*

Table 3 summarizes the osmotic permeability parameters obtained from this study that were used to model the responses of human corneal cells at low temperatures in the absence of cryoprotectant. As an example of the calculations, Fig. 5 shows the calculated volume as a function of temperature for human corneal endothelial cells during cooling at different rates. As extracellular ice forms, extracellular solutes concentrate and the cells respond osmotically to the increased extracellular osmotic pressure. As the cooling rate increases the cells are unable to lose water quickly enough in response to the increasing extracellular osmotic pressure and the amount of supercooling increases. The amount of supercooling was calculated from the difference between the curve for each cooling rate and the equilibrium curve. Fig. 6 shows the maximum

intracellular supercooling at different cooling rates in human corneal endothelial, keratocyte, and epithelial cells.

### **3.4 Discussion**

The osmotically-inactive fraction ( $V_b$ ) obtained from the Boyle van't Hoff plot for human corneal endothelial (0.28), keratocyte (0.27), and epithelial cells (0.41) are within the range reported for a variety of cell types (0.2-0.41), including human lymphocytes (15), granulocytes (28), cord blood stem cells (40), and human chondrocytes (27). However, the results in this study differed from reported  $V_b$  values for rabbit corneal endothelial cells (0.34) (33) and rabbit corneal keratocytes (0.44) (1), indicating differences between rabbit and human corneal tissue.

The difference in the osmotically-inactive fraction for human corneal endothelial and keratocytes, compared to the epithelial cells will impact the design of cryopreservation protocols, in particular during freezing and addition of cryoprotectants when cells are exposed to hypertonic conditions. According to Meryman's minimum critical volume theory (32), which states that a higher  $V_b$  results in increased tolerance to hypertonic stress, the endothelial and keratocytes will reach their minimum critical volume at lower osmolalities than the epithelial cells, rendering them more susceptible to damage from cell shrinkage.

The deviation from linearity in hypotonic solutions by the human corneal endothelial and keratocytes shown in the Boyle van't Hoff plot (Fig. 4) is also important to consider when developing a cryopreservation protocol, as this may indicate a greater susceptibility of the endothelial and keratocytes to swelling-

induced lysis compared to the epithelial cells that behaved ideally under hypotonic conditions. The non-linearity of the Boyle van't Hoff in the hypotonic region may be caused by mechanical resistance to swelling, which would increase the probability of swelling-induced lysis, or may indicate the activation of cell volume regulatory mechanisms (16,37).

Values for the membrane hydraulic conductivity reported in this study for human corneal endothelial, keratocyte, and epithelial cells are within the typical range of  $L_p$  values reported for mammalian cells (30), although, endothelial and keratocytes have higher values than epithelial cells at 22°C. The equivalence of  $L_p$  values for endothelial and keratocytes at 22°C would indicate similar responses to low temperatures, but different activation energies lead to important differences in osmotic responses at low temperatures as demonstrated by Mazur (22,24); therefore conclusions drawn from  $L_p$  values at 22°C are misleading.

The Arrhenius activation energies of human corneal endothelial (14.8kcal/mol) and epithelial cells (14.1 kcal/mol) reported in this study are higher than values of 9-12 kcal/mol typically seen in mammalian cells (30). The  $E_a$  for human corneal keratocytes (12.0 kcal/mol) is characteristic of reported  $E_a$  values in mammalian cells, showing less temperature dependence of water permeability than the endothelial and epithelial cells. Verkmann et al. has characterized an  $E_a$  of less than 6 kcal/mol as indicative of the presence of channel-mediated water transport (36). Using this criterion,  $E_a$  values from this study indicate the absence of channel-mediated water transport in all three cell lines. Previous studies, however, reported evidence of aqueous pores in bovine corneal

endothelial (8,14,18,38), keratocyte (14,38), and epithelial cells (9,11,14). Recent findings (2) show mRNA levels encoding for aquaporins decreases rapidly in culture, consistent with the activation energies reported here. Membrane transport functions after culture may not be indicative of transport functions in primary cells from fresh tissue.

Activation energies together with the  $L_p$  values used to simulate low temperature responses give a clearer understanding of the differences between cell types in a tissue during cryopreservation. As ice forms in the extracellular space, solutes are excluded, resulting in loss of water from the cells or if cooling is too rapid the cytoplasm supercools and intracellular ice forms. The cooling rate is a strong determinant of cell survival during cryopreservation, since it must be high enough to avoid damaging exposures to the increased solute concentrations, and low enough to allow water loss thereby avoiding supercooling and lethal intracellular ice formation (25). Modelling the supercooling of human corneal cells during freezing (Fig. 6), using experimentally obtained  $L_p$  and  $E_a$  values, shows that the human corneal endothelial, keratocyte, and epithelial cells have different optimal cooling rates, that minimize exposure to concentrated solutes while avoiding intracellular freezing. The simulations (Fig. 6) suggest that keratocytes in the human cornea are unlikely to freeze intracellularly at cooling rates as high as 20°C/min (<10°C supercooling), a cooling rate that would likely result in intracellular freezing for endothelial and epithelial cells (>25°C supercooling). The optimal cooling rates calculated in this study are much higher than the current protocol to freeze corneas at 1°C/min; however, the

addition of cryoprotectants may alter these responses and will have to be taken into consideration when optimizing cryopreservation strategies. These results indicate that the differences in osmotic parameters between constituent cells will be a significant factor with physiological consequences during freezing and thawing of the bioengineered human corneal constructs and makes clear the challenge in optimizing a cryopreservation strategy.

Defining the osmotic parameters of the constituent cells in a tissue is the first step in developing a cryopreservation protocol for these bioengineered human corneal constructs. Cryopreservation of tissues is a complex problem that is facilitated by taking smaller, manageable steps to first define low temperature responses of individual components of the tissue of interest and using these to simulate low temperature responses. Osmotic parameters used in simulation of low temperature responses can supplement purely empirical approaches to the cryopreservation of bioengineered human corneal constructs.

### **3.5 References**

1. Armitage, W.J., and Juss, B.K. Osmotic response of mammalian cells: effects of permeating cryoprotectants on nonsolvent volume. *J Cell Physiol.* **168**, 532-538 (1996).
2. Bildin, V.N., Iserovich, P., Fischbarg, J., and Reinach, P.S. Differential expression of Na:K:2Cl cotransporter, glucose transporter, and aquaporin 1 in freshly isolated and cultured bovine corneal tissues. *Exp Biol Med (Maywood).* **226**, 919-926 (2001).

3. Bourne, W.M., and Nelson, L.R. Human corneal studies with a vitrification solution containing dimethyl sulfoxide, formamide, and 1,2-propanediol. *Cryobiology*. **31**, 522-530 (1994).
4. Bourne, W.M., Nelson, L.R., and Hodge, D.O. Comparison of three methods for human corneal cryopreservation that utilize dimethyl sulfoxide. *Cryobiology*. **39**, 47-57 (1999).
5. Brunette, I., Le Francois, M., Tremblay, M.C., and Guertin, M.C. Corneal transplant tolerance of cryopreservation. *Cornea*. **20**, 590-596 (2001).
6. Canals, M., Costa, J., Potau, J.M., Merindano, M.D., Pita, D., and Ruano, D. Long-term cryopreservation of human donor corneas. *Eur J Ophthalmol*. **6**, 234-241 (1996).
7. Canals, M., Garcia, J., Potau, J.M., Dalmases, C., Costa-Vila, J., and Miralles, A. Optimization of a method for the cryopreservation of rabbit corneas: Attempted application to human corneas. *Cell and Tissue Banking*. **1**, 271-278 (2000).
8. Echevarria, M., Kuang, K., Iserovich, P., Li, J., Preston, G.M., Agre, P., and Fischbarg, J. Cultured bovine corneal endothelial cells express CHIP28 water channels. *Am J Physiol*. **265**, C1349-C1355 (1993).
9. Fengying, K., Kuang, K., Li, J., and Fischbarg, J. Cultured bovine corneal epithelial cells express a functional aquaporin water channel. *Invest Ophthalmol Vis Sci*. **40**, 253-257 (1999).

10. Fong, L.P., Hunt, C.J., Taylor, M.J., and Pegg, D.E. Cryopreservation of rabbit corneas: assessment by microscopy and transplantation. *Br J Ophthalmol.* **70**, 751-760 (1986).
11. Funaki, H., Yamamoto, T., Koyama, Y., Kondo, D., Yaoita, E., Kawasaki, K., Kobayashi, H., Sawaguchi, S., Abe, H., and Kihara, I. Localization and expression of AQP5 in cornea, serous salivary glands, and pulmonary epithelial cells. *Am J Physiol.* **275**, C1151-C1157 (1998).
12. Griffith, M., Osborne, R., Munger, R., Xiong, X., Doillon, C.J., Laycock, N.L.C, Hakim, M., Song, Y., and Watsky, M.A. Functional human corneal equivalents constructed from cell lines. *Science* **286**, 2169-2172 (1999).
13. Hagenah, M., and Bohnke, M. Corneal cryopreservation with chondroitin sulfate. *Cryobiology.* **30**, 396-406 (1993).
14. Hamann, S., Zeuthen, T., La Cour, M., Nagelhus, E.A., Ottersen, O.P., Agre, P., and Nielsen, S. Aquaporins in complex tissues: distribution of aquaporins 1-5 in human and rat eye. *Am J Physiol.* **274**, C1332-C1345 (1998).
15. Hempling, H.G., Thompson, S., and DuPre, A. Osmotic properties of human lymphocytes. *J Cell Physiol.* **93**, 293-302 (1977).
16. Henson, J.H. Relationships between the actin cytoskeleton and cell volume regulation. *Microsc Res Tech.* **47**, 155-162 (1999).
17. Jacobs, M.H., and Stewart, D.R. A simple method for the quantitative measurement of cell permeability. *J Cell Comp Physiol.* **1**, 71-82 (1932).

18. Li, J., Kuang, K., Neilsen, S., and Fischbarg, J. Molecular identification of the water channel protein aquaporin 1 in CBCECs. *Invest Ophthalmol Vis Sci.* **40**, 1288-1292 (1999).
19. Liu, C., Benson, C.T., Gao, D., Haag, B.W., McGann, L.E., and Critser, J.K. Water permeability and its activation energy for individual hamster pancreatic islet cells. *Cryobiology.* **32**, 493-502 (1995).
20. Madden, P.W., and Easty, D.L. An investigation of damage during corneal cryopreservation II. With temperature reduction to  $-196^{\circ}\text{C}$ . *Cryo-Letters.* **7**, 162-169 (1986).
21. Madden, P.W., Taylor, M.J., Hunt, C.J., and Pegg, D.E. The effect of polyvinylpyrrolidone and the cooling rate during corneal cryopreservation. *Cryobiology.* **30**, 135-157 (1993).
22. Mazur, P. Kinetics of water loss from cells at subzero temperatures and the likelihood of intracellular freezing. *Journal of General Physiology.* **47**, 347-369 (1963).
23. Mazur, P. Cryobiology: The freezing of biological systems. *Science.* **168**, 939-949 (1970).
24. Mazur, P. The role of intracellular freezing in the death of cells cooled at supraoptimal rates. *Cryobiology.* **14**, 251-272 (1977).
25. Mazur, P., Leibo, S.P., and Chu, E.H.Y. A two-factor hypothesis of freezing injury. *Experimental Cell Research.* **70**, 345-355 (1972).

26. Mazur, P., and Schneider, U. Osmotic responses of preimplantation mouse and bovine embryos and their cryobiological implications. *Cell Biophys.* **8**, 259-285 (1986).
27. McGann, L.E., Stevenson, M., Muldrew, K., and Schachar, N. Kinetics of osmotic water movement in chondrocytes isolated from articular cartilage and applications to cryopreservation. *J Orthop Res.* **6**, 109-115 (1988).
28. McGann, L.E., Turner, A.R., Mannoni, P., and Turc, J. Calculated osmometric responses of human granulocytes during freezing. *In "Proceeding of the XVIth International Congress on Refrigeration, Paris, III*, pp. 121-126, 1984.
29. McGann, L.E., Turner, A.R., and Turc, J. Microcomputer interface for rapid measurements of average volume using an electronic particle counter. *Med & Biol Eng & Comput.* **20**, 117-120 (1982).
30. McGrath, J.J. Membrane transport proteins. *In "Low Temperature Biotechnology Emerging Applications and Engineering Contributions"* (J.J. McGrath and K.R. Diller, Eds.), pp. 273-330. The American Society of Mechanical Engineers, New York, 1988.
31. McNally, R.T., and McCaa, C. Cryopreserved tissues for transplant. *In "Low Temperature Biotechnology Emerging Applications and Engineering Contributions"* (J.J. McGrath and K.R. Diller, Eds.), pp. 91-112. The American Society of Mechanical Engineers, New York, 1988.
32. Meryman, H.T. Freezing injury and its prevention in living cells. *In "Annual Review of Biophysics and Bioengineering"* (Mullins, Hagins, Stryer, Newton, Eds.), pp 344-363. Annual Review Inc., 1974.

33. Pegg, D.E., Hunt, C.J., and Fong, L.P. Osmotic properties of the rabbit corneal endothelium and their relevance to cryopreservation. *Cell Biophys.* **10**, 169-189 (1987).
34. Rich, S.J., and Armitage, W.J.. The potential of an equimolar combination of propane-1,2-diol and glycerol as a vitrification solution for corneas. *Cryobiology.* **28**, 314-326 (1991).
35. Song, Y.C., Kharabadi, B.S., Lightfoot, F., Brockbank, K.G., and Taylor, M.J. Vitreous cryopreservation maintains function of vascular grafts. *Nat Biotech.* **18**, 296-299 (2000).
36. Verkman, A.S., Van Hoek, A.F., Ma, T., Frigeri, A., Skach, W.R., Mitra, A., Tamarappoo, B.K., and Farinas, J. Water transport across mammalian cell membranes. *Am J Physiol.* **270**, C12-C30 (1996).
37. Waldegger, S., Steuer, S., Risler, T., Heidland, A., Capasso, G., Massry, S., and Lang, F. Mechanisms and clinical significance of cell volume regulation. *Nephrol Dial Transplant.* **13**, 867-874 (1998).
38. Wen, Q., Diecke, F.P., Iserovich, P., Kuang, K., Sparrow, J., and Fischbarg, J. Immunocytochemical localization of aquaporin-1 in bovine corneal endothelial cells and keratocytes. *Exp Biol Med (Maywood).* **226**, 463-467 (2001).
39. Wolf, A.V., Brown, M.G., and Prentiss, P.G. Concentrative properties of aqueous solutions. In "Handbook of chemistry and physics" (Weast, Eds.). pp D-258, D-261. CRC press, 1982.
40. Woods, E.J., Liu, J., Darrow, C.W., Smith, F.O., Williams, D.A., and Critser, J.K. Osmometric and permeability characteristics of human

placental/umbilical cord blood CD34+ cells and their application to cryopreservation. *J hematol & stem cell res.* **9**, 161-173 (2000).

41. Woods, E.J., Zieger, M.A.J., Lakey, J.R.T., Liu, J., and Critser, J.K. Osmotic characteristics of isolated human and canine pancreatic islets. *Cryobiology.* **35**, 106-113 (1997).

42. Wusteman, M.C., Boylan, S., and Pegg, D.E. Cryopreservation of rabbit corneas in dimethyl sulfoxide. *Invest Ophthalmol Vis Sci.* **38**, 1934-1943 (1997).

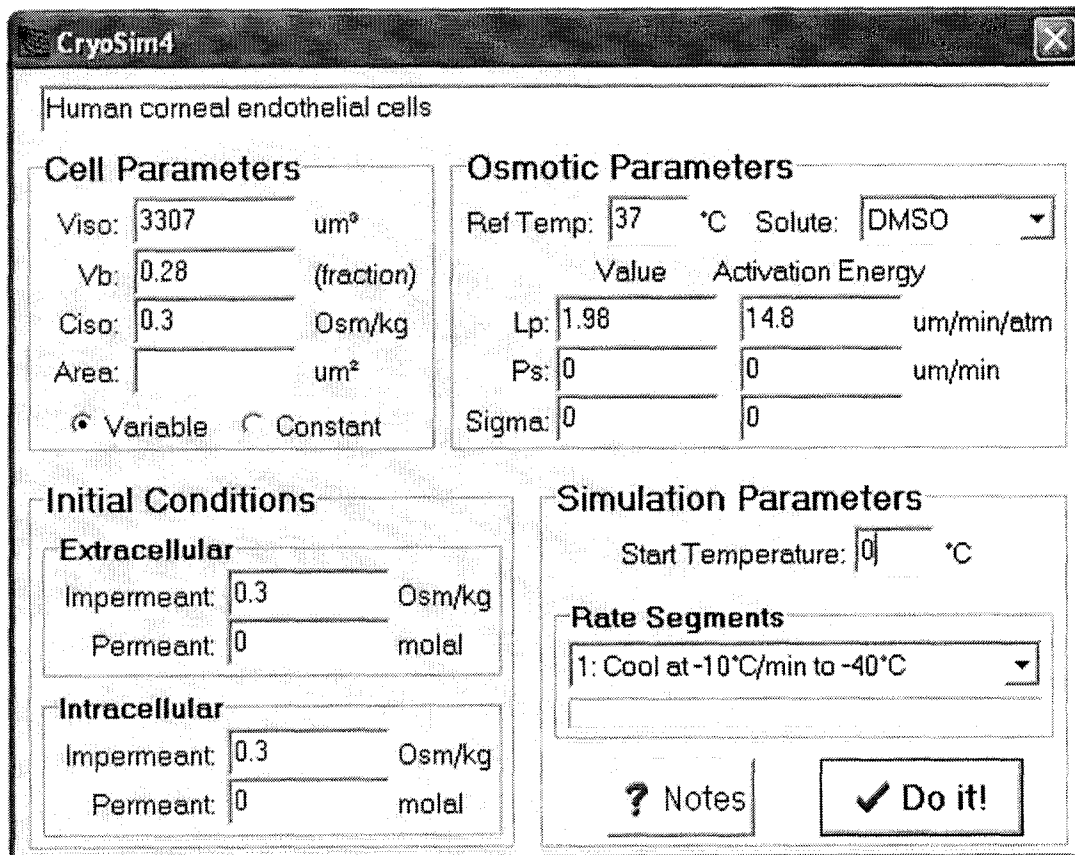


Fig. 1. Schematic of CryoSim4 program used to simulate cellular responses.

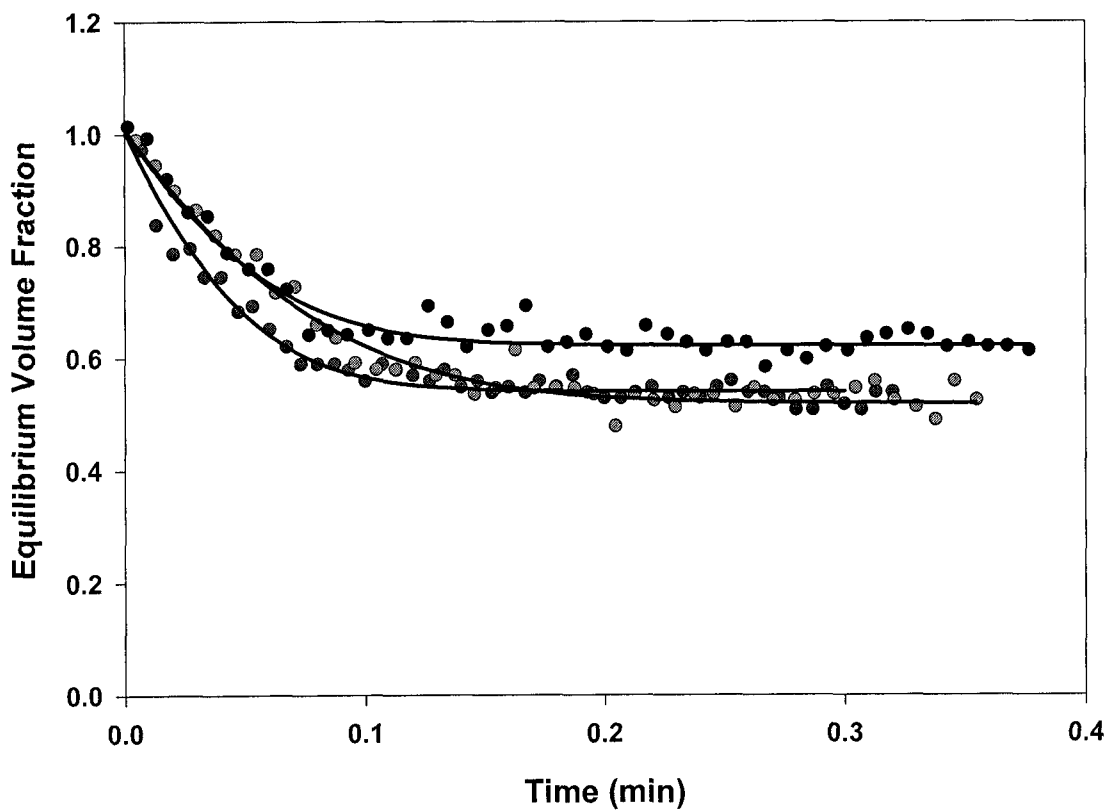


Fig. 2. A representative plot of volume versus time for human corneal endothelial, keratocyte, and epithelial cells exposed to 862mosm/kg PBS at 37°C. The solid lines represent the best fit for  $L_p$  and  $V_b$  using the membrane mass transport model developed by Jacobs and Stewart (17).

TABLE 1A.  $L_p$  ( $\mu\text{m}/\text{atm}/\text{min}$ ) for human corneal endothelial cells (mean  $\pm$  SD).

<b>A</b>	150 (mosm/kg)	210 (mosm/kg)	600 (mosm/kg)	900 (mosm/kg)	1200 (mosm/kg)	1500 (mosm/kg)
4°C	0.07 $\pm$ 0.01	0.07 $\pm$ 0.07	0.12 $\pm$ 0.02	0.11 $\pm$ 0.01	0.10 $\pm$ 0.02	0.10 $\pm$ 0.01
13°C	0.13 $\pm$ 0.02	0.19 $\pm$ 0.11	0.25 $\pm$ 0.02	0.28 $\pm$ 0.03	0.27 $\pm$ 0.03	0.26 $\pm$ 0.02
22°C	0.46 $\pm$ 0.13	0.64 $\pm$ 0.16	0.62 $\pm$ 0.05	0.61 $\pm$ 0.06	0.60 $\pm$ 0.08	0.63 $\pm$ 0.10
37°C	1.10 $\pm$ 0.14	1.44 $\pm$ 0.36	1.80 $\pm$ 0.30	2.02 $\pm$ 0.42	1.95 $\pm$ 0.32	1.83 $\pm$ 0.21

TABLE 1B.  $L_p$  ( $\mu\text{m}/\text{atm}/\text{min}$ ) for human corneal keratocytes (mean  $\pm$  SD).

<b>B</b>	150 (mosm/kg)	210 (mosm/kg)	600 (mosm/kg)	900 (mosm/kg)	1200 (mosm/kg)	1500 (mosm/kg)
4°C	0.16 $\pm$ 0.11	0.15 $\pm$ 0.10	0.13 $\pm$ 0.01	0.13 $\pm$ 0.01	0.12 $\pm$ 0.01	0.14 $\pm$ 0.02
13°C	0.22 $\pm$ 0.10	0.17 $\pm$ 0.08	0.36 $\pm$ 0.10	0.34 $\pm$ 0.06	0.30 $\pm$ 0.04	0.31 $\pm$ 0.05
22°C	0.38 $\pm$ 0.08	0.45 $\pm$ 0.07	0.61 $\pm$ 0.05	0.63 $\pm$ 0.05	0.62 $\pm$ 0.04	0.63 $\pm$ 0.03
37°C	0.72 $\pm$ 0.18	0.98 $\pm$ 0.23	1.36 $\pm$ 0.40	1.44 $\pm$ 0.33	1.30 $\pm$ 0.19	1.34 $\pm$ 0.25

TABLE 1C.  $L_p$  values ( $\mu\text{m}/\text{atm}/\text{min}$ ) for human corneal epithelial cells (mean  $\pm$  SD).

<b>C</b>	150 (mosm/kg)	210 (mosm/kg)	600 (mosm/kg)	900 (mosm/kg)	1200 (mosm/kg)	1500 (mosm/kg)
4°C	0.12 $\pm$ 0.03	0.12 $\pm$ 0.05	0.10 $\pm$ 0.02	0.08 $\pm$ 0.01	0.08 $\pm$ 0.02	0.08 $\pm$ 0.01
13°C	0.21 $\pm$ 0.02	0.21 $\pm$ 0.08	0.17 $\pm$ 0.01	0.16 $\pm$ 0.02	0.18 $\pm$ 0.04	0.17 $\pm$ 0.02
22°C	0.50 $\pm$ 0.07	0.34 $\pm$ 0.06	0.39 $\pm$ 0.05	0.36 $\pm$ 0.03	0.36 $\pm$ 0.05	0.37 $\pm$ 0.07
37°C	1.44 $\pm$ 0.21	1.37 $\pm$ 0.19	1.20 $\pm$ 0.15	1.27 $\pm$ 0.12	1.23 $\pm$ 0.13	1.13 $\pm$ 0.17

TABLE 1D. Pooled  $L_p$  values ( $\mu\text{m}/\text{atm}/\text{min}$ ) for human corneal cells in hypertonic solutions (600 – 1500 mosm/kg).

	Endothelial Cells	Keratocytes	Epithelial Cells
4°C	0.11 $\pm$ 0.02	0.13 $\pm$ 0.01	0.08 $\pm$ 0.01
13°C	0.26 $\pm$ 0.02	0.33 $\pm$ 0.07	0.17 $\pm$ 0.02
22°C	0.62 $\pm$ 0.07	0.62 $\pm$ 0.04	0.37 $\pm$ 0.05
37°C	1.91 $\pm$ 0.32	1.36 $\pm$ 0.30	1.21 $\pm$ 0.14

TABLE 2A.  $V_b$  for human corneal endothelial cells (mean  $\pm$  SD).

<b>A</b>	150 (mosm/kg)	210 (mosm/kg)	600 (mosm/kg)	900 (mosm/kg)	1200 (mosm/kg)	1500 (mosm/kg)
4°C	0.81 $\pm$ 0.04	0.73 $\pm$ 0.37	0.31 $\pm$ 0.01	0.34 $\pm$ 0.02	0.34 $\pm$ 0.03	0.33 $\pm$ 0.03
13°C	0.67 $\pm$ 0.03	0.51 $\pm$ 0.22	0.30 $\pm$ 0.02	0.30 $\pm$ 0.03	0.29 $\pm$ 0.02	0.30 $\pm$ 0.02
22°C	0.57 $\pm$ 0.08	0.38 $\pm$ 0.07	0.31 $\pm$ 0.04	0.32 $\pm$ 0.04	0.31 $\pm$ 0.03	0.31 $\pm$ 0.03
37°C	0.69 $\pm$ 0.02	0.53 $\pm$ 0.06	0.26 $\pm$ 0.03	0.28 $\pm$ 0.03	0.26 $\pm$ 0.02	0.26 $\pm$ 0.01

TABLE 2B.  $V_b$  for human corneal keratocytes (mean  $\pm$  SD).

<b>B</b>	150 (mosm/kg)	210 (mosm/kg)	600 (mosm/kg)	900 (mosm/kg)	1200 (mosm/kg)	1500 (mosm/kg)
4°C	0.55 $\pm$ 0.13	0.23 $\pm$ 0.22	0.30 $\pm$ 0.04	0.36 $\pm$ 0.05	0.34 $\pm$ 0.03	0.32 $\pm$ 0.03
13°C	0.45 $\pm$ 0.09	0.48 $\pm$ 0.14	0.24 $\pm$ 0.08	0.24 $\pm$ 0.05	0.26 $\pm$ 0.02	0.26 $\pm$ 0.03
22°C	0.53 $\pm$ 0.02	0.20 $\pm$ 0.05	0.23 $\pm$ 0.03	0.23 $\pm$ 0.05	0.24 $\pm$ 0.02	0.25 $\pm$ 0.02
37°C	0.62 $\pm$ 0.03	0.41 $\pm$ 0.04	0.26 $\pm$ 0.10	0.29 $\pm$ 0.10	0.29 $\pm$ 0.05	0.27 $\pm$ 0.04

TABLE 2C.  $V_b$  for human corneal epithelial cells (mean  $\pm$  SD).

<b>C</b>	150 (mosm/kg)	210 (mosm/kg)	600 (mosm/kg)	900 (mosm/kg)	1200 (mosm/kg)	1500 (mosm/kg)
4°C	0.48 $\pm$ 0.19	0.63 $\pm$ 0.20	0.42 $\pm$ 0.05	0.42 $\pm$ 0.04	0.42 $\pm$ 0.03	0.40 $\pm$ 0.03
13°C	0.43 $\pm$ 0.04	0.58 $\pm$ 0.05	0.38 $\pm$ 0.01	0.37 $\pm$ 0.01	0.38 $\pm$ 0.02	0.35 $\pm$ 0.01
22°C	0.38 $\pm$ 0.05	0.52 $\pm$ 0.04	0.42 $\pm$ 0.02	0.43 $\pm$ 0.02	0.44 $\pm$ 0.03	0.43 $\pm$ 0.06
37°C	0.52 $\pm$ 0.02	0.62 $\pm$ 0.03	0.43 $\pm$ 0.04	0.44 $\pm$ 0.02	0.42 $\pm$ 0.01	0.42 $\pm$ 0.02

TABLE 2D. Pooled  $V_b$  for human corneal cells in hypertonic solutions (600 – 1500 mosm/kg).

	Osmotically Inactive Fraction
Endothelial Cells	0.28 $\pm$ 0.02
Keratocytes	0.27 $\pm$ 0.05
Epithelial Cells	0.41 $\pm$ 0.03

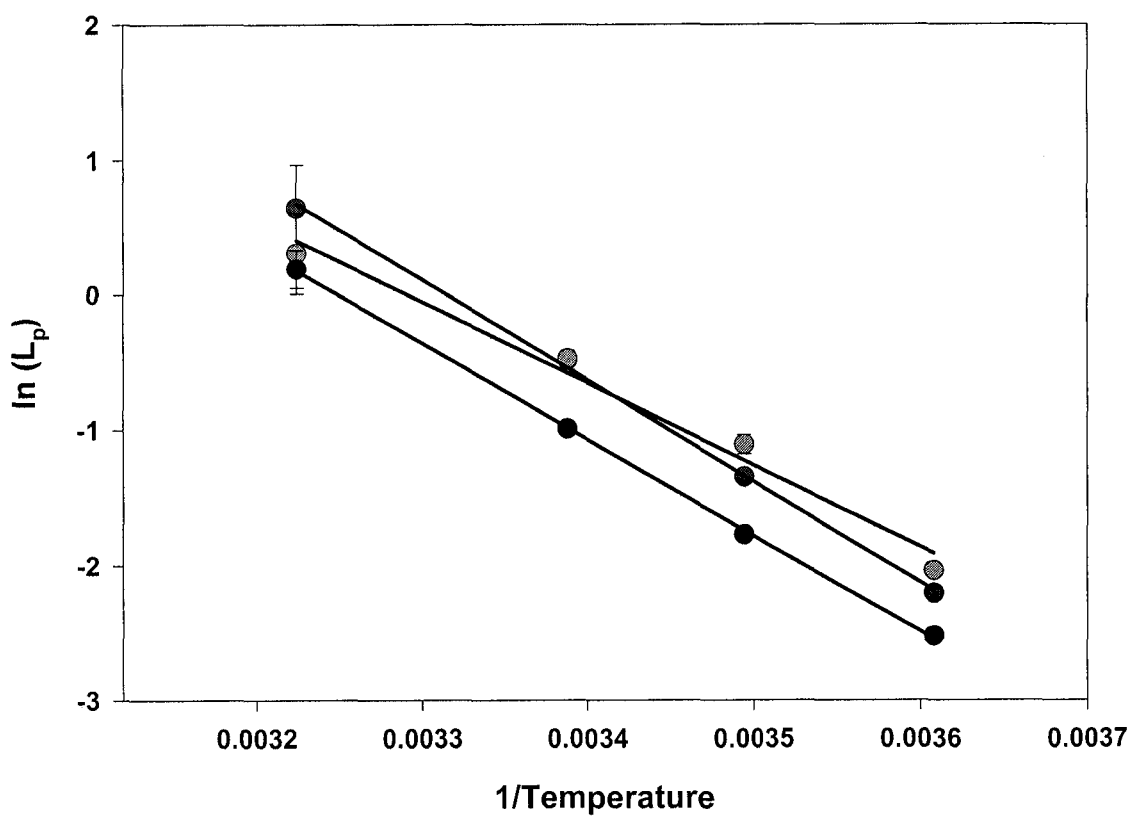


Fig. 3. Arrhenius plot of the natural logarithm of  $L_p$  of human corneal endothelial, keratocyte, and epithelial cells as a function of the reciprocal of the absolute temperature. The solid lines represent the linear regression of the data for calculation of activation energy using the Arrhenius equation.

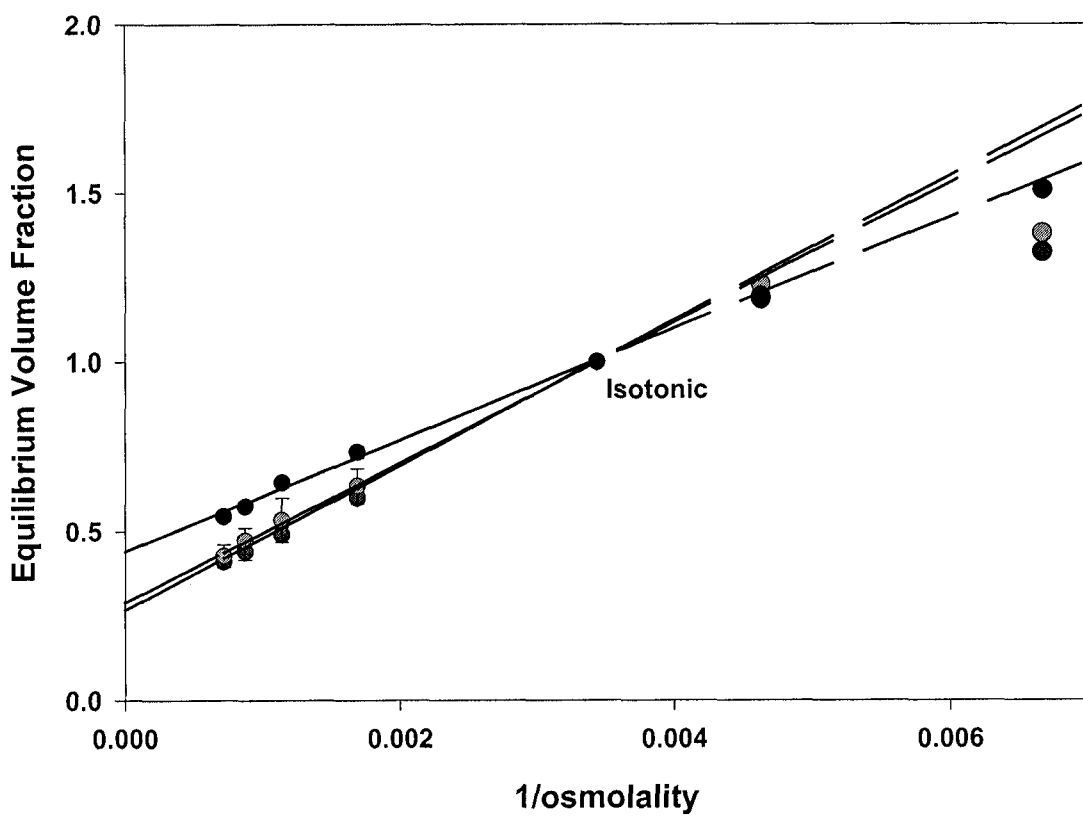


Fig. 4. Boyle van't Hoff plot of human corneal endothelial, keratocyte, and epithelial cells. The solid lines represent the linear regression fit to the equilibrium volume of the cells in hypertonic solutions and the dashed lines represent this fit extrapolated to hypotonic conditions. The fitted lines were not constrained to pass through the isotonic point.

TABLE 3. Summary of osmotic parameters for human corneal cells.

	$V_{iso}$ ( $\mu\text{m}^3$ )	Diameter ( $\mu\text{m}$ )	$V_b$	$L_p$ at 37°C ( $\mu\text{m}/\text{atm}/\text{min}$ )	$E_a$ (kcal/mol)
Endothelium	3307±292 <sup>a</sup>	18.5±0.50	0.28±0.02	1.98±0.32 <sup>b</sup>	14.8
Keratocytes	3186±297	18.3±0.60	0.27±0.05	1.50±0.30	12.0
Epithelium	4134±169	19.9±0.30	0.41±0.03	1.19±0.14	14.1

a: mean ± SD

b:  $L_p$  values calculated from Eq. 3.

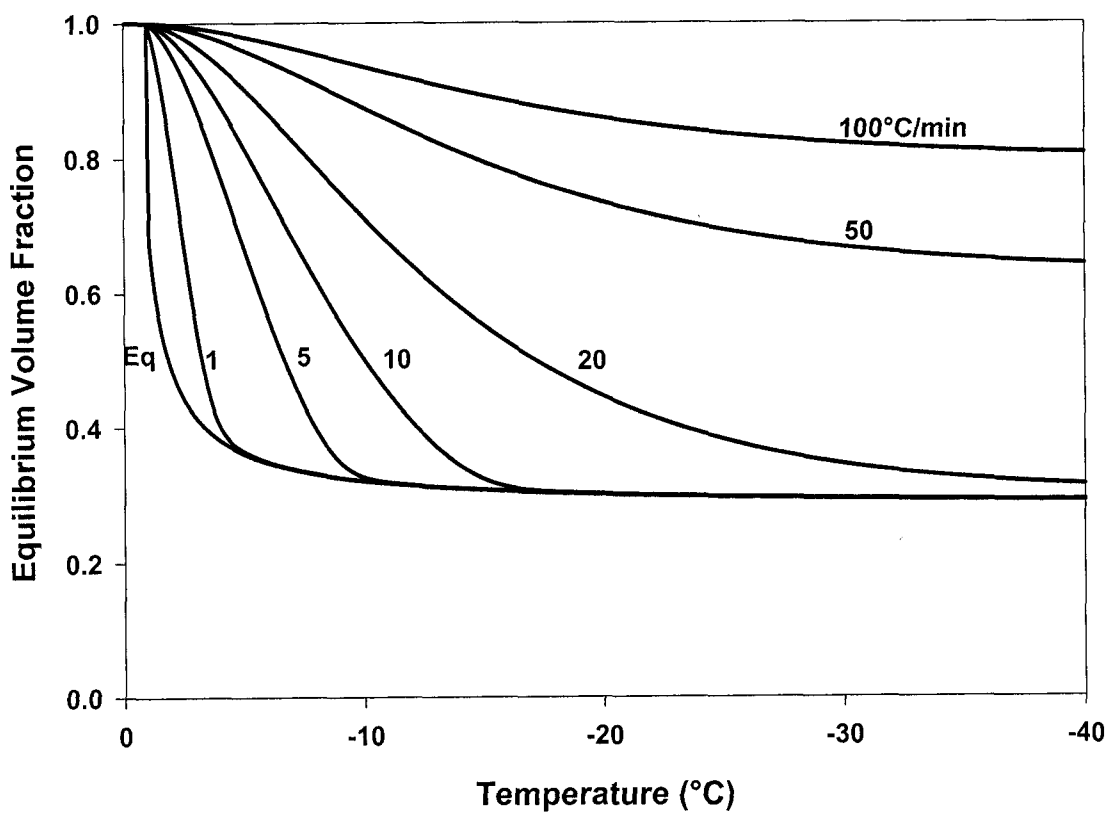


Fig. 5. Simulated volume response of human corneal endothelial cells during freezing at different rates using the measured osmotic parameters. The curve labelled Eq shows the endothelial cell volume in osmotic equilibrium with the extracellular solution during cooling.

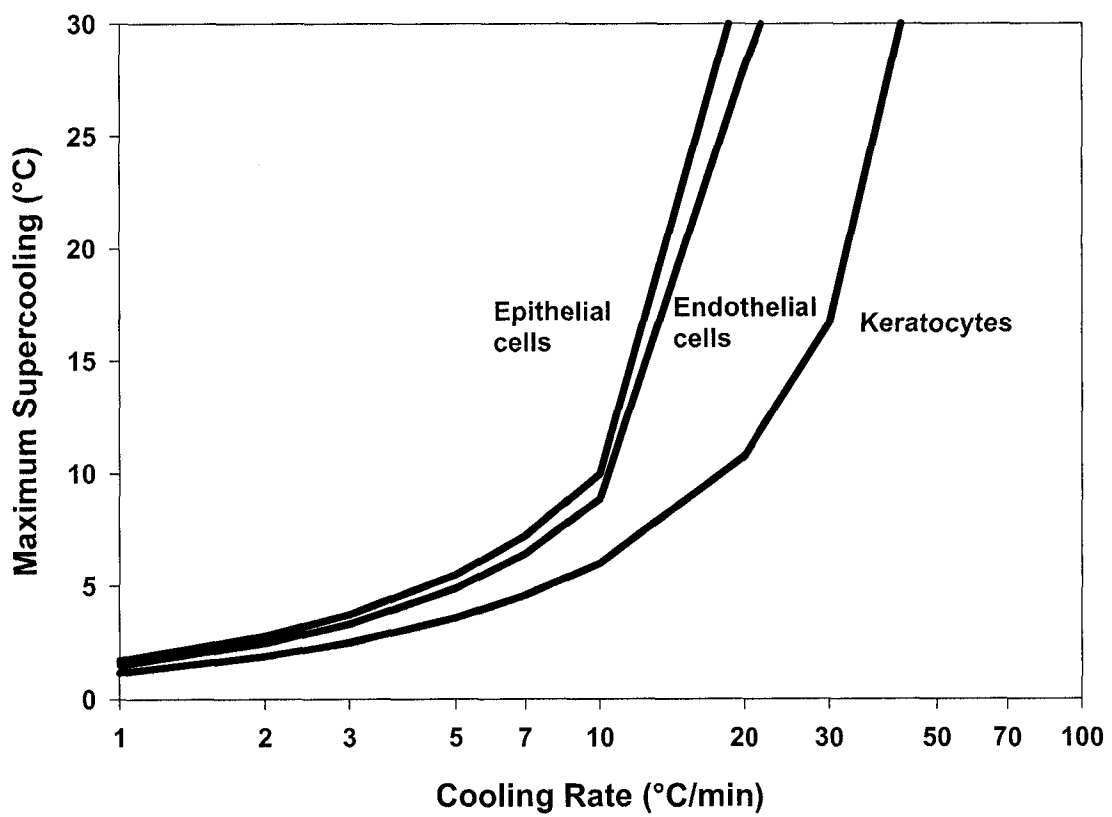


Fig. 6. Maximum supercooling calculated for human corneal endothelial, keratocyte, and epithelial cells at different cooling rates.

## **Chapter 4: Determination of Cryoprotectant Permeability for Cells from a Bioengineered Human Corneal Equivalent and Applications for Cryopreservation**

### **4.1 Introduction**

Successful cryopreservation of cells and tissues depends on the presence of cryoprotective agents (CPA) during cooling and warming, and has been recognized since the discovery and characterization of the protective nature of glycerol by Polge et al. (19). Permeating cryoprotectants, such as DMSO and PG, protect by colligative actions by decreasing the extra- and intracellular solute concentrations and decreasing the amount of extracellular ice formed. However, the presence of cryoprotectants can also be the source of damage, from osmotic stresses on the cells due to solute and water flux during addition and removal and cooling and warming, or direct toxicity.

The addition of a permeating CPA causes cells to shrink as water exits in response to the increased extracellular osmotic pressure, and then re-swell as the CPA (as well as water) permeates the cell membrane returning the cell to isotonic volume (8). When cells are returned to an isotonic solution to remove the permeating CPA, cells typically swell to greater than isotonic volume as water moves into the cell down the concentration gradient; the cell then returns to isotonic volume as CPA and water exit the cell.

As cells are cooled below the freezing point of the suspending solution, ice initially forms extracellularly, concentrating the extracellular solution, causing the cells to shrink as water leaves the cells in response to the increased osmotic pressure. At low cooling rates, cells become increasingly dehydrated which

concentrates the intracellular electrolytes and intracellular CPA, and at high cooling rates the cytoplasm becomes supercooled, increasing the probability of intracellular ice formation. All of these occurrences can damage cells during cooling, and optimal cooling conditions exist that minimize exposure to damaging solute concentrations and the formation of intracellular ice.

This study uses primary human corneal endothelial, keratocyte, and epithelial cell lines, which are the constituent cells of the biosynthetic corneal construct (5) we are interested in cryopreserving. The objective of this study is to determine membrane permeability ( $P_s$ ) of DMSO and PG, membrane hydraulic conductivity ( $L_p$ ) in the presence of these cryoprotectants, and the Arrhenius activation energies for  $L_p$  and  $P_s$  for human corneal cells and to use these values to model addition and removal of cryoprotectants and low temperature responses of the biosynthetic human corneal construct to optimize cooling conditions.

## **4.2 Materials and Methods**

### *Human Corneal Cell Culture*

Human corneal endothelial, keratocyte, and epithelial cells (a gift from Dr. May Griffiths, University of Ottawa) were incubated at 37°C in 5% carbon dioxide in Medium 199 with 10% v/v fetal bovine serum (GIBCO BRL, Burlington, Canada), and supplemented with 1% v/v insulin transferrin selenium (Sigma, Mississauga, Canada). Cells were grown in 75cm<sup>2</sup> Falcon tissue culture flasks (VWR, Edmonton, Canada) and harvested by exposure to 0.05% trypsin-EDTA (GIBCO BRL) solution at 37°C for 2-3 minutes. The corneal cells were re-

suspended in supplemented M199 to obtain cell suspensions for use in permeability measurements.

### *Experimental Solutions*

Experimental solutions were 0.5M, 1M, and 2M DMSO and PG (Sigma), with calculated osmolalities of 631,1227, and 2589 mosm/kg for the DMSO solutions and 529, 1087, and 2653 mosm/kg for the PG solutions, respectively. Solution osmolalities were calculated using Eq. 1, where values for freezing point depression were obtained from the phase diagrams for DMSO (20) and PG (23).

$$\Delta fp = K * osm \quad (1)$$

Where,  $\Delta fp$  is the freezing point depression in °C, K is a constant, representing the depression of the freezing point of water by 1osmol of solute (-1.86°C/osmol), and osm is the osmolality of the solution.

### *Permeability Measurements of Human Corneal Cells*

Electronic particle counters have been used extensively to determine cryoprotectant permeabilities of cells in suspension (2,9,25,26). After rapid addition and mixing of cells with the test solution, the cells pass through a 100-120 $\mu$ m aperture that displaces a volume of the conducting fluid resulting in a voltage pulse proportional to the cell volume. A Coulter counter (model ZB1; Coulter Inc, Hialeah, FL) was connected to a personal computer via a pulse-height analyzer (The Great Canadian Computer Company, Spruce Grove, Canada), with the accompanying cell size analyzer software, which recorded the time and relative volume of each cell passing through the aperture (13). Experimental solutions were maintained within 0.1°C of the test temperatures (4,

13, 22 and 37°C) with a custom-made insulated jacket connected to a circulating water bath. Spherical latex beads (15µm diameter; Coulter Inc.) were used as calibrators to convert relative volumes to actual volumes. In-house software allowed kinetic analysis of mean cell volume as a function of time. Triplicate runs with each experimental solution were repeated with three different passages of cultured human corneal endothelial, keratocyte, and epithelial cells.

#### *Determination of Permeability Parameters*

The hydraulic conductivity, solute permeability, and reflection coefficient were calculated using differential equations developed by Johnson and Wilson (6), which describe volume changes and solute movement across a membrane as a function of time.

$$\frac{dV}{dt} = L_p A R T \left[ (\pi_n^i - \pi_n^e) + \sigma (\pi_s^i - \pi_s^e) \right] \quad (2)$$

$$\frac{dS}{dt} = P_s (\Delta C_s) + (1 - \sigma) \frac{\bar{c}_s}{2} * \frac{dV}{dt} \quad (3)$$

Where  $P_s$  is the solute permeability,  $\Delta C_s$  is the difference between extracellular and intracellular solute concentration,  $\sigma$  (sigma) is the reflection coefficient,  $L_p$  is the membrane hydraulic conductivity,  $A$  is the cell surface area,  $R$  is the universal gas constant,  $T$  is the absolute temperature,  $\pi^i$  is the intracellular osmolality, and  $\pi^e$  is the extracellular osmolality and the subscript  $n$  refers to the nonpermeating solute and the subscript  $s$  refers to the permeating solute. Intracellular osmolality was determined from the Boyle van't Hoff relationship (Eq. 4):

$$\frac{V}{V_{\text{iso}}} = \frac{\pi_o}{\pi} (1 - V_b) + V_b \quad (4)$$

Where  $V$  is the equilibrium cell volume,  $\pi$  is the experimental osmolality,  $\pi_o$  is the isotonic osmolality,  $V_{\text{iso}}$  is the isotonic cell volume and  $V_b$  is the osmotically inactive fraction of the isotonic cell volume, which was previously determined (chapter 1).  $L_p$ ,  $P_s$ , and  $\sigma$  were determined by fitting the experimental data to Eq. 2 and 3 using the least-square error method.

The Arrhenius activation energy (Eq. 5) was used to describe the temperature dependence of  $P_s$  and  $L_p$ . The activation energy was calculated from the slope of an Arrhenius plot of the natural logarithm of  $P_s$  and  $L_p$  as a function of inverse absolute temperature.

$$P_s \text{ or } L_p = K * \exp\left(\frac{-E_a}{RT}\right) \quad (5)$$

Where  $P_s$  is the solute permeability,  $L_p$  is the membrane hydraulic conductivity,  $K$  is a fitting constant,  $R$  is the universal gas constant,  $T$  is temperature (K) for  $P_s$  or  $L_p$ , and  $E_a$  is the activation energy.

#### *Statistical Analysis*

A one way ANOVA was used with a level of significance set at 5%.

#### *Simulation of Low Temperature Responses*

Simulations were performed by calculating cellular osmotic responses to the concentration of solutes in the residual liquid in the presence of ice at low temperatures. Phase diagrams were used to calculate concentrations in the liquid phase for NaCl-H<sub>2</sub>O (23), KCl-H<sub>2</sub>O (23) (for the intracellular compartment), DMSO-H<sub>2</sub>O (20) and PG-H<sub>2</sub>O (23). Coupled equations (Eqs. 2 and 3) describing

the water and solute transport across the plasma membrane were used to calculate osmotic cellular responses to the changing extracellular conditions. The experimentally-determined Arrhenius activation energies were used to describe temperature dependencies of hydraulic conductivity and solute permeabilities, and the temperature as a function of time was calculated from the cooling rate.

### **4.3 Results**

#### *Permeability Parameters*

Mean cell volumes after exposure to 1M DMSO at 22°C are shown in Fig. 1 for human corneal endothelial, keratocyte, and epithelial cells. Changes in mean volume as a function of time were used to calculate the  $L_p$ ,  $P_s$ , and  $\sigma$ , and the resulting values for each cell type for all experimental solutions and temperatures tested are summarized in Tables 1, 2, and 3, respectively.

#### *Arrhenius Activation Energies for $L_p$ and $P_s$*

Fig. 2 shows the temperature dependence for  $L_p$  at 4, 13, 22, and 37°C of the human corneal cells calculated from the Arrhenius relationship, and resulted in activation energies for  $L_p$  in the presence of DMSO of 16.0, 13.9, and 15.0 kcal/mol and in the presence of PG of 14.5, 15.1, and 14.1 kcal/mol for human corneal endothelial, keratocyte, and epithelial cells, respectively.

The Arrhenius activation energy for  $P_s$ , shown in Fig. 3, at 4, 13, 22, and 37°C of the human corneal endothelial, keratocyte, and, epithelial cells in the presence of DMSO was 15.9, 15.0, and 17.3 kcal/mol and in the presence of PG was 18.1, 15.3, and 18.1 kcal/mol, respectively.

The activation energies indicate that membrane permeability to water and cryoprotectant will change considerably with temperature and cryoprotectant permeability is more sensitive to changes in temperature than membrane permeability to water.

#### *Simulations of Low Temperature Responses*

Table 4A (values from chapter 3), 4B and 4C summarize the permeability parameters obtained in this study, which were used to model the responses of human corneal cells. The  $L_p$  and  $P_s$  values were calculated using the Arrhenius equation (Figs. 2 and 3).

Simulated volume responses of addition and removal of DMSO and PG for human corneal endothelial, keratocyte, and epithelial cells are shown in Figs. 4 and 5 respectively. Fig. 6 shows the simulated volume response of the removal of 2M DMSO and 2M PG using the sucrose dilution technique.

Simulations of the volume response, amount of supercooling, intracellular electrolyte concentration, and intracellular cryoprotectant concentration as human corneal endothelial, keratocyte, and epithelial cells are cooled down to  $-40^{\circ}\text{C}$  at various cooling rates in the presence of 1M and 4M DMSO are shown in Figs. 7, 8, and 9, and cooled in the presence of 1M and 4M PG are shown in Figs. 10, 11, and 12, respectively. From these simulations, the maximum values for supercooling, intracellular electrolyte, and intracellular cryoprotectant concentration were determined down to  $-40^{\circ}\text{C}$  at each cooling rate, plotted as a function of the cooling rate and are shown in Fig. 13 and 14 in the presence of DMSO and PG, respectively.

#### 4.4 Discussion

The membrane hydraulic conductivity and cryoprotectant permeability values reported in this study were temperature dependent, as expected, and the results were pooled for each experimental temperature. In regards to cryoprotectant concentration dependence, some, but not all of the conditions showed statistical differences ( $p < 0.05$ ), however all values for  $L_p$  fell within 1 standard deviation of the others and some of the  $P_s$  values also fell within 1 standard deviation of the others, so these values were considered to have no concentration dependence and were pooled for cryoprotectant type as shown in Tables 1D and 2D. Another factor to consider regarding the  $P_s$  values is that, in all cases, it was the  $P_s$  in the presence of 2M cryoprotectant that showed a statistical difference, which may be a result of a limitation of the osmofit program, used to calculate the permeability parameters (i.e. the Johnson and Wilson model). The program assumes linearity, which is not entirely correct because of the non-equivalence of molality and osmolality, which may be significant at the higher concentrations of cryoprotectant.

CPAs have been shown to alter the  $L_p$  of cell membranes by decreasing the  $L_p$  in the presence of increased solute concentration (14) or in other instances increasing the apparent  $L_p$  of a cell (15) however this varies considerably with cell and solute type (15). Comparing the  $L_p$  for human corneal cells in the presence and absence of a permeating solute (results in chapter 3) shows that the  $L_p$  values remain the same under both conditions for human corneal endothelial

cells and keratocytes, although for human corneal epithelial cells the  $L_p$  is higher in the presence of DMSO and PG.

Values for  $P_s$  at 22°C in the presence of DMSO and PG reported in this study for human corneal endothelial, keratocyte, and epithelial cells are similar to values found for a variety of cell types (14) (7.9 – 17  $\mu\text{m}/\text{min}$  for DMSO, 23  $\mu\text{m}/\text{min}$  for PG), including hamster islets (2), porcine aortic smooth muscle and endothelial cells (27), human granulocytes (22), and human sperm (4). The  $P_s$  values also show that human corneal cells are more permeable to PG than DMSO, which is generally accepted for other cell types (15).

The Arrhenius activation energy for  $L_p$  in the presence of DMSO or PG of human corneal endothelial (16.0, 14.5 kcal/mol), keratocyte (13.9, 15.1 kcal/mol), and epithelial cells (15.0, 14.1 kcal/mol) reported in this study are typical for what has been reported for other cells types, such as human platelets (1,25) and rat embryos (18).  $E_a$  for  $L_p$  in the presence of a CPA was similar to the  $E_a$  for  $L_p$  in the absence of a CPA (see chapter 3).

The Arrhenius activation energy for  $P_s$  in the presence of DMSO and PG of human corneal endothelial (15.9, 18.1 kcal/mol), keratocyte (15.0, 15.3 kcal/mol), and epithelial cells (17.3, 18.1 kcal/mol) reported in this study are typical for values reported for other cell types (15), such as rat liver tissue (21) and rat embryos (18). The  $E_a$  for  $L_p$  and  $P_s$  indicates that osmotically driven transport of cryoprotectants is more sensitive to decreasing temperatures than transport of water and the importance of cryoprotectant transport decreases with lower temperatures, as previously noted by Mazur (12).

The reflection coefficient was poorly constrained by the experimental data in this study as  $L_p$  and  $P_s$  primarily determine the best fit to the experimental volume responses. Others have also recognized this when measuring permeability parameters of platelets (25), islets (2), and human sperm (4). Some values for  $\sigma$  reported in this study were also found to have statistical differences ( $p < 0.05$ ), but with overlapping errors for most of the reported values, therefore  $\sigma$  was considered to have no concentration or temperature dependence and the values were pooled for each type of cryoprotectant as shown in Table 3D. Arnaud and Pegg has also stated that there is no reason to think that  $\sigma$  would be temperature or concentration dependent (1) and there are no reports of a concentration or temperature dependence found for  $\sigma$ . The values for  $\sigma$  reported in this study indicate that there is a physical interaction between the water and solute flux.

Pegg et al. have previously reported the osmotic tolerance limits for rabbit corneal endothelium as 50-140% isotonic volume (17). These are the limits that will be used to interpret the simulated responses of human corneal endothelial, keratocyte, and epithelial cells, as there are no reported tolerance limits for corneal keratocytes and epithelial cells.

Addition and dilution of permeating cryoprotectants cause cells to undergo potentially damaging volume excursions by shrinking below tolerated osmotic limits during addition or by swelling above tolerated osmotic limits during dilution. Figs. 4 and 5 show that addition of 1M DMSO, 1M PG, 2M DMSO, and 2M PG, and the dilution of 1M DMSO and 1M PG are tolerated in a single step procedure

by human corneal endothelial, keratocyte, and epithelial cells. However, a single step dilution of 2M DMSO and 2M PG as shown in Figs. 4 and 5 results in volume excursions greater than the tolerance limits ( $140\% V_{iso}$ ) for all human corneal cells. Therefore it is necessary to remove the cryoprotectant in a step-wise procedure or use the sucrose dilution technique that is depicted in Fig. 6. The sucrose dilution technique uses the addition of a non-permeating solute (i.e. sucrose) to the diluting solution to control the amount of water that moves into the cell in response to the high internal osmotic pressure caused by the intracellular CPA, thus controlling the extent to which the cell swells. The cell then starts to shrink as water and CPA leave the cell in response to the increased external osmotic pressure, and shrinks below isotonic volume, still within tolerable limits, because of the increased osmolality of the external non-permeating sucrose. The cells can then be returned to isotonic volume without the risk of damaging volume excursions. These simulations will be necessary to develop appropriate addition and removal strategies for the bioengineered human corneal equivalent once optimal cryoprotectant type and concentration is determined.

Simulations of human corneal cells cooled at various cooling rates in the presence of 1M or 4M DMSO and PG, shown in Figs 7-12, give extensive information about the responses of cells as they are cooled, such as volume changes, supercooling, intracellular electrolyte concentration, and intracellular cryoprotectant concentration and can be used to develop a cryopreservation procedure. I will discuss each of these events in regards to the development of a cryopreservation procedure individually. Ultimately all of these factors need to be

considered as a whole to propose an optimal cooling rate, choice and concentration of cryoprotectant for cryopreservation of the bioengineered human corneal equivalent, and is shown in Fig. 13 and 14 which is discussed later.

When cell volume as a function of temperature is plotted (Figs. 7-12A), it clearly demonstrates the loss of water by cells in response to extracellular ice formation and increasing extracellular solute concentration as temperature is decreased. Human corneal endothelial cells and keratocytes cooled in the presence of low concentrations of DMSO or PG (1M) are more susceptible to low cooling rates as the cells shrink below tolerable limits. Therefore avoiding damaging volume changes would require a cooling rate of 10°C/min for the endothelial cells and 15°C/min for the keratocytes. The human corneal epithelial cells remain within tolerable volume limits at all cooling rates simulated and are less susceptible to damaging volume excursions during cooling. Increasing the concentration of cryoprotectant during cooling results in less ice formation and lower concentrations of solutes in the unfrozen extracellular solution, therefore the cells do not lose as much water and do not shrink to damaging volumes. It has long been that this is the mechanism by which cryoprotectants offer protection. 2M DMSO and PG is the lowest concentration that controls shrinking of the human corneal cells within their tolerable limits (simulations not shown).

Supercooling is defined as the difference between the freezing point of the internal solution and the actual temperature of the unfrozen intracellular solution. As the amount of supercooling increases so does the probability of intracellular ice formation, which is lethal to cells. It is thought that intracellular ice will likely

form at  $>10^{\circ}\text{C}$  of supercooling (10). Figs 7-12B shows that increasing cryoprotectant concentration decreases the amount of supercooling, thus protecting the human corneal cells from intracellular ice formation.

The simulations in Figs. 7-12C show that as cells are cooled in the presence of lower concentrations (1M) of permeating CPAs, the intracellular electrolytes concentrate significantly at the lower cooling rates and will be a significant source of damage as stated by Mazur's two-factor hypothesis of freezing injury (9). However, increasing the CPA concentration is a very effective method to protect against the damaging effects of increased intracellular electrolyte concentration as shown in Figs. 7-12C, as there is virtually no increase in intracellular electrolyte concentration at all cooling rates simulated.

Figs. 7-12D show the increase in intracellular cryoprotectant concentration as cells are cooled at various cooling rates. This is an important consideration when deciding at what temperature slow cooling can be stopped before rapid cooling to the final storage temperature. A protective CPA concentration can be achieved at higher subzero temperatures and therefore rapid cooling to the final storage temperatures from higher subzero temperatures would avoid damaging exposure to increasing solute and cryoprotectant concentrations. The simulations show that as cells are cooled slowly, the intracellular cryoprotectant will reach vitrifiable concentrations, and upon subsequent rapid cooling intracellular vitrification will occur, thus avoiding solute effects and intracellular ice formation damage. Intracellular vitrification has also been proposed for cryopreservation of

embryos (3,18) and oocytes (7). This concept will be further developed in chapter 5.

Simulations allow insight into the protective mechanisms of CPA, such as controlling the volume excursions of cells within tolerable limits as they are cooled, decreasing the amount of supercooling and intracellular electrolyte concentrations, which helps to avoid conditions that will result in damage from increasing solute concentrations or formation of intracellular ice. Considering these factors as a whole (Figs. 13 and 14) can aid in developing a cryopreservation protocol by determining optimal cooling rates and CPA type and concentration, which can be tested experimentally.

Considering a maximum supercooling of 10°C in Figs. 13A, C, E and Figs. 14A, C, E of the low temperature responses of human corneal cells cooled in the presence of 1M DMSO and 1M PG, the optimal cooling rate is 3°C/min for human corneal endothelial cells, 7°C/min for human corneal keratocytes and epithelial cells in the presence of 1M DMSO and 7°C/min for endothelial cells, 5°C/min for keratocytes, and 10°C/min for epithelial cells in the presence of 1M PG. Under these cooling conditions the maximum intracellular electrolyte concentration reaches appreciable levels that are likely damaging, and to control the magnitude of the concentration of these solutes would require a higher cooling rate that would result in significant supercooling and intracellular ice formation. The intracellular DMSO and PG concentrations are vitrifiable if cooled to -40°C at the identified optimal cooling rates above, if cells are subsequently cooled rapidly below their glass transformation temperature, and this would have

to be considered during warming because warming would have to be rapid enough to avoid lethal devitrification. Figs. 7-12A also shows that cooling corneal cells at the rates identified from the supercooling graphs, results in the endothelial cells and keratocytes shrinking below their tolerable volumes. From these simulations it can be concluded that 1M DMSO and 1M PG is of insufficient concentration to protect human corneal cells during cryopreservation. The simulations also clearly show the difference in low temperature responses of the constituent cells of the bioengineered human corneal construct, which is a major barrier to the successful cryopreservation of tissues versus cells in suspension.

Figs. 13B, D, and F, and 14B, D, and F show the maximum amount of supercooling, intracellular electrolyte concentration and intracellular DMSO and PG concentration after cooling human corneal cells at various cooling rates in the presence of 4M CPA. The minimum volume excursions of the human corneal endothelial, keratocyte, and epithelial cells are within tolerable limits at all cooling rates simulated as discussed previously. The simulations also show that intracellular electrolyte concentration is kept at a minimum at all cooling rates tested and will not be a source of damage when high concentrations of cryoprotectant are used. The maximum cooling rate that results in  $<10^{\circ}\text{C}$  of supercooling during cooling are  $2^{\circ}\text{C}/\text{min}$  for endothelial and epithelial cells, and  $3^{\circ}\text{C}/\text{min}$  for keratocytes in 4M DMSO, and  $2^{\circ}\text{C}/\text{min}$  for endothelial cells and keratocytes and  $4^{\circ}\text{C}/\text{min}$  for epithelial cells in 4M PG, although from the simulations it appears that any cooling rate lower than these aforementioned maximums would be successful. Therefore, it appears that as CPA concentration

is increased, cooling rate is less important if the maximum supercooling is  $<10^{\circ}\text{C}$ , decreasing the probability of lethal intracellular ice formation. This less discriminatory effect of cooling rate virtually eliminates the differences in the low temperature responses of the constituent cells of the bioengineered human corneal equivalent and suggests that complex tissues require higher concentrations of CPA for successful cryopreservation. One factor to consider when using high concentrations of cryoprotectant is toxicity, which is directly proportional to exposure time. So, although the simulations show that any cooling rates  $\leq 2^{\circ}\text{C}/\text{min}$  could be used, a higher cooling rate will limit exposure and decrease toxicity of high concentrations of cryoprotectant.

The ability to simulate low temperature responses of cells is important to theoretically describe a cryopreservation protocol that can be verified experimentally. This approach is simpler than empirically developing cryopreservation procedures as it decreases the number of variables to be examined and establishes a theoretical basis for choice and concentration of cryoprotectant and cooling rate, which were derived from specific cell parameters measured for the tissue or cells of interest. Most tissues cannot be cryopreserved successfully (16), but the ability to simulate low temperature responses will enhance our ability to develop successful cryopreservation strategies for tissues, like the bioengineered human corneal construct.

#### **4.5 References**

1. Arnaud, F.G., and Pegg, D.E. Permeation of glycerol and propane-1,2-diol into human platelets. *Cryobiology*. **27**, 107-118 (1990).

2. Benson, C.T., Liu, C., Gao, D.Y., Critser, E.S., Benson, J.D., and Critser, J.K. Hydraulic conductivity ( $L_p$ ) and its activation energy ( $E_a$ ), Cryoprotectant agent permeability ( $P_s$ ) and its  $E_a$ , and reflection coefficients ( $\sigma$ ) for golden hamster individual pancreatic islet cell membranes. *Cryobiology*. **37**, 290-299 (1998).
3. Critser, J.K., Arneson, B.W., Aaker, D.V., Huse-Benda, A.R., and Ball, G.D. Factors affecting the cryosurvival of mouse two-cell embryos. *J Reprod Fertil*. **82**, 27-33 (1988).
4. Gilmore, J.A., McGann, L.E., Liu, J., Gao, D.Y., Peter, A.T., Kleinhaus, F.W., and Critser, J.K. Effect of cryoprotectant solutes on water permeability of human spermatozoa. *Biol Reprod*. **53**, 985-995 (1995).
5. Griffith, M., Osborne, R., Munger, R., Xiong, X., Doillon, C.J., Laycock, N.L.C, Hakim, M., Song, Y., and Watsky, M.A. Functional human corneal equivalents constructed from cell lines. *Science* **286**, 2169-2172 (1999).
6. Johnson, J.A., and Wilson, T.A. Osmotic volume changes induced by a permeable solute. *J Theoret Biol*. **17**, 304-311 (1967).
7. Karlsson, J.O., Eroglu, A., Toth, T.L., Cravalho, E.G., and Toner, M. Rational design and theoretical optimization of a cryopreservation protocol. In "Advances in Heat and Mass Transfer in Biotechnology, HTD. Bol. 322éBED, vol. 32" (L.J. Hayes, Ed.), pp. 85-89. The American Society of Mechanical Engineers, New York, 1995.
8. Levin, R.L., and Miller, T.W. An optimum method for the introduction or removal of permeable cryoprotectants: Isolated cells. *Cryobiology*. **18**, 32-48 (1981).

9. Liu, J., Zieger, M.A.J., Lakey, J.R.T., Woods, E.J., and Critser, J.K. The determination of membrane permeability coefficients of canine pancreatic islet cells and their application to islet cryopreservation. *Cryobiology*. **35**, 1-13 (1997).
10. Mazur, P. Kinetics of water loss from cells at subzero temperatures and the likelihood of intracellular freezing. *Journal of General Physiology*. **47**, 347-369 (1963).
11. Mazur, P., Leibo, S.P., and Chu, E.H.Y. A two-factor hypothesis of freezing injury. *Experimental Cell Research*. **70**, 345-355 (1972).
12. Mazur, P., Rall, W.F., and Leibo, S.P. Kinetics of water loss and the likelihood of intracellular freezing in mouse ova. *Cell Biophys*. **6**, 197-213 (1984).
13. McGann, L.E., Turner, A.R., and Turc, J. Microcomputer interface for rapid measurements of average volume using an electronic particle counter. *Med & biol eng & comput*. **20**, 117-120 (1982).
14. McGrath, J.J. Membrane transport proteins. In "Low Temperature Biotechnology Emerging Applications and Engineering Contributions" (J.J. McGrath and K.R. Diller, Eds.), pp. 273-330. The American Society of Mechanical Engineers, New York, 1988.
15. McGrath, J.J. Quantitative measurement of cell membrane transport: Technology and applications. *Cryobiology*. **34**, 315-334 (1997).
16. Pegg, D.E. The current status of tissue cryopreservation. *Cryo-letters*. **22**, 105-114 (2001).

17. Pegg, D.E., Hunt, C.J., and Fong, L.P. Osmotic properties of the rabbit corneal endothelium and their relevance to cryopreservation. *Cell Biophys.* **10**, 169-189 (1987).
18. Pfaff, R.T., Agca, Y., Liu, J., Woods, E.J., Peter, A.J., and Critser, J.K. Cryobiology of rat embryos I: Determination of zygote membrane permeability coefficients for water and cryoprotectants, their activation energies, and the development of improved cryopreservation methods. *Biol Reprod.* **63**, 1294-1302 (2000).
19. Polge, C., Smith, A.U., and Parkes, A.S. Revival of spermatozoa after vitrification and dehydration at low temperatures. *Nature.* **164**, 666-676 (1949).
20. Rasmussen, D.H., and MacKenzie, A.P. Phase diagram for the system water-dimethylsulphoxide. *Nature.* **220**, 1315-1317 (1968).
21. Smith, D.J., Pham, L.D., and Bischof, J.C. The effect of dimethylsulfoxide on the water transport response of rat liver tissue during freezing. *Cryo-letters.* **19**, 343-354 (1998).
22. Toupin, C.J., Le Maguer, M., and McGann, L.E. Permeability of human granulocytes to dimethyl sulfoxide. *Cryobiology.* **26**, 422-430 (1989).
23. Wolf, A.V., Brown, M.G., and Prentiss, P.G. Concentrative properties of aqueous solutions. In "Handbook of chemistry and physics" (Weast, Eds.). pp D-227 - D-276. CRC press, 1982.

24. Woods, E.J., Liu, J., Zieger, M.A.J., Lakey, J.R.T., and Critser, J.K. Water and cryoprotectant permeability characteristics of isolated human and canine pancreatic islets. *Cell Transplantation*. **8**, 549-559 (1999).
25. Woods, E.J., Liu, J., Gilmore, J.A., Reid, T.J., Gao, D.Y., and Critser, J.K. Determination of human platelet membrane permeability coefficients using the Kedem-Katchalsky formalism: estimates from two- vs three-parameter fits. *Cryobiology*. **38**, 200-208 (1999).
26. Woods, E.J., Liu, J., Derrow, C.W., Smith, F.O., Williams, D.A., and Critser, J.K. Osmometric and permeability characteristics of human placental/umbilical cord blood CD34+ cells and their application to cryopreservation. *J hematol & stem cell res*. **9**, 161-173 (2000).
27. Wusteman, M.C., and Pegg, D.E. Differences in the requirements for cryopreservation of porcine aortic smooth muscle and endothelial cells. *Tissue Engineering*. **7**, 507-518 (2001).

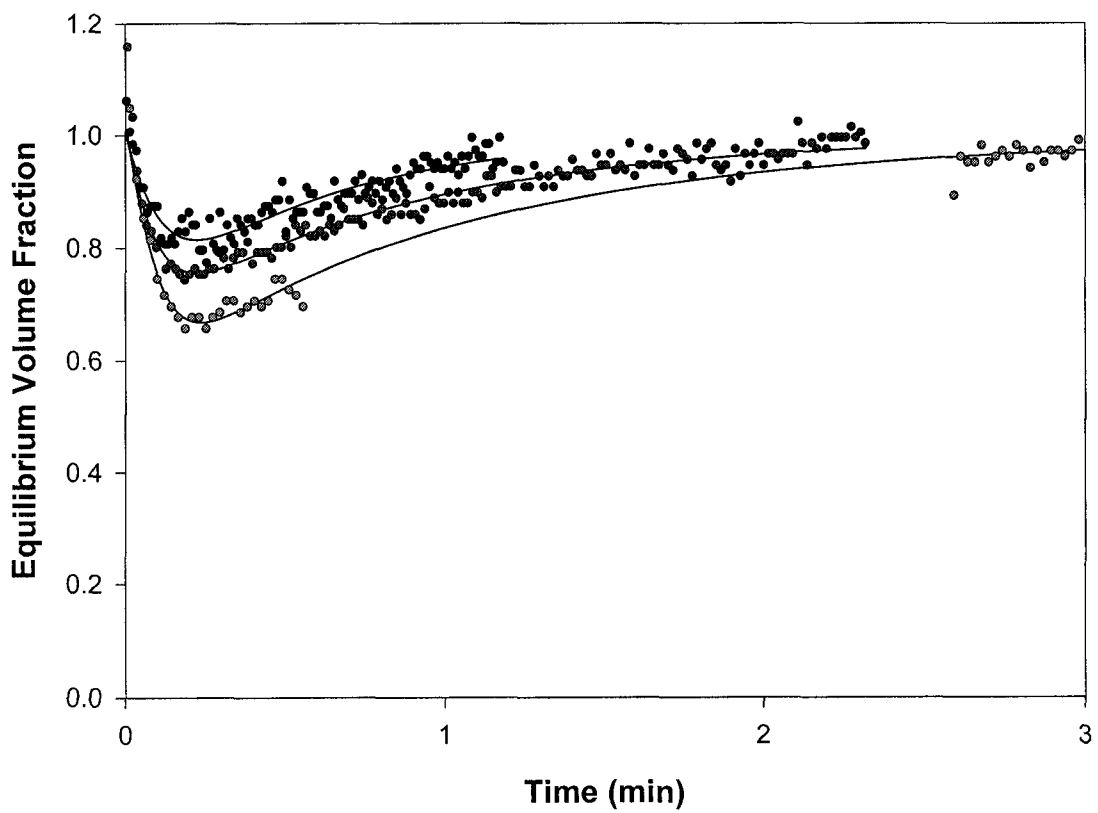


Fig. 1. A representative plot of volume versus time for human corneal endothelial, keratocyte, and epithelial cells exposed to 1M DMSO at 22°C. The solid lines represent the best fit for  $L_p$ ,  $P_s$ , and  $\sigma$  using the equations developed by Johnson and Wilson (6).

TABLE 1A.  $L_p$  ( $\mu\text{m}/\text{atm}/\text{min}$ ) for human corneal endothelial cells (mean  $\pm$  SD).

<b>A</b>	0.5M DMSO	1M DMSO	2M DMSO	0.5M PG	1 M PG	2M PG
4°C	0.06 $\pm$ 0.02	0.08 $\pm$ 0.03	0.08 $\pm$ 0.01 <sup>a</sup>	0.08 $\pm$ 0.04	0.04 $\pm$ 0.03	0.11 $\pm$ 0.02 <sup>a</sup>
13°C	0.33 $\pm$ 0.08	0.29 $\pm$ 0.04	0.25 $\pm$ 0.02 <sup>a</sup>	0.33 $\pm$ 0.06	0.31 $\pm$ 0.03	0.26 $\pm$ 0.03 <sup>a</sup>
22°C	0.56 $\pm$ 0.08	0.66 $\pm$ 0.06	0.66 $\pm$ 0.05 <sup>a</sup>	0.70 $\pm$ 0.14	0.75 $\pm$ 0.13	0.73 $\pm$ 0.09
37°C	2.27 $\pm$ 0.91	1.38 $\pm$ 0.50	1.36 $\pm$ 0.31 <sup>a</sup>	1.72 $\pm$ 0.56	1.74 $\pm$ 0.69	2.01 $\pm$ 0.60

TABLE 1B.  $L_p$  ( $\mu\text{m}/\text{atm}/\text{min}$ ) for human corneal keratocytes (mean  $\pm$  SD).

<b>B</b>	0.5M DMSO	1M DMSO	2M DMSO	0.5M PG	1 M PG	2M PG
4°C	0.08 $\pm$ 0.01	0.10 $\pm$ 0.03	0.10 $\pm$ 0.01	0.08 $\pm$ 0.01	0.08 $\pm$ 0.01	0.10 $\pm$ 0.01 <sup>a</sup>
13°C	0.22 $\pm$ 0.09	0.49 $\pm$ 0.11 <sup>b</sup>	0.31 $\pm$ 0.03 <sup>a</sup>	0.24 $\pm$ 0.14	0.40 $\pm$ 0.10	0.27 $\pm$ 0.06 <sup>a</sup>
22°C	0.59 $\pm$ 0.17	0.52 $\pm$ 0.05	0.50 $\pm$ 0.04	0.60 $\pm$ 0.19	0.52 $\pm$ 0.06	0.54 $\pm$ 0.06
37°C	1.88 $\pm$ 0.64	1.41 $\pm$ 0.24	1.23 $\pm$ 0.14 <sup>a</sup>	2.01 $\pm$ 1.01	1.69 $\pm$ 0.22	1.78 $\pm$ 0.94

TABLE 1C.  $L_p$  values ( $\mu\text{m}/\text{atm}/\text{min}$ ) for human corneal epithelial cells (mean  $\pm$  SD).

<b>C</b>	0.5M DMSO	1M DMSO	2M DMSO	0.5M PG	1 M PG	2M PG
4°C	0.10 $\pm$ 0.02	0.13 $\pm$ 0.04	0.08 $\pm$ 0.01 <sup>a</sup>	0.10 $\pm$ 0.03	0.15 $\pm$ 0.05	0.18 $\pm$ 0.04 <sup>a</sup>
13°C	0.22 $\pm$ 0.05	0.33 $\pm$ 0.12	0.21 $\pm$ 0.03 <sup>a</sup>	0.28 $\pm$ 0.07	0.31 $\pm$ 0.11	0.25 $\pm$ 0.02
22°C	1.02 $\pm$ 0.14	1.16 $\pm$ 0.24	1.03 $\pm$ 0.36	1.14 $\pm$ 0.13	1.17 $\pm$ 0.36	0.76 $\pm$ 0.05 <sup>a</sup>
37°C	1.75 $\pm$ 0.63	1.62 $\pm$ 0.25	1.44 $\pm$ 0.07	2.04 $\pm$ 0.77	1.94 $\pm$ 0.26	1.65 $\pm$ 0.16

a:  $p < 0.05$       b: outside of the error

TABLE 1D. Pooled  $L_p$  values ( $\mu\text{m}/\text{atm}/\text{min}$ ) for human corneal cells in DMSO and PG.

	Endothelial Cells		Keratocytes		Epithelial Cells	
	DMSO	PG	DMSO	PG	DMSO	PG
4°C	0.07 $\pm$ 0.02	0.11 $\pm$ 0.03	0.09 $\pm$ 0.02	0.09 $\pm$ 0.01	0.10 $\pm$ 0.03	0.14 $\pm$ 0.04
13°C	0.29 $\pm$ 0.06	0.30 $\pm$ 0.04	0.35 $\pm$ 0.09	0.31 $\pm$ 0.10	0.25 $\pm$ 0.08	0.28 $\pm$ 0.08
22°C	0.62 $\pm$ 0.07	0.72 $\pm$ 0.12	0.53 $\pm$ 0.10	0.56 $\pm$ 0.12	1.07 $\pm$ 0.26	1.02 $\pm$ 0.22
37°C	1.67 $\pm$ 0.62	1.83 $\pm$ 0.62	1.51 $\pm$ 0.40	1.83 $\pm$ 0.81	1.60 $\pm$ 0.39	1.88 $\pm$ 0.49

TABLE 2A.  $P_s$  values ( $\mu\text{m}/\text{min}$ ) for human corneal endothelial cells (mean  $\pm$  SD).

<b>A</b>	0.5M DMSO	1M DMSO	2M DMSO	0.5M PG	1 M PG	2M PG
4°C	1.51 $\pm$ 0.31	2.41 $\pm$ 0.85	4.48 $\pm$ 1.20 <sup>a,b</sup>	1.65 $\pm$ 0.43	1.53 $\pm$ 0.68	5.02 $\pm$ 1.07 <sup>a,b</sup>
13°C	3.20 $\pm$ 0.77	5.61 $\pm$ 1.11	11.00 $\pm$ 1.48 <sup>a,b</sup>	5.08 $\pm$ 1.58	7.43 $\pm$ 1.44	12.25 $\pm$ 1.72 <sup>a,b</sup>
22°C	14.24 $\pm$ 2.38	13.78 $\pm$ 2.08	20.55 $\pm$ 2.91 <sup>a,b</sup>	15.78 $\pm$ 2.15	16.99 $\pm$ 3.56	25.35 $\pm$ 4.91 <sup>a</sup>
37°C	58.38 $\pm$ 20.99	50.58 $\pm$ 18.53	63.45 $\pm$ 12.20	67.56 $\pm$ 14.68	84.53 $\pm$ 39.16	123.29 $\pm$ 53.37 <sup>a</sup>

TABLE 2B.  $P_s$  values ( $\mu\text{m}/\text{min}$ ) for human corneal keratocytes (mean  $\pm$  SD).

<b>B</b>	0.5M DMSO	1M DMSO	2M DMSO	0.5M PG	1 M PG	2M PG
4°C	0.95 $\pm$ 0.27	1.06 $\pm$ 0.62	3.58 $\pm$ 0.82 <sup>a,b</sup>	0.99 $\pm$ 0.13	1.07 $\pm$ 0.21	4.38 $\pm$ 0.54 <sup>a,b</sup>
13°C	2.24 $\pm$ 0.45	2.76 $\pm$ 0.41	8.15 $\pm$ 0.87 <sup>a,b</sup>	2.15 $\pm$ 0.26	3.40 $\pm$ 0.79	8.42 $\pm$ 2.23 <sup>a,b</sup>
22°C	9.84 $\pm$ 3.33	8.55 $\pm$ 1.52	10.90 $\pm$ 1.36	9.50 $\pm$ 1.77	9.97 $\pm$ 0.79	14.74 $\pm$ 2.91 <sup>a,b</sup>
37°C	27.17 $\pm$ 8.57	40.46 $\pm$ 14.14	39.60 $\pm$ 21.93	31.04 $\pm$ 9.41	42.28 $\pm$ 14.01	44.99 $\pm$ 18.38

TABLE 2C.  $P_s$  values ( $\mu\text{m}/\text{min}$ ) for human corneal epithelial cells (mean  $\pm$  SD).

<b>C</b>	0.5M DMSO	1M DMSO	2M DMSO	0.5M PG	1 M PG	2M PG
4°C	0.74 $\pm$ 0.19	0.89 $\pm$ 0.32	2.61 $\pm$ 0.26 <sup>a,b</sup>	0.87 $\pm$ 0.21	0.80 $\pm$ 0.28	3.03 $\pm$ 0.25 <sup>a,b</sup>
13°C	2.16 $\pm$ 0.61	2.94 $\pm$ 1.24	5.31 $\pm$ 0.96 <sup>a,b</sup>	2.13 $\pm$ 0.42	3.94 $\pm$ 2.62	5.99 $\pm$ 0.67 <sup>a</sup>
22°C	7.06 $\pm$ 0.67	7.77 $\pm$ 1.05	15.13 $\pm$ 5.73 <sup>a,b</sup>	7.49 $\pm$ 0.83	8.94 $\pm$ 2.00	17.52 $\pm$ 2.90 <sup>a,b</sup>
37°C	34.80 $\pm$ 11.62	38.82 $\pm$ 9.86	42.29 $\pm$ 7.87	39.29 $\pm$ 11.27	51.74 $\pm$ 15.29	62.62 $\pm$ 23.03 <sup>a</sup>

a:  $p < 0.05$       b: outside of the error

TABLE 2D. Pooled  $P_s$  values ( $\mu\text{m}/\text{min}$ ) for human corneal cells in DMSO and PG.

	Endothelial Cells		Keratocytes		Epithelial Cells	
	DMSO	PG	DMSO	PG	DMSO	PG
4°C	2.71 $\pm$ 0.84	2.73 $\pm$ 0.77	1.99 $\pm$ 0.62	2.15 $\pm$ 0.34	1.41 $\pm$ 0.26	1.57 $\pm$ 0.25
13°C	6.64 $\pm$ 1.16	8.25 $\pm$ 1.58	4.27 $\pm$ 0.60	4.28 $\pm$ 1.23	3.47 $\pm$ 0.97	4.02 $\pm$ 1.58
22°C	16.21 $\pm$ 2.49	19.24 $\pm$ 3.68	9.76 $\pm$ 2.19	11.40 $\pm$ 2.02	9.99 $\pm$ 3.38	11.32 $\pm$ 2.09
37°C	57.47 $\pm$ 17.63	92.63 $\pm$ 42.15	35.74 $\pm$ 15.86	39.44 $\pm$ 14.41	38.64 $\pm$ 9.90	50.74 $\pm$ 17.01

TABLE 3A. Reflection coefficient ( $\sigma$ ) for human corneal endothelial cells (mean  $\pm$  SD).

<b>A</b>	0.5M DMSO	1M DMSO	2M DMSO	0.5M PG	1 M PG	2M PG
4°C	0.88 $\pm$ 0.20	0.65 $\pm$ 0.28	0.94 $\pm$ 0.99	0.78 $\pm$ 0.24	0.35 $\pm$ 0.12	0.61 $\pm$ 0.15 <sup>a</sup>
13°C	0.33 $\pm$ 0.11	0.38 $\pm$ 0.08	0.51 $\pm$ 0.09 <sup>a,b</sup>	0.46 $\pm$ 0.18	0.50 $\pm$ 0.12	0.51 $\pm$ 0.09
22°C	0.62 $\pm$ 0.12	0.51 $\pm$ 0.09	0.44 $\pm$ 0.08 <sup>a</sup>	0.63 $\pm$ 0.17	0.51 $\pm$ 0.15	0.38 $\pm$ 0.07 <sup>a</sup>
37°C	0.70 $\pm$ 0.37	0.62 $\pm$ 0.19	0.56 $\pm$ 0.12	0.76 $\pm$ 0.17	0.67 $\pm$ 0.27	0.52 $\pm$ 0.28

TABLE 3B. Reflection coefficient ( $\sigma$ ) for human corneal keratocytes (mean  $\pm$  SD).

<b>B</b>	0.5M DMSO	1M DMSO	2M DMSO	0.5M PG	1 M PG	2M PG
4°C	0.99 $\pm$ 0.01	0.92 $\pm$ 0.21	0.76 $\pm$ 0.08 <sup>a</sup>	1	1	0.80 $\pm$ 0.09 <sup>a,b</sup>
13°C	0.72 $\pm$ 0.23	0.32 $\pm$ 0.08 <sup>b</sup>	0.50 $\pm$ 0.08 <sup>a</sup>	0.68 $\pm$ 0.31	0.44 $\pm$ 0.18	0.46 $\pm$ 0.08
22°C	0.73 $\pm$ 0.19	0.70 $\pm$ 0.12	0.54 $\pm$ 0.14 <sup>a</sup>	0.78 $\pm$ 0.19	0.79 $\pm$ 0.10	0.40 $\pm$ 0.08 <sup>a,b</sup>
37°C	0.50 $\pm$ 0.17	0.54 $\pm$ 0.20	0.38 $\pm$ 0.08	0.61 $\pm$ 0.28	0.51 $\pm$ 0.18	0.32 $\pm$ 0.17 <sup>a</sup>

TABLE 3C. Reflection coefficient( $\sigma$ ) for human corneal epithelial cells (mean  $\pm$  SD).

<b>C</b>	0.5M DMSO	1M DMSO	2M DMSO	0.5M PG	1 M PG	2M PG
4°C	0.60 $\pm$ 0.16	0.46 $\pm$ 0.17	0.71 $\pm$ 0.04 <sup>a</sup>	0.73 $\pm$ 0.22	0.49 $\pm$ 0.14	0.97 $\pm$ 0.04 <sup>a</sup>
13°C	0.46 $\pm$ 0.13	0.38 $\pm$ 0.15	0.50 $\pm$ 0.12	0.53 $\pm$ 0.16	0.52 $\pm$ 0.27	0.65 $\pm$ 0.07
22°C	0.27 $\pm$ 0.04	0.23 $\pm$ 0.06	0.26 $\pm$ 0.11	0.30 $\pm$ 0.03	0.30 $\pm$ 0.12	0.43 $\pm$ 0.10 <sup>a</sup>
37°C	0.64 $\pm$ 0.27	0.57 $\pm$ 0.16	0.49 $\pm$ 0.11	0.69 $\pm$ 0.17	0.69 $\pm$ 0.17	0.64 $\pm$ 0.22

a:  $p < 0.05$       b: outside of the error

TABLE 3D. Pooled reflection coefficient ( $\sigma$ ) for human corneal cells in DMSO and PG.

	Endothelial Cells		Keratocytes		Epithelial Cells	
	DMSO	PG	DMSO	PG	DMSO	PG
4°C	0.83 $\pm$ 0.59	0.58 $\pm$ 0.18	0.89 $\pm$ 0.12	0.93 $\pm$ 0.05	0.59 $\pm$ 0.14	0.73 $\pm$ 0.16
13°C	0.41 $\pm$ 0.10	0.49 $\pm$ 0.13	0.50 $\pm$ 0.14	0.52 $\pm$ 0.22	0.44 $\pm$ 0.13	0.57 $\pm$ 0.19
22°C	0.53 $\pm$ 0.10	0.51 $\pm$ 0.14	0.65 $\pm$ 0.15	0.66 $\pm$ 0.13	0.25 $\pm$ 0.08	0.34 $\pm$ 0.09
37°C	0.63 $\pm$ 0.25	0.65 $\pm$ 0.25	0.48 $\pm$ 0.16	0.48 $\pm$ 0.21	0.56 $\pm$ 0.19	0.67 $\pm$ 0.22

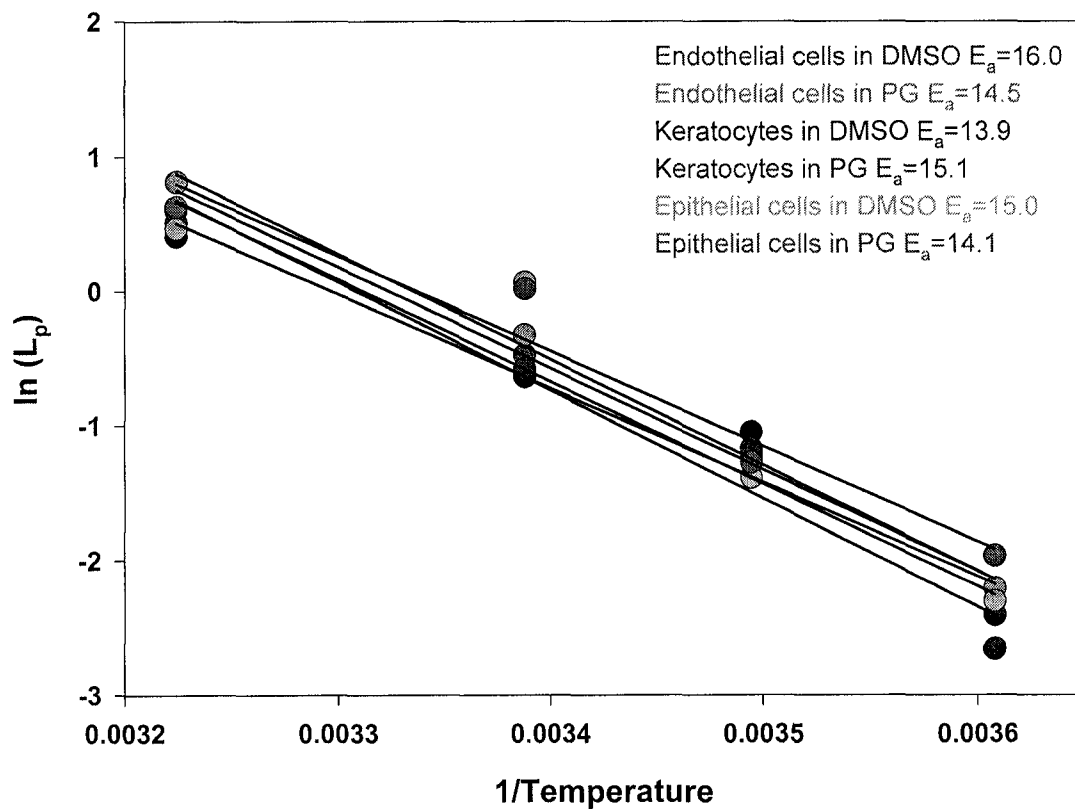


FIG. 2. Arrhenius plot of the natural logarithm for  $L_p$  of human corneal cells as a function of inverse absolute temperature. The solid lines represent the linear regression of the data for calculation of activation energy (kcal/mol) from the slope.

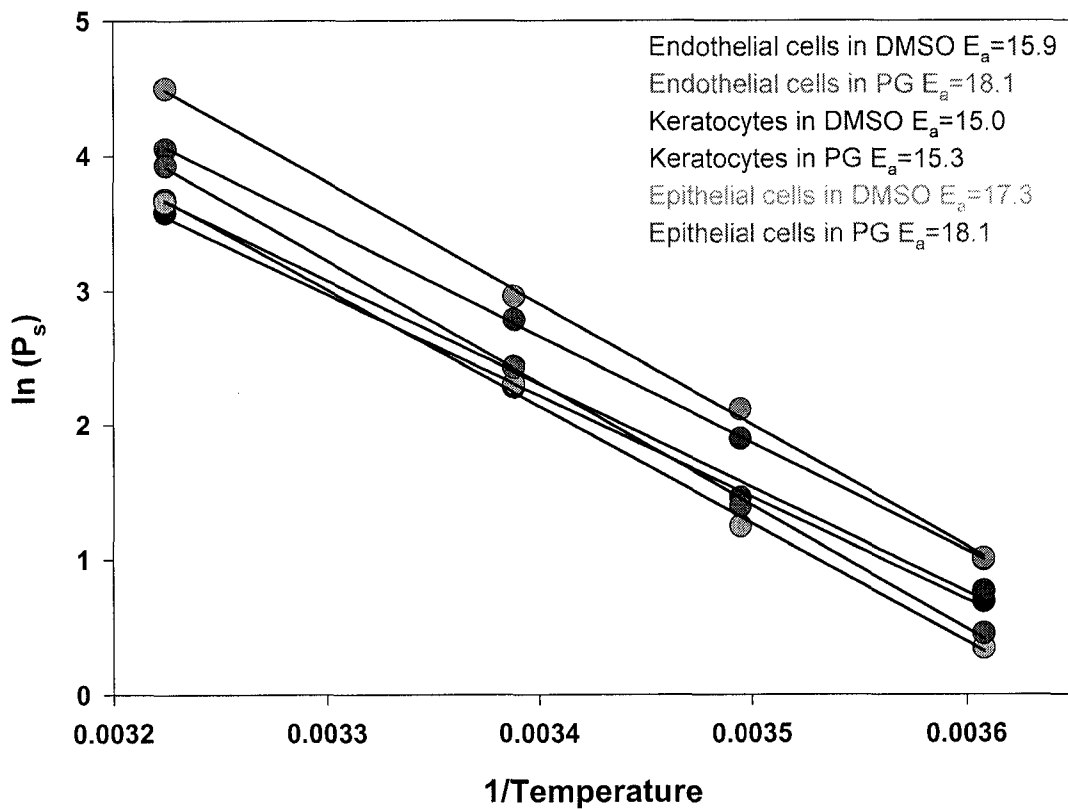


FIG. 3. Arrhenius plot of the natural logarithm of  $P_s$  of human corneal cells as a function of inverse absolute temperature. The solid lines represent the linear regression of the data for calculation of activation energy (kcal/mol) from the slope.

TABLE 4A. Summary of osmotic parameters for human corneal cells<sup>a</sup>.

	$V_{iso}$ ( $\mu\text{m}^3$ )	Diameter ( $\mu\text{m}$ )	$V_b$
Endothelium	3307 $\pm$ 292 <sup>b</sup>	18.5 $\pm$ 0.50	0.28 $\pm$ 0.02
Keratocytes	3186 $\pm$ 297	18.3 $\pm$ 0.60	0.27 $\pm$ 0.05
Epithelium	4134 $\pm$ 169	19.9 $\pm$ 0.30	0.41 $\pm$ 0.03

a: From: Ebertz, S.L. Chapter 2: Cellular osmotic parameters for a bioengineered human cornea equivalent and consequences for cryopreservation. Ph.D. Thesis.

b: mean  $\pm$  SD

Table 4B. Summary of osmotic parameters for human corneal cells in the presence of DMSO.

	Value at 22°C (mean ± SD)	Activation Energy (kcal/mol)
<b>Endothelium</b>		
Lp(μm/atm/min)	0.53±0.07	16.0
Ps(μm/min)	15.7±2.5	15.9
σ	0.60±0.34	
<b>Keratocytes</b>		
Lp(μm/atm/min)	0.53±0.10	13.9
Ps(μm/min)	10.0±2.2	15.0
σ	0.63±0.14	
<b>Epithelium</b>		
Lp(μm/atm/min)	0.62±0.26	15.0
Ps(μm/min)	9.4±3.4	17.3
σ	0.46±0.14	

Table 4C. Summary of osmotic parameters for human corneal cells in the presence of PG.

	Value at 22°C (mean ± SD)	Activation Energy (kcal/mol)
<b>Endothelium</b>		
Lp(μm/atm/min)	0.62±0.12	14.5
Ps(μm/min)	20.5±3.7	18.1
σ	0.56±0.18	
<b>Keratocytes</b>		
Lp(μm/atm/min)	0.56±0.12	15.1
Ps(μm/min)	11.0±2.0	15.3
σ	0.51±0.17	
<b>Epithelium</b>		
Lp(μm/atm/min)	0.62±0.22	14.1
Ps(μm/min)	11.2±2.1	18.1
σ	0.58±0.17	

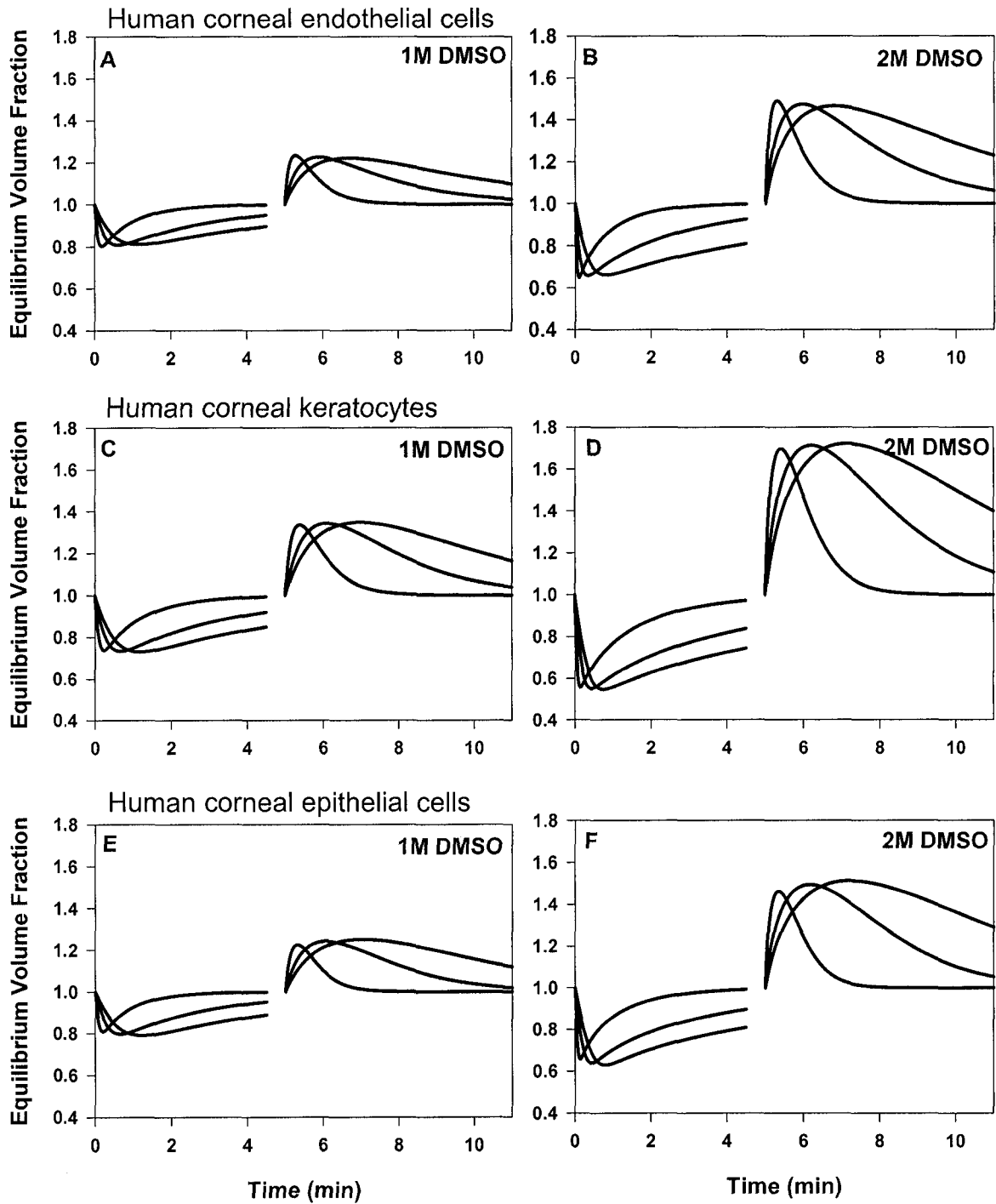


Fig. 4. Simulated cell volume response of human corneal endothelial (A,B), keratocyte (C,D), and epithelial cells (E,F) upon addition and removal of 1 or 2M DMSO at 4°C, 10°C, and 22°C.

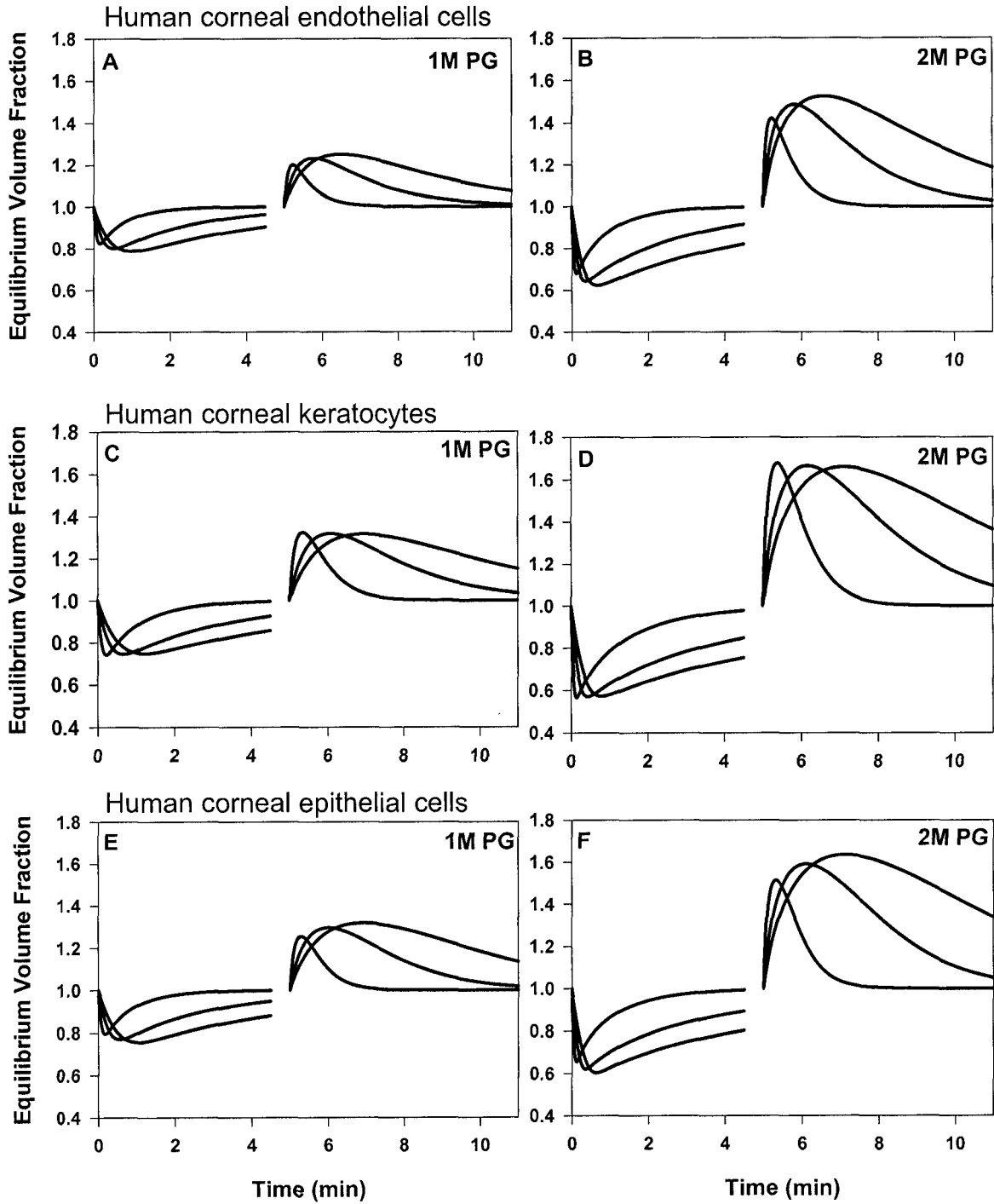


Fig. 5. Simulated cell volume response of human corneal endothelial (A,B), keratocyte (C,D), and epithelial cells (E,F) upon addition and removal of 1 or 2M PG at 4°C, 10°C, and 22°C.

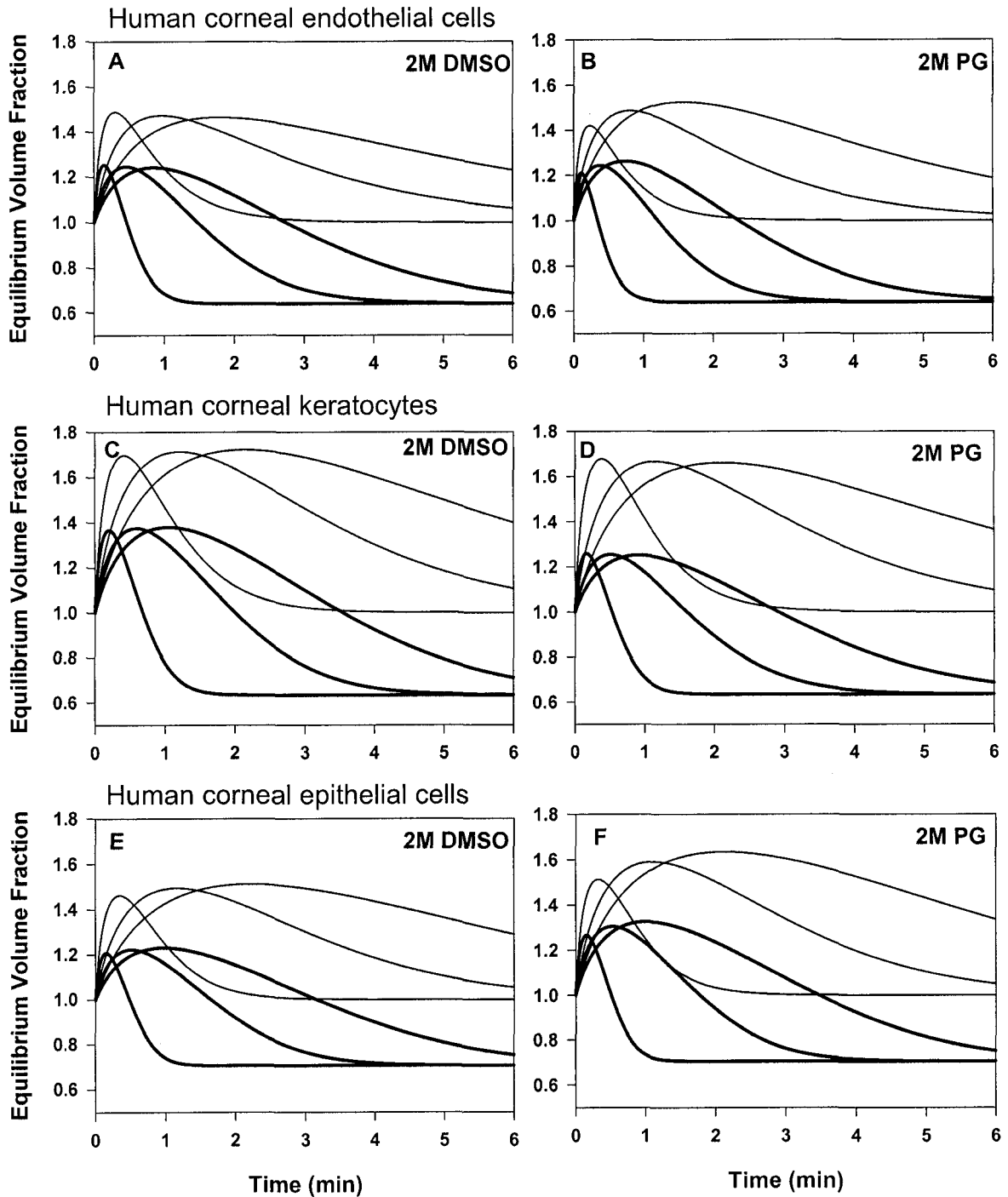


Fig. 6. Simulated cell volume response of human corneal endothelial (A,B), keratocyte (C,D), and epithelial cells (E,F) upon removal of 2M DMSO or 2M PG using the sucrose dilution technique at 4°C, 10°C, and 22°C. The gray lines represent the direct dilution of CPA from the corneal cells as shown in Figs. 4 and 5.

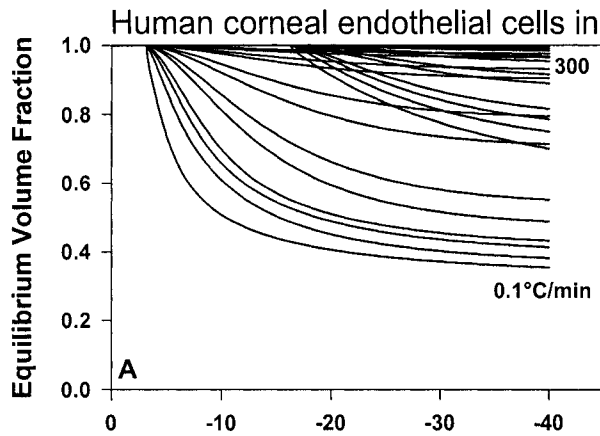


Fig. 7A. Simulated volume response of human corneal endothelial cells cooled at various cooling rates in the presence of 1M DMSO or 4M DMSO.

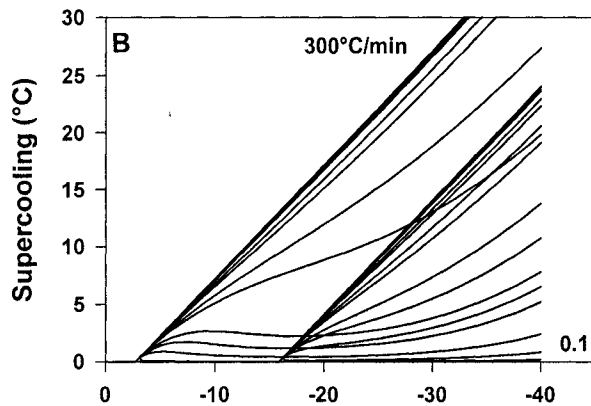


Fig. 7B. Amount of supercooling calculated for human corneal endothelial cells cooled at various cooling rates in the presence of 1M DMSO or 4M DMSO.

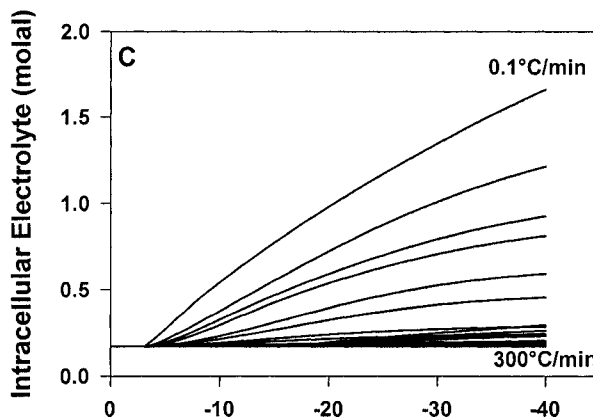


Fig. 7C. Intracellular electrolyte concentration calculated for human corneal endothelial cells at various cooling rates in the presence of 1M DMSO or 4M DMSO.

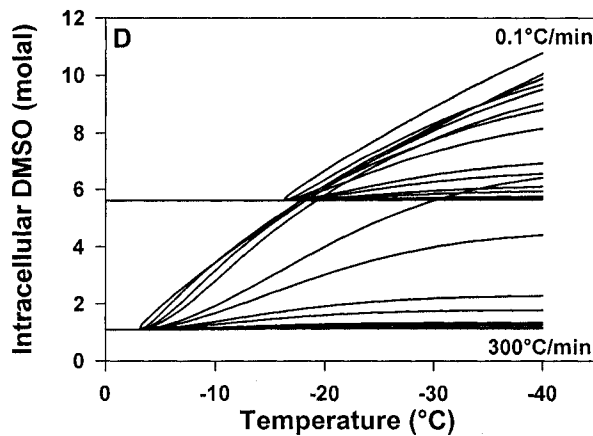


Fig. 7D. Intracellular DMSO concentration calculated for human corneal endothelial cells at various cooling rates in the presence of 1M DMSO or 4M DMSO.

Cooling rates used in simulations were 0.1, 1, 2, 3, 7, 10, 20, 30, 70, 100, 200, and 300°C/min.

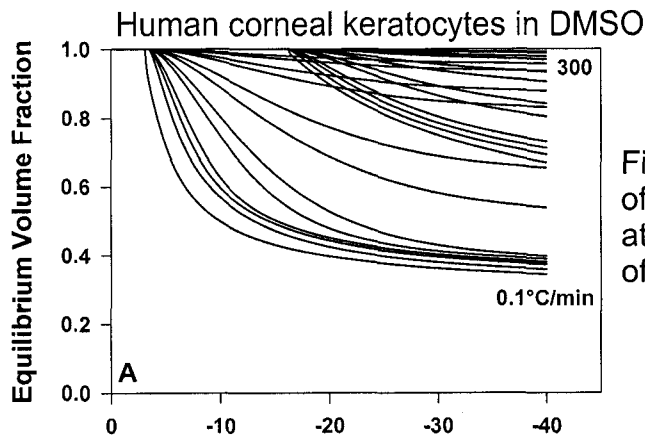


Fig. 8A. Simulated volume response of human corneal keratocytes cooled at various cooling rates in the presence of 1M DMSO or 4M DMSO.

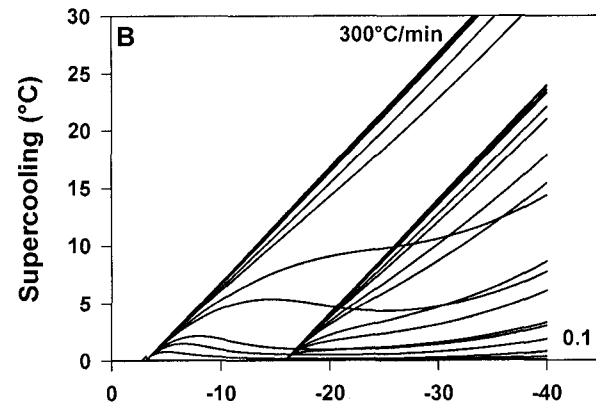


Fig. 8B. Amount of supercooling calculated for human corneal keratocytes cooled at various cooling rates in the presence of 1M DMSO or 4M DMSO.

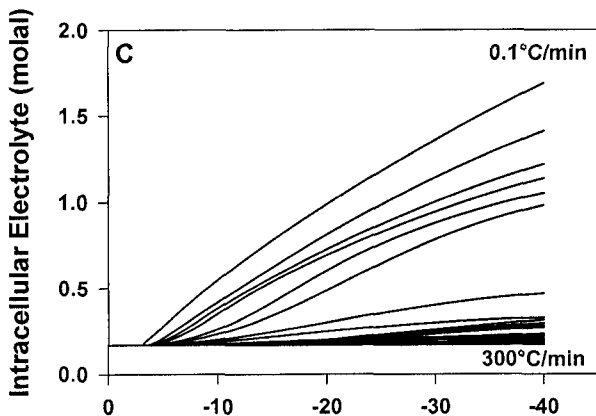


Fig. 8C. Intracellular electrolyte concentration calculated for human corneal keratocytes at various cooling rates in the presence of 1M DMSO or 4M DMSO.

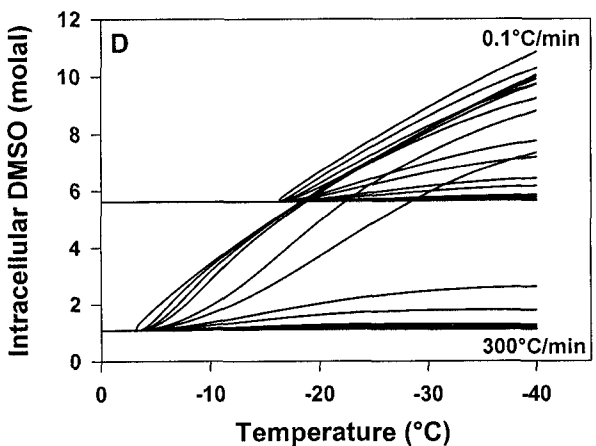


Fig. 8D. Intracellular DMSO concentration calculated for human corneal keratocytes at various cooling rates in the presence of 1M DMSO or 4M DMSO.

Cooling rates used in simulations were 0.1, 1, 2, 3, 7, 10, 20, 30, 70, 100, 200, and 300°C/min.

Human corneal epithelial cells in DMSO

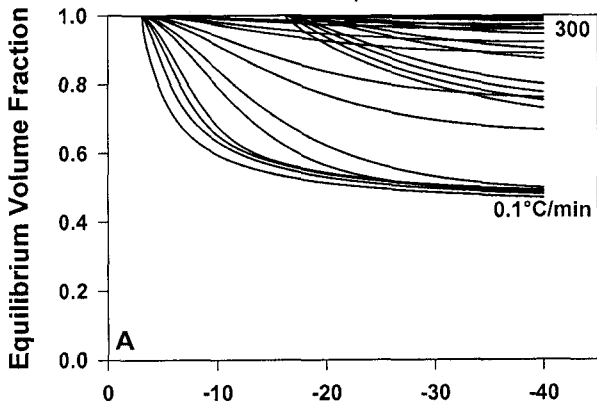


Fig. 9A. Simulated volume response of human corneal epithelial cells cooled at various cooling rates in the presence of 1M DMSO or 4M DMSO.

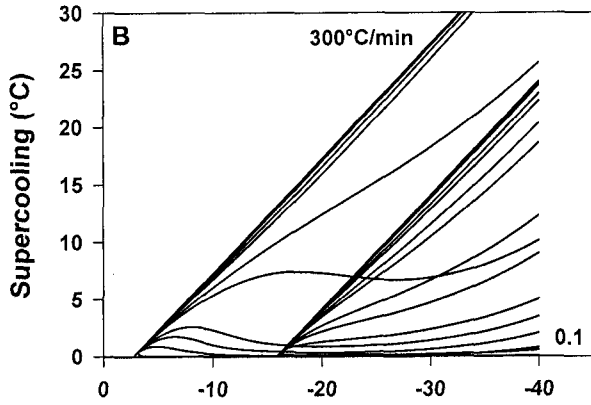


Fig. 9B. Amount of supercooling calculated for human corneal epithelial cells cooled at various cooling rates in the presence of 1M DMSO or 4M DMSO.

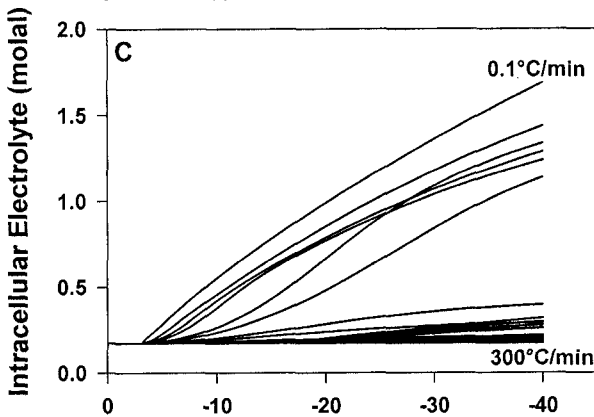


Fig. 9C. Intracellular electrolyte concentration calculated for human corneal epithelial cells at various cooling rates in the presence of 1M DMSO or 4M DMSO.

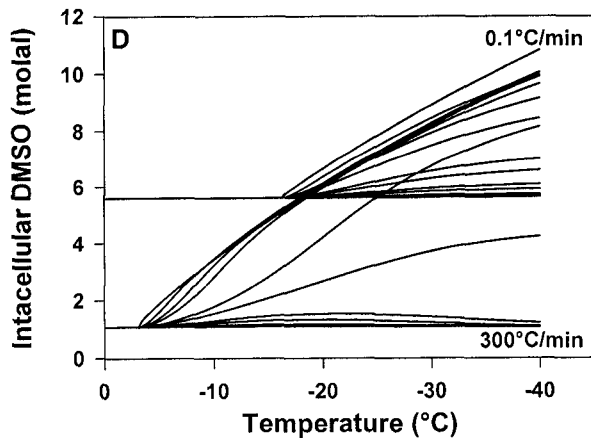


Fig. 9D. Intracellular DMSO concentration calculated for human corneal epithelial cells at various cooling rates in the presence of 1M DMSO or 4M DMSO.

Cooling rates used in simulations were 0.1, 1, 2, 3, 7, 10, 20, 30, 70, 100, 200, and 300°C/min.

Human corneal endothelial cells in PG

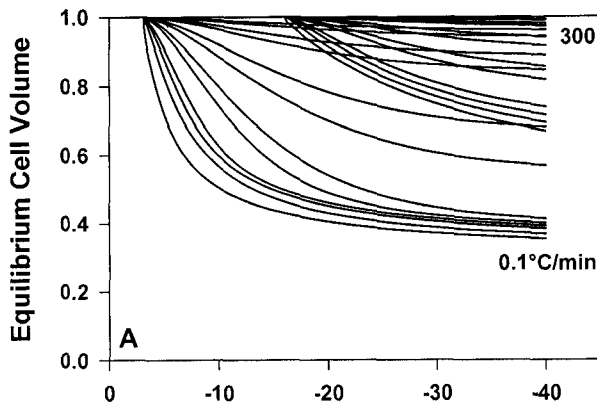


Fig. 10A. Simulated volume response of human corneal endothelial cells cooled at various cooling rates in the presence of 1M PG or 4M PG.

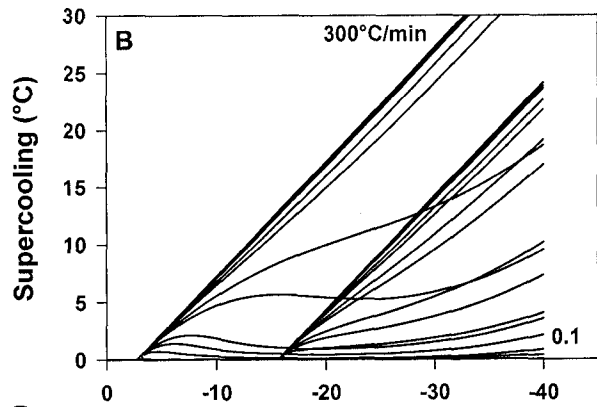


Fig. 10B. Amount of supercooling calculated for human corneal endothelial cells cooled at various cooling rates in the presence of 1M PG or 4M PG.

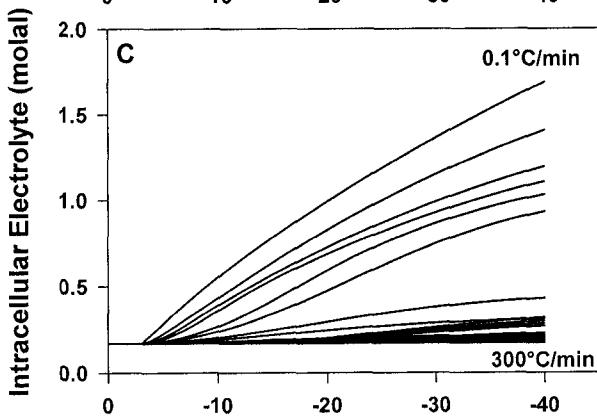


Fig. 10C. Intracellular electrolyte concentration calculated for human corneal endothelial cells at various cooling rates in the presence of 1M PG or 4M PG.

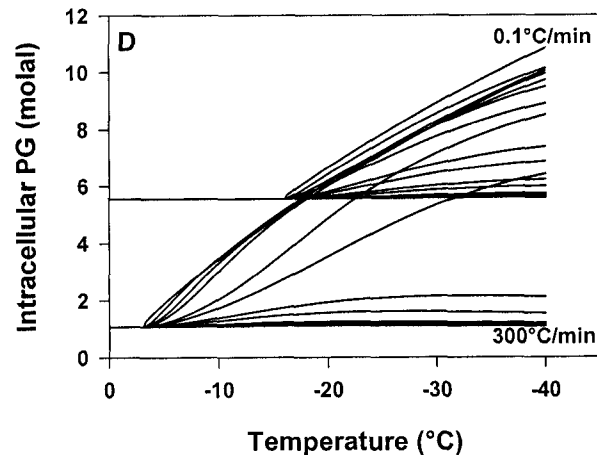


Fig. 10D. Intracellular PG concentration calculated for human corneal endothelial cells at various cooling rates in the presence of 1M PG or 4M PG.

Cooling rates used in simulations were 0.1, 1, 2, 3, 7, 10, 20, 30, 70, 100, 200, and 300 °C/min.

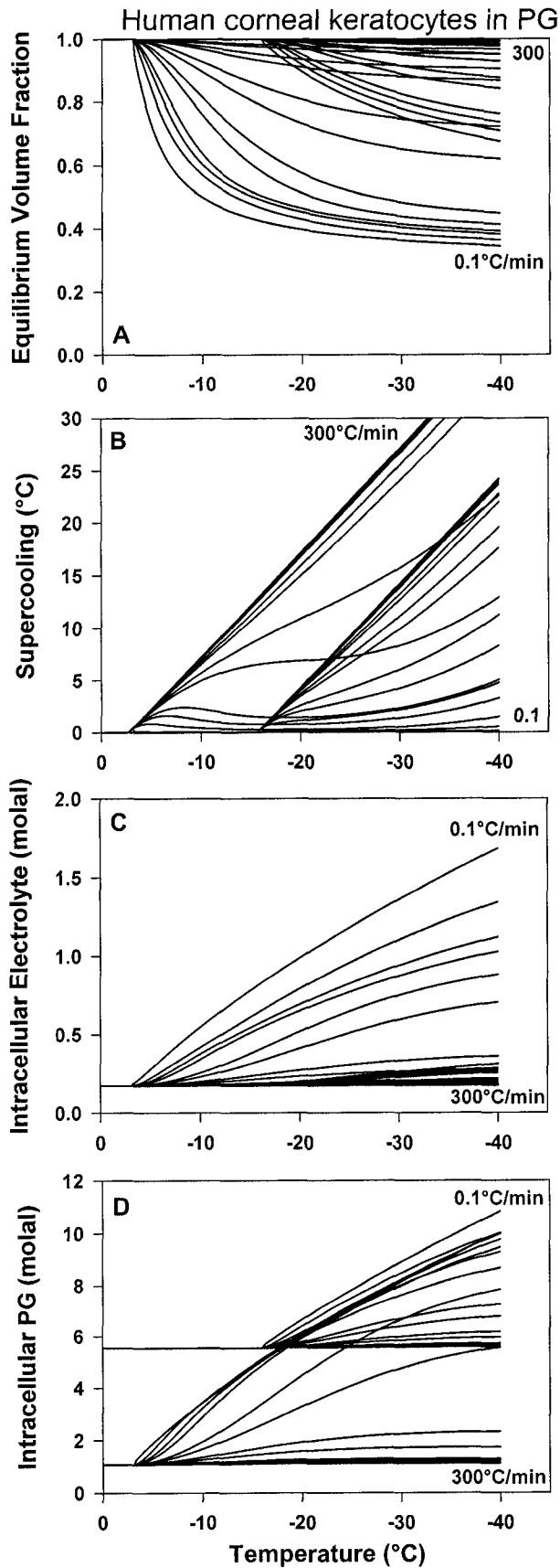


Fig. 11A. Simulated volume response of human corneal keratocytes cooled at various cooling rates in the presence of 1M PG or 4M PG.

Fig. 11B. Amount of supercooling calculated for human corneal keratocytes cooled at various cooling rates in the presence of 1M PG or 4M PG.

Fig. 11C. Intracellular electrolyte concentration calculated for human corneal keratocytes at various cooling rates in the presence of 1M PG or 4M PG.

Fig. 11D. Intracellular PG concentration calculated for human corneal keratocytes at various cooling rates in the presence of 1M PG or 4M PG.

Cooling rates used in simulations were 0.1, 1, 2, 3, 7, 10, 20, 30, 70, 100, 200, and 300°C/min.

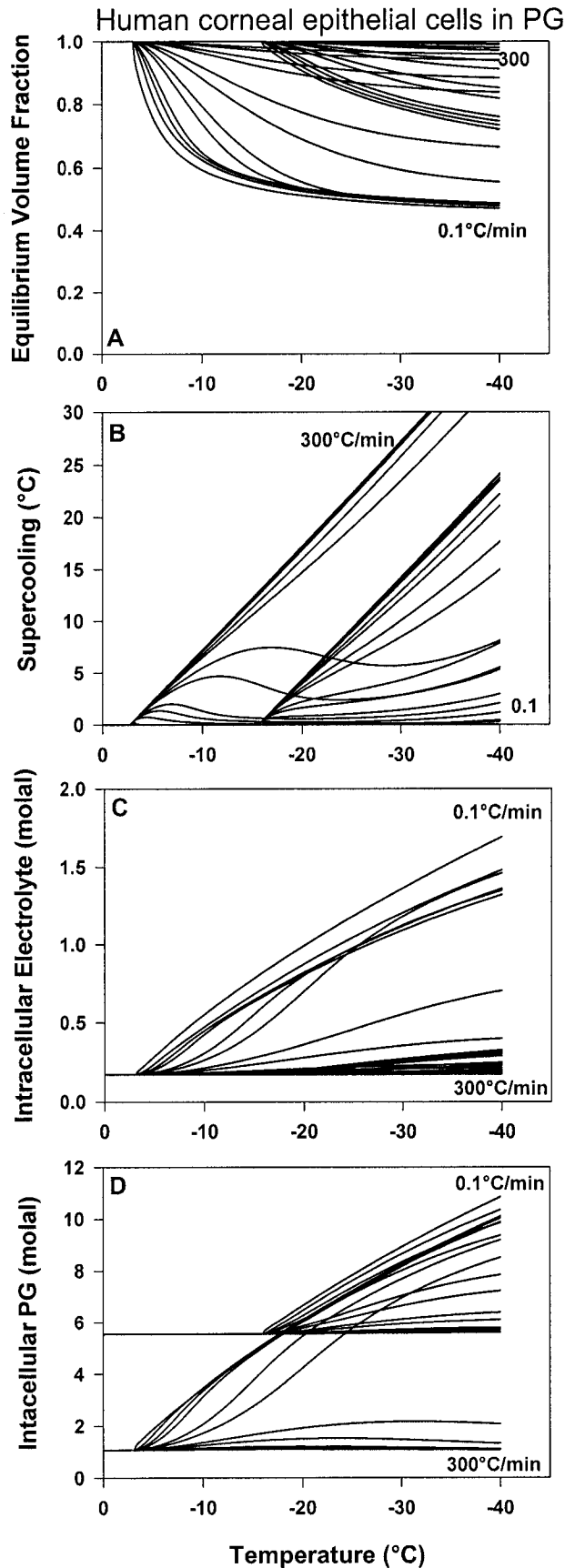


Fig. 12A. Simulated volume response of human corneal epithelial cells cooled at various cooling rates in the presence of 1M PG or 4M PG.

Fig. 12B. Amount of supercooling calculated for human corneal epithelial cells cooled at various cooling rates in the presence of 1M PG or 4M PG.

Fig. 12C. Intracellular electrolyte concentration calculated for human corneal epithelial cells at various cooling rates in the presence of 1M PG or 4M PG.

Fig. 12D. Intracellular PG concentration calculated for human corneal epithelial cells at various cooling rates in the presence of 1M PG or 4M PG.

Cooling rates used in simulations were 0.1, 1, 2, 3, 7, 10, 20, 30, 70, 100, 200, and 300 °C/min.

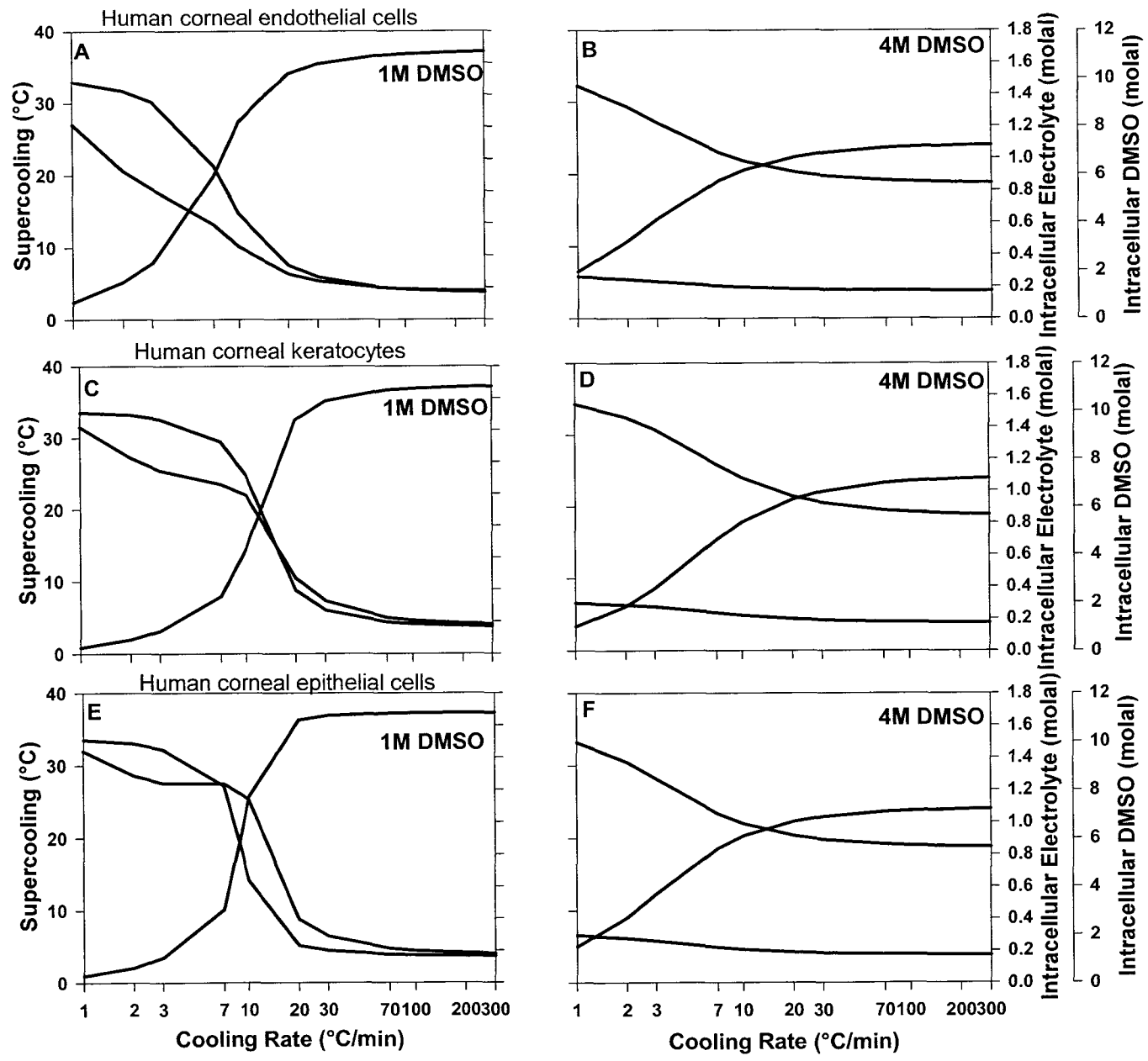


Fig. 13. Maximum supercooling, intracellular electrolyte concentration, and intracellular DMSO concentration calculated at various cooling rates for human corneal endothelial (A,B), keratocyte (C,D), and epithelial (E,F) cells in the presence of 1M or 4M DMSO.

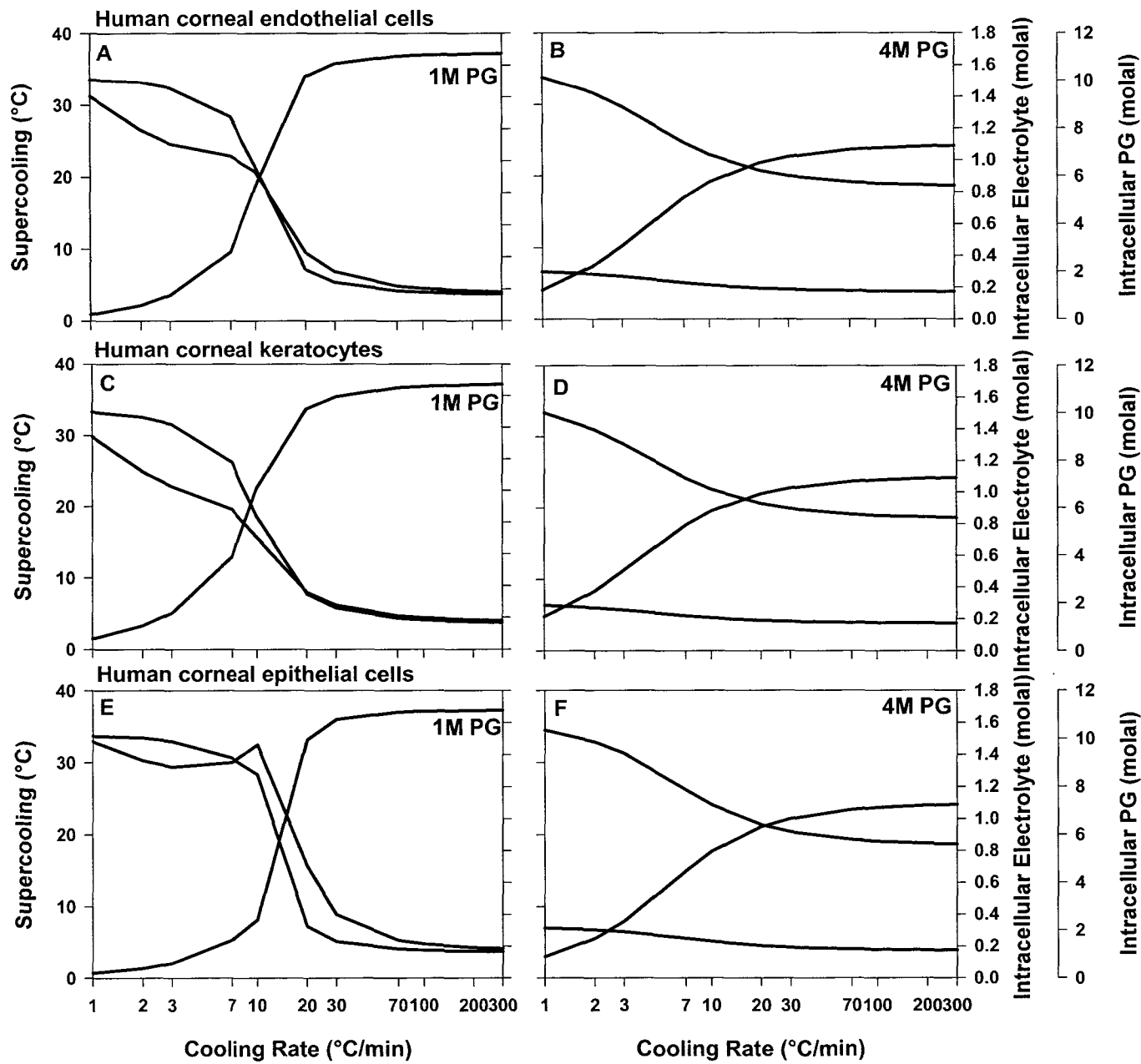


Fig. 14. Maximum supercooling, intracellular electrolyte concentration, and intracellular DMSO concentration calculated at various cooling rates for human corneal endothelial (A,B), keratocyte (C,D), and epithelial (E,F) cells in the presence of 1M or 4M PG.

## **Chapter 5: Simulations of Low Temperature Responses of Cells from a Bioengineered Human Corneal Equivalent**

### **5.1 Introduction**

Recovery of function and viability of cells and tissues following cryopreservation requires the addition of a cryoprotective agent (CPA). There are two categories of CPAs: permeating (DMSO, PG, glycerol) that can pass through cell membranes; and non-permeating (hydroxyethyl starch, polyvinylpyrrolidone, sugars) that cannot pass through cell membranes. Permeating and non-permeating CPAs act colligatively, reducing the amount of ice formed in the external and internal solutions during cooling, thereby decreasing the potentially damaging concentrations of electrolytes inside and outside the cell (8,11,15).

Conventional cryopreservation procedures involve the formation of ice in the external solution during cooling at an optimal controlled cooling rate that allows enough water to be lost from the cell to avoid excessive supercooling and intracellular ice formation and to avoid prolonged exposure to damaging solute concentrations as cells are cooled and more external ice is formed (14). Cells in suspension can be cryopreserved successfully using conventional cryopreservation procedures.

This is not true for tissues, and because of this many researchers are turning to vitrification as the possible solution. Vitrification is the solidification of a liquid into a glassy state rather than into a crystalline or frozen state, and offers the prospect of ice-free cryopreservation as there is evidence that the formation of ice within tissues is the damaging action (3,10). High concentrations of permeating CPAs are required to achieve vitrification and it is the increased

viscosity of these CPAs during cooling at high rates that suppresses nucleation of ice and crystal growth, resulting in a glass transformation (3,10). However, vitrification still presents its own problems, such as cryoprotectant toxicity and severe osmotic stress from the addition and removal of high concentrations of CPAs, achieving high enough cooling and warming rates, cracking of aqueous glasses at low storage temperatures, and devitrification (ice formation upon warming) (3,10).

The first objective of this chapter is to simulate the low temperature responses of the graded freezing protocol of human corneal endothelial cell (HCEC) monolayers from chapter 2 and relate these simulations to the graded freezing results obtained. The second objective of this chapter is to simulate low temperature responses of human corneal endothelial, keratocyte, and epithelial cells, which are the constituent cells of a bioengineered human corneal equivalent, using permeating and non-permeating CPAs. Then, from these simulations, discuss the implications for cryopreservation and how simulations can help in the development of cryopreservation procedures.

## **5.2 Methods**

The simulations were performed using the osmotic parameters determined in chapters 3 and 4 of this thesis, and were performed using the same procedures outlined in those chapters. The first set of simulations used the conditions from the graded freezing experiments in chapter 2, cool at 1°C/min to -15°C or -40°C, followed by a rapid cool at 235°C/min to -80°C or 325°C/min to -196°C. The second set of simulations were performed cooling the human

corneal cells from 0°C to -40°C at various cooling rates (0.1, 1, 2, 3, 7, 10, 20, 30, 70, 100, 200, and 300°C/min) in the presence: of no cryoprotectant, 1M DMSO, 1M PG, 4M DMSO, 4M PG, 1M DMSO + 0.3M sucrose, and 1M PG + 0.3M sucrose.

### **5.3 Results**

Fig. 1 and 2 shows the simulated low temperature responses (volume, supercooling, and intracellular electrolyte concentration as a function of temperature) and Fig. 3 shows the intracellular cryoprotectant concentration of human corneal endothelial cells under the graded freezing conditions used in chapter 2. Briefly, the cell monolayers were cooled at 1°C/min to -15°C or -40°C, and then rapidly cooled at 235°C/min to -80°C or 325°C/min to -196°C in the presence of 1M, 2M, or 4M DMSO or PG.

Simulated volume responses for human corneal endothelial, keratocyte, and epithelial cells cooled at varying cooling rates with no CPA, in the presence of permeating CPAs, and a combination of a permeating and non-permeating CPAs are shown in Figs. 4 and 5.

Figs. 6, 7, and 8 show the maximum amount of supercooling, intracellular electrolyte concentration, and intracellular cryoprotectant concentration, respectively as human corneal endothelial, keratocyte, and epithelial cells are cooled at varying cooling rates without cryoprotectant, in the presence of permeating CPAs, and a combination of a permeating and non-permeating CPA.

## 5.4 Discussion

When HCEC monolayers were subjected to the graded freezing protocol in chapter 2, rapid cooling to  $-196^{\circ}\text{C}$  after controlled cooling to  $-15^{\circ}\text{C}$  or  $-40^{\circ}\text{C}$ , there was no recovery of membrane integrity regardless of the cryoprotectant type or concentration. However, when the monolayers were rapidly cooled to  $-80^{\circ}\text{C}$  after controlled cooling to  $-15^{\circ}\text{C}$  or  $-40^{\circ}\text{C}$ , there was 30-45% membrane integrity after initial cooling to  $-15^{\circ}\text{C}$ , and 60% membrane integrity after initial cooling to  $-40^{\circ}\text{C}$  in the presence of 1M DMSO and 1M PG. 2M DMSO and 2M PG protected the membrane integrity of the HCEC monolayers equally well, but 4M DMSO and PG resulted in lower recovery of membrane integrity.

Consider the simulations in Figs. 1 and 2 in relation to the results from the graded freezing experiments of the HCEC monolayers. The simulations show that rapid cooling at  $235^{\circ}\text{C}/\text{min}$  to  $-80^{\circ}\text{C}$  and  $325^{\circ}\text{C}/\text{min}$  to  $-196^{\circ}\text{C}$  following cooling at  $1^{\circ}\text{C}/\text{min}$  to  $-15^{\circ}\text{C}$  and  $-40^{\circ}\text{C}$  follow the same pattern when plotted as volume, supercooling, and intracellular electrolyte concentration are plotted as functions of temperature; therefore the discussion applies to all these variables.

When HCEC monolayers were slowly cooled in 1M DMSO or 1M PG to  $-15^{\circ}\text{C}$ , followed by rapid cooling, simulations show that the cells do not shrink below their tolerable volume (50-140% of isotonic volume) as described by Pegg (16). Therefore, they are not likely damaged by osmotic stresses. However, the amount of supercooling is high during rapid cooling, and because the cells were slowly cooled to a relatively high subzero temperature, less external ice forms, external solute concentrations remain low, and not much intracellular water was

lost. Furthermore, there was little additional loss of intracellular water during rapid cooling, resulting in a high probability of intracellular ice formation. Under these conditions, the intracellular electrolyte concentration also remained low. It appeared from the simulations that HCEC monolayers cooled at 1°C/min to –15°C, followed by rapid cooling were likely damaged by intracellular ice formation, which was consistent with the resulting 100% membrane integrity seen in the direct thaw experiments and the loss of membrane integrity after rapid cooling experiments.

Simulations of HCEC monolayers slowly cooled to –40°C, followed by rapid cooling in 1M DMSO and 1M PG showed that the cells shrank below their tolerable limits, indicating that there should have been a loss of membrane integrity in the direct thaw experiments, which was not the case. Damage due to osmotic stresses is dependent on time and temperature, therefore decreasing the length of time of exposure or decreasing the temperature, protects against osmotic damage. The tolerance limits defined by Pegg et al. were established with exposure for 5 minutes at 20°C (16), therefore at subzero temperatures these limits may be different, as seen by the recovery of the HCEC monolayers in the graded freezing experiments. Although simulations are extremely important in predicting low temperature responses, it is still important to perform experiments, as there are a number of variables that can affect the cryopreservation outcomes that cannot be accurately predicted by the simulations as shown in this example. Also shown by the simulations is the high degree of supercooling during rapid cooling, and, if the cells still contain osmotically active intracellular water, the

probability of intracellular ice formation is high. The intracellular electrolyte concentration was high under these conditions, due to the large amount of intracellular water lost during slow cooling in response to external ice formation and increasing extracellular solute concentrations. However, from the direct thaw experiments, with virtually 100% membrane integrity, we saw that this electrolyte concentration was not damaging. Therefore, the HCEC monolayers have most likely been damaged by intracellular ice formation upon rapid cooling.

Simulations of the HCEC monolayers in 2M or 4M DMSO and PG with slow cooling to  $-15^{\circ}\text{C}$  or  $-40^{\circ}\text{C}$  followed by rapid cooling predict responses that have similar conclusions to the simulations of graded freezing experiments in 1M DMSO and 1M PG. The endothelial cells did not shrink below tolerable volume limits and intracellular electrolyte concentrations were maintained at low levels, indicating that these were not the likely causes of damage. Again, there are high degrees of supercooling, demonstrating that intracellular ice formation is the likely cause of damage after rapid cooling of HCEC monolayers. The next step to validate these simulations experimentally would be to slowly cool the HCEC monolayers to temperatures below the eutectic temperature to ensure that all external water has been frozen and the cells have lost all osmotically active water to avoid intracellular ice formation.

Something not explained by the simulations is the difference in recovery of HCEC monolayers between rapid cooling to  $-80^{\circ}\text{C}$  and  $-196^{\circ}\text{C}$ . Figs. 1 and 2 show that the HCEC monolayer response to low temperatures is the same whether they are rapidly cooled from experimental temperatures at  $235^{\circ}\text{C}/\text{min}$  to

$-80^{\circ}\text{C}/\text{min}$  or at  $325^{\circ}\text{C}/\text{min}$  to  $-196^{\circ}\text{C}$ , therefore the simulations predict that rapid cooling to  $-80^{\circ}\text{C}$  and  $-196^{\circ}\text{C}$  should have resulted in the same recovery of membrane integrity. This was not supported by the experimental observations. Mazur has shown that cell survival is dependent on the amount of unfrozen water, and, as the unfrozen fraction decreased, so did survival of cells (14). Rapatz et al. observed that as cells froze, they were sequestered between narrow channels of unfrozen solution between the ice, and as the temperature was lowered the channels became narrower (17). The unfrozen fraction may damage cells by the physical forces imposed by the growing ice (14). These physical forces may be responsible for the increased detachment of endothelial cells from the monolayer after rapid cooling to  $-196^{\circ}\text{C}$  versus  $-80^{\circ}\text{C}$ . At  $-80^{\circ}\text{C}$  there would be a higher unfrozen fraction, than at  $-196^{\circ}\text{C}$  (because liquid water does not exist below  $-130^{\circ}\text{C}$  (14)), which may explain the differences in membrane integrity and detachment results of the HCEC monolayers. However, the difference in the unfrozen fraction will be small.

Another hypothesis, discussed in chapter 2, to explain the differences in recovery of HCEC monolayers after rapid cooling to  $-80^{\circ}\text{C}$  and  $-196^{\circ}\text{C}$ , is a glass transformation of the intracellular contents upon rapid cooling to  $-196^{\circ}\text{C}$ , with damaging devitrification upon warming. The simulations in Fig. 3 when HCEC monolayers are cooled at  $1^{\circ}\text{C}/\text{min}$  to  $-40^{\circ}\text{C}$ , show that the intracellular concentrations of DMSO and PG reach vitrifiable levels. Subsequent rapid cooling to  $-196^{\circ}\text{C}$  cools cells below their glass transformation temperatures ( $-130^{\circ}\text{C}$  for DMSO and  $-110^{\circ}\text{C}$  for PG (10)), therefore intracellular vitrification

could occur. Whereas, rapid cooling to  $-80^{\circ}\text{C}$ , is higher than the glass transformation temperature and the intracellular solution could not vitrify. It has been shown that devitrification is damaging to corneas (4,18,19), and Fahy et al. state that avoiding devitrification is essential to the survival of cells after warming (10). Therefore, if the intracellular solution vitrifies upon rapid cooling to  $-196^{\circ}\text{C}$ , its devitrification upon warming would explain the decrease in membrane integrity after rapid cooling of HCEC monolayers to  $-196^{\circ}\text{C}$  versus  $-80^{\circ}\text{C}$ .

In chapter 2 it was concluded that using a single cryoprotectant for cryopreservation of HCEC monolayers may not be possible, and a combination of cryoprotectants may be required. The next set of simulations examined the low temperature responses of the human corneal endothelial, keratocyte, and epithelial cells in the presence of no cryoprotectant, a permeating cryoprotectant, and a combination of permeating and non-permeating cryoprotectants, and the implications for cryopreservation are discussed.

Figs. 4 and 5 show the volume response of human corneal endothelial, keratocyte, and epithelial cells in the presence of no cryoprotectant, 1M DMSO or PG, and 1M DMSO or PG + 0.3M sucrose. The simulations show that the addition of CPAs (permeating and non-permeating) protects cells by limiting the decrease in volume, compared to cooling without CPA. The addition of non-permeating CPAs increases the amount of intracellular water lost, shown by the lower cell volumes when cells are cooled in the presence of a non-permeating and permeating CPA, compared to a permeating CPA alone. Therefore non-permeating CPAs protect against intracellular ice formation. The addition of a

non-permeating CPA also increases the optimum cooling rate. If 50% of the isotonic volume is considered as the tolerable lower limit, the optimum cooling rates for endothelial, keratocyte, and epithelial cells is around 7, 15, and 1°C/min in 1M DMSO and 30, 30-70, and 20°C/min in 1M DMSO + 0.3M sucrose, respectively. An important consideration when developing cryopreservation procedures is that optimum cooling rates depend on the combination of cryoprotectants chosen, and simulations can be used to estimate optimal cooling rates to be tested experimentally.

Fig. 6 shows the maximum supercooling at varying cooling rates without CPA, in the presence of permeating CPAs and a combination of non-permeating and permeating CPAs. The simulations indicate that the presence of DMSO and PG as well as increasing their concentrations, increases the amount of supercooling. Therefore the optimal cooling rate for the human corneal cells will decrease as permeating CPAs are added and their concentrations increased as was discussed in chapter 4. However, when 0.3M sucrose is combined with 1M DMSO or PG the maximum supercooling is decreased, therefore increasing the optimal cooling rate as compared to adding only a permeating CPA. The optimal cooling rates for human corneal endothelial cells in 1M DMSO and 1M PG are 3 and 7°C/min respectively, and in 1M DMSO or 1M PG + 0.3M sucrose are 7 and 10°C/min, respectively. Again the simulations show that non-permeating CPAs will protect against intracellular ice formation by decreasing the amount of supercooling.

Fig. 7 shows the maximum intracellular electrolyte concentration calculated at various cooling rates for human corneal endothelial, keratocyte, and epithelial cells. When human corneal cells are frozen without CPA the simulations show that the intracellular electrolyte concentration is high if cooled at practical cooling rates, which would damage the cells. The addition of permeating CPAs buffers the electrolyte concentrations, a known mechanism of protection, which is supported by the simulations. DMSO and PG, in low or high concentrations, protect equally well against solution effects damage caused by increasing intracellular electrolyte concentrations as cells are cooled. The addition of sucrose to the CPA mixture also protects cells against increasing intracellular electrolyte concentrations compared to freezing without CPA. However compared to DMSO and PG alone, cells are exposed to higher intracellular electrolyte concentrations when a non-permeating CPA is added. Therefore the addition of non-permeating CPAs to a cryoprotectant mixture increases the optimal cooling rate needed to avoid solution effects injury and maintain the intracellular electrolyte concentration at the same amounts as with a permeating CPA alone.

Fig. 8 shows the maximum intracellular cryoprotectant concentration achieved after cooling to  $-40^{\circ}\text{C}$  at various cooling rates. At cooling rates of  $7^{\circ}\text{C}/\text{min}$  or lower the human corneal endothelial, keratocyte, and epithelial cells achieve high concentrations of intracellular cryoprotectants by losing intracellular water as external ice is formed. These results show that intracellular vitrification, can be achieved after slow cooling of human corneal cells to concentrate the

intracellular cryoprotectants to vitrifiable amounts, warranting further investigation of this cryopreservation protocol. A major obstacle in achieving complete vitrification of a tissue is cellular toxicity of the high concentrations of cryoprotectants needed for equilibration in the tissue before cooling is initiated (3,10). Whereas to achieve intracellular vitrification, vitrifiable intracellular cryoprotectant concentrations can result from concentrating the intracellular solution by loss of cell water as external ice forms during slow cooling. The intracellular solution will vitrify upon rapid cooling to temperatures lower than the glass transformation temperature of the CPA. Concentrating the intracellular solution by loss of intracellular water during slow cooling also enhances vitrification by concentrating intracellular proteins, which has been shown to decrease the concentration of cryoprotectant required for vitrification (10). Intracellular vitrification through this mechanism proposed, would overcome the problems of toxicity and osmotic stresses during addition and removal of high concentrations of cryoprotectants needed for complete vitrification of a tissue. Intracellular vitrification is an attractive idea for bioengineered human corneal equivalents as there has been limited success with conventional cryopreservation of corneas (5,6,7,9,12,13), and vitrification has been difficult because of the toxicity of vitrifiable concentrations of CPAs to corneal endothelial cells (1,2).

Knowledge of osmotic and permeability parameters of the human corneal endothelial, keratocyte, and epithelial cells of the bioengineered human corneal equivalent is critical to theoretically predict low temperature responses and develop cryopreservation procedures that can be tested experimentally. Purely

empirical development of procedures is time consuming and the conditions chosen may not yield optimal conditions for the cryoprotectant being used or the cells being cryopreserved. This was seen in chapter 2 where many conditions were tested experimentally, but recovery of the HCEC monolayers was not improved. Simulating and theoretically predicting the low temperature responses of the HCEC monolayers during graded freezing explained these results. The ability to simulate and predict low temperature responses of the constituent cells of the bioengineered human corneal equivalent will provide a rationale basis for choosing cryoprotectants, concentrations of cryoprotectants, and cooling rates, and will also facilitate and hasten the development of a cryopreservation procedure.

## **5.5 References**

1. Armitage, W.J. Survival of corneal endothelium following exposure to a vitrification solution. *Cryobiology*. **26**, 318-328 (1989).
2. Armitage, W.J., and Easty, D.E. Toxicity to rabbit corneal endothelium of solutions for vitrification. In "Acta XXV Concilium Ophthalmologicum" (F. Blodi et al., Eds.), pp. 375-377. Kugler & Ghedini, Amsterdam, 1987.
3. Armitage, W.J., and Rich, S.J. Vitrification of Organized Tissue. *Cryobiology*. **27**, 483-491 (1990).
4. Bourne, W.M., and Nelson, L.R. Human Corneal Studies with a Vitrification Solution Containing Dimethyl Sulfoxide, Formamide, and 1,2-Propanediol. *Cryobiology*. **31**, 522-530 (1994).

5. Bourne, W.M., Nelson, L.R., and Hodge, D.O. Comparison of Three Methods for Human Corneal Cryopreservation That Utilize Dimethyl Sulfoxide. *Cryobiology*. **39**, 47-57 (1999).
6. Canals, M., Costa, J., Potau, J.M., Merindano, M.D., Pita, D., and Ruano, D. Long-term cryopreservation of human donor corneas. *Eur J Ophthalmol*. **6**, 234-241 (1996).
7. Canals, M., Garcia, J., Potau, J.M., Dalmases, C., Costa-Vila, J., and Miralles, A. Optimization of a method for the cryopreservation of rabbit corneas: Attempted application to human corneas. *Cell and Tissue Banking*. **1**, 271-278 (2000).
8. Doebbler, G.F. Cryoprotective compounds. Review and discussion of structure and function. *Cryobiology*. **3**, 2-11 (1966).
9. Hagenah, M., and Bohnke, M. Corneal Cryopreservation with Chondroitin Sulfate. *Cryobiology*. **30**, 396-406 (1993).
10. Fahy, G.M., MacFarlane, D.R., Angell, C.A., and Meryman, H.T. Vitrification as an approach to cryopreservation. *Cryobiology*. **21**, 407-426 (1984).
11. Karlsson, J.O.M., and Toner, M. Long-term storage of tissues by cryopreservation: critical issues. *Biomaterials*. **17**, 243-256 (1996).
12. Madden, P.W., and Easty, D.L. An Investigation of Damage During Corneal Cryopreservation II. With temperature reduction to  $-196^{\circ}\text{C}$ . *Cryo-Letters*. **7**, 162-169 (1986).

13. Madden, P.W., Taylor, M.J., Hunt, C.J., and Pegg, D.E. The Effect of Polyvinylpyrrolidone and the Cooling Rate during Corneal Cryopreservation. *Cryobiology*. **30**, 135-157 (1993).
14. Mazur, P. Freezing of living cells: mechanisms and implications. *Am J Physiol*. **247**, C125-C142 (1984).
15. Meryman, H.T. Cryoprotective agents. *Cryobiology*. **8**, 173-183 (1971).
16. Pegg, D.E., Hunt, C.J, and Fong, L.P. Osmotic properties of the rabbit corneal endothelium and their relevance to cryopreservation. *Cell Biophys*. **10**, 169-189 (1987).
17. Rapatz, G.L, Menz, L.J., and Luyet, B.J. Anatomy of the freezing process in biological materials. *In* "Cryobiology" (H.T. Meryman, Ed.) pp. 139-162. Academic, New York, 1966.aa
18. Rich, S.J., and Armitage, W.J. Corneal Tolerance of Vitrifiable Concentrations of Propane-1,2-diol. *Cryobiology*. **28**, 159-170 (1991).
19. Rich, S.J., and Armitage, W.J. The Potential of an Equimolar combination of Propane-1,2-Diol and Glycerol as a Vitrification Solution for Corneas. *Cryobiology*. **28**, 314-326 (1991).

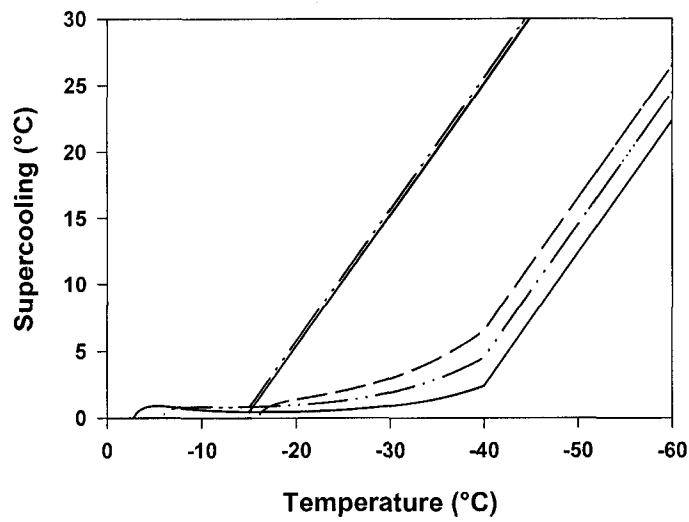
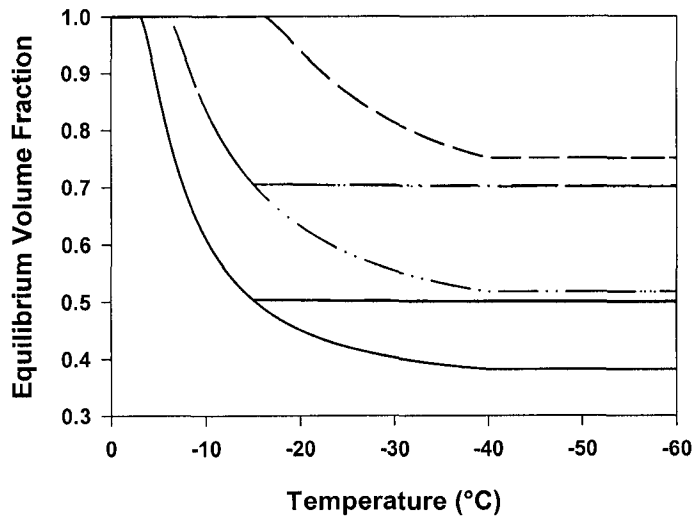
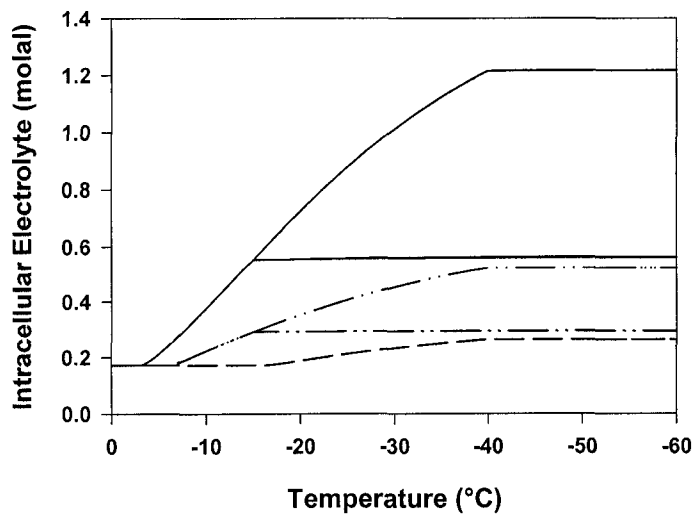


Fig. 1. Simulated responses of human corneal endothelial cells using the graded freezing conditions in chapter 2. Cool at 1°C/min to -15°C or -40°C, in 1M DMSO (solid lines), 2M DMSO (dash-dot lines), and 4M DMSO (dashed lines).



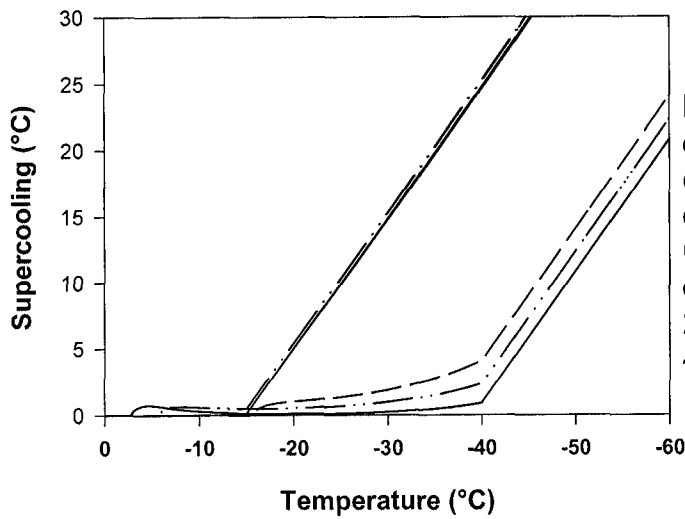
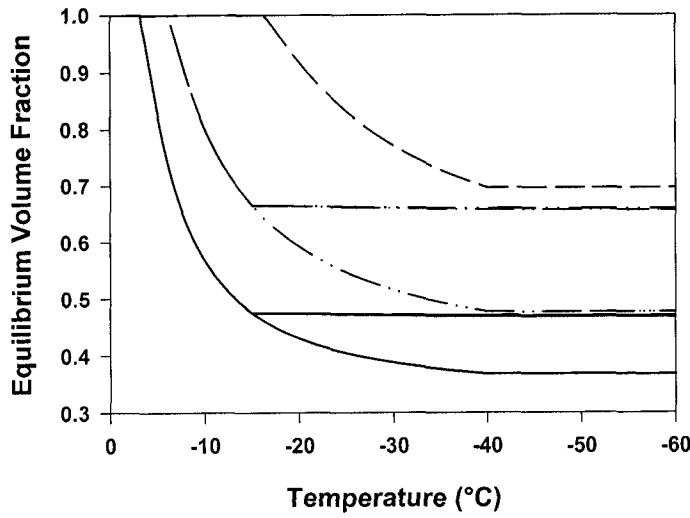
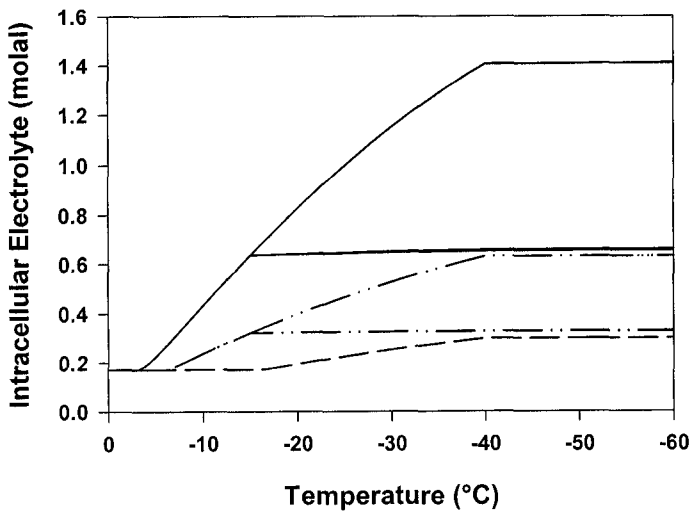


Fig. 2. Simulated responses of human corneal endothelial cells using the graded freezing conditions in chapter 2. Cool at 1°C/min to -15°C or -40°C, in 1M PG (solid lines), 2M PG (dash-dot lines), and 4M PG (dashed lines).



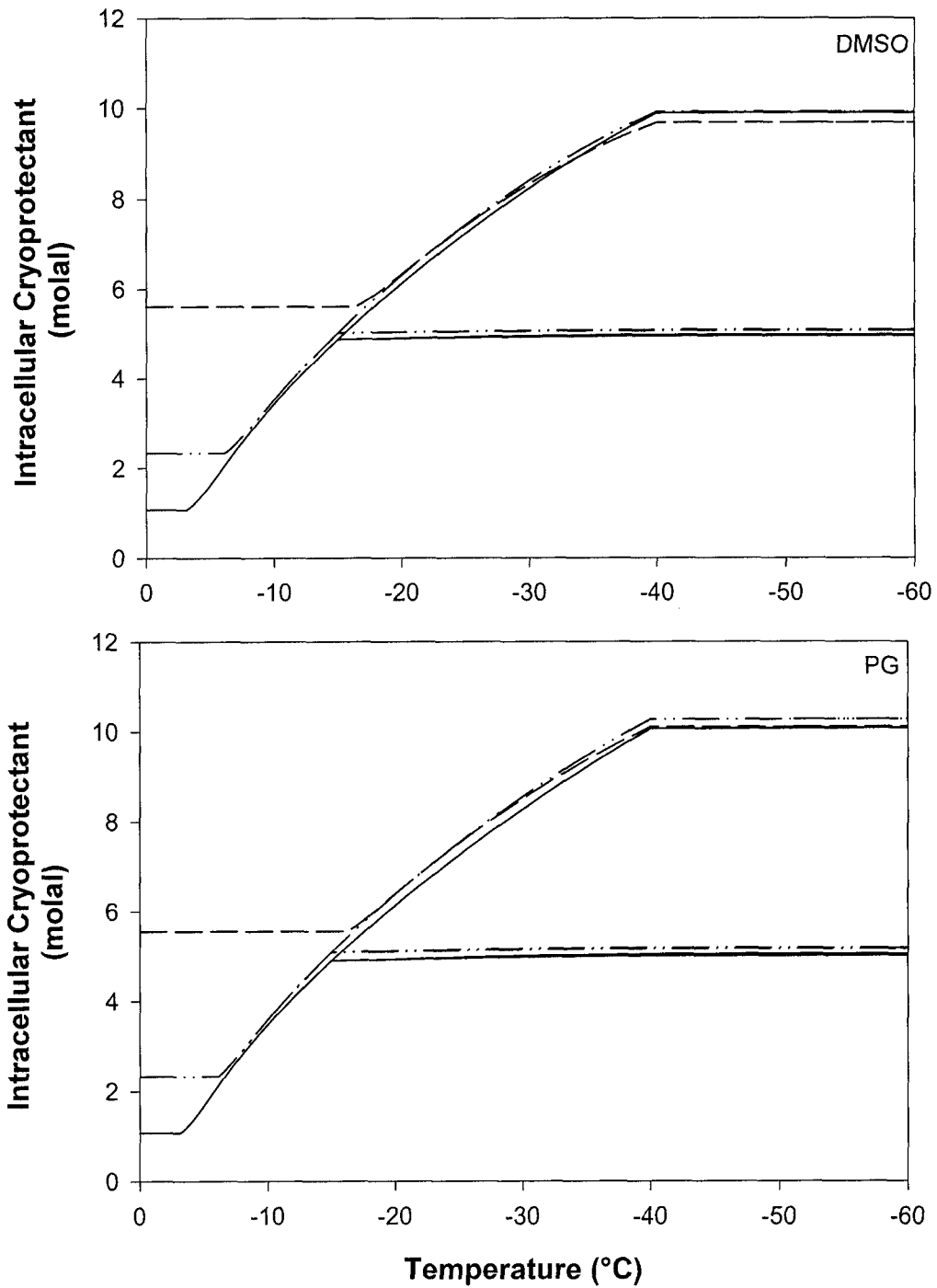


Fig. 3. Simulated responses of intracellular cryoprotectant concentrations of human corneal endothelial cells using the graded freezing conditions in chapter 2. Cool at 1°C/min to -15°C or -40°C, in 1M DMSO or PG (solid lines), 2M DMSO or PG (dash-dot lines), and 4M DMSO or PG (dashed lines).

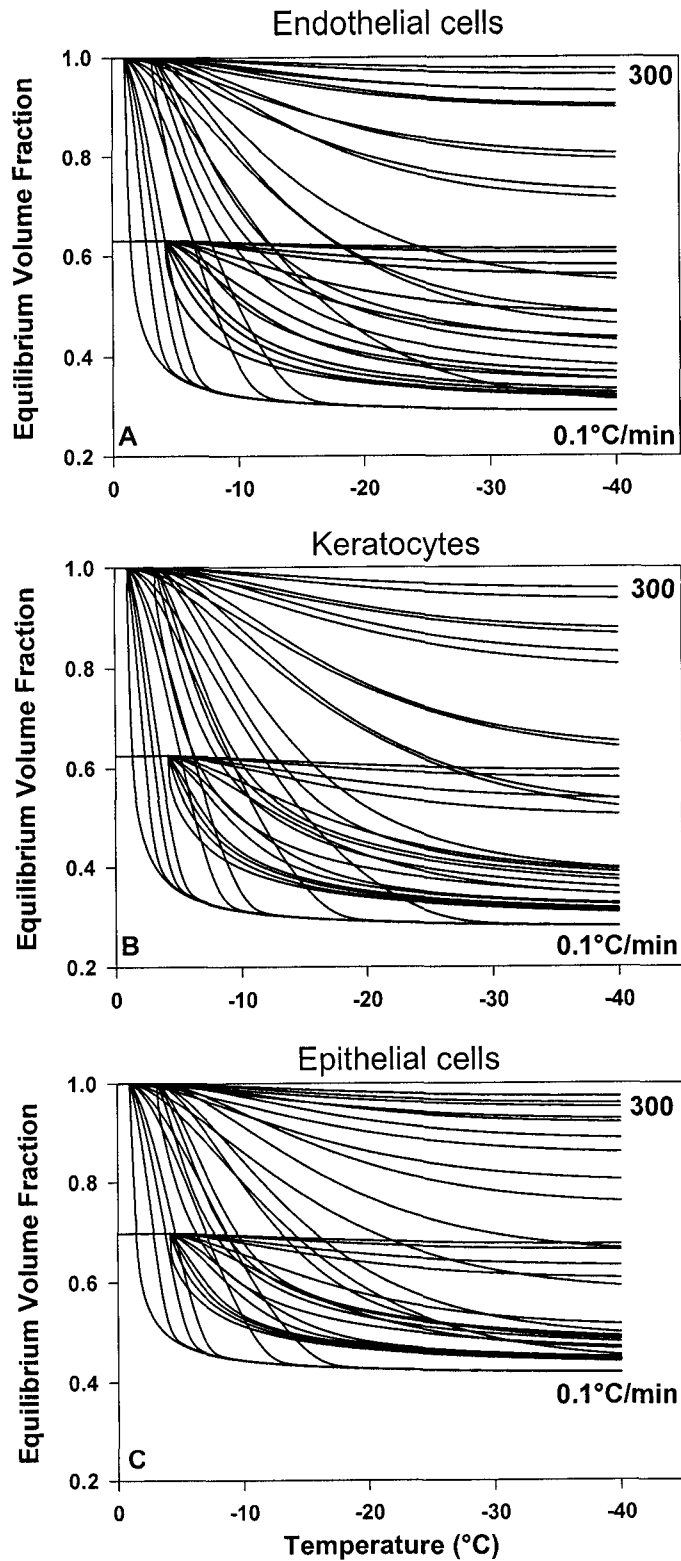


Fig. 4. Simulated volume response of human corneal endothelial (A), keratocyte (B), and epithelial (C) cells cooled at various cooling rates in the presence of no cryoprotectant, 1M DMSO, and 1M DMSO + 0.3M sucrose. Cooling rates were 0.1, 1, 2, 3, 7, 10, 20, 30, 70, 100, 200, and 300°C/min.

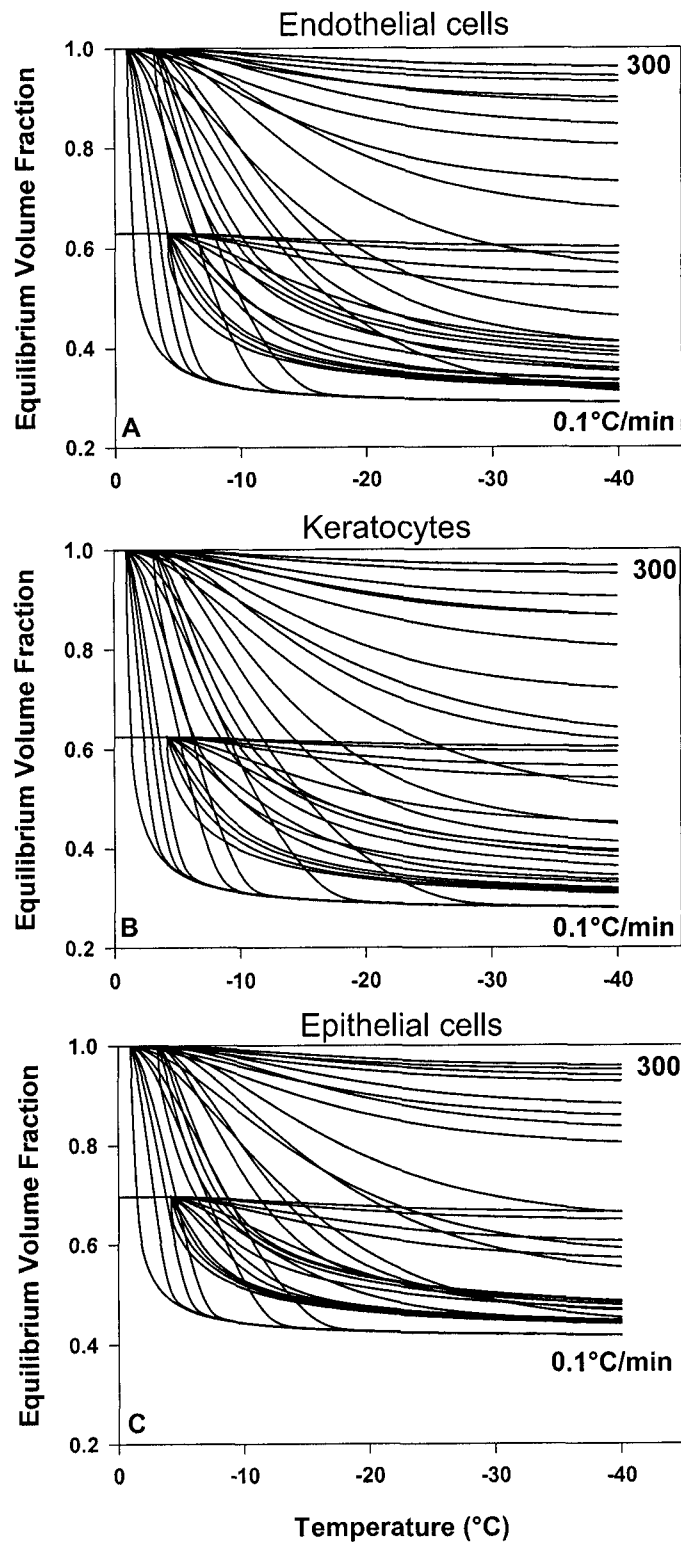


Fig. 5. Simulated volume response of human corneal endothelial (A), keratocyte (B), and epithelial (C) cells cooled at various cooling rates in the presence of no cryoprotectant, 1M PG, and 1M PG + 0.3M sucrose. Cooling rates were 0.1, 1, 2, 3, 7, 10, 20, 30, 70, 100, 200, and 300°C/min.

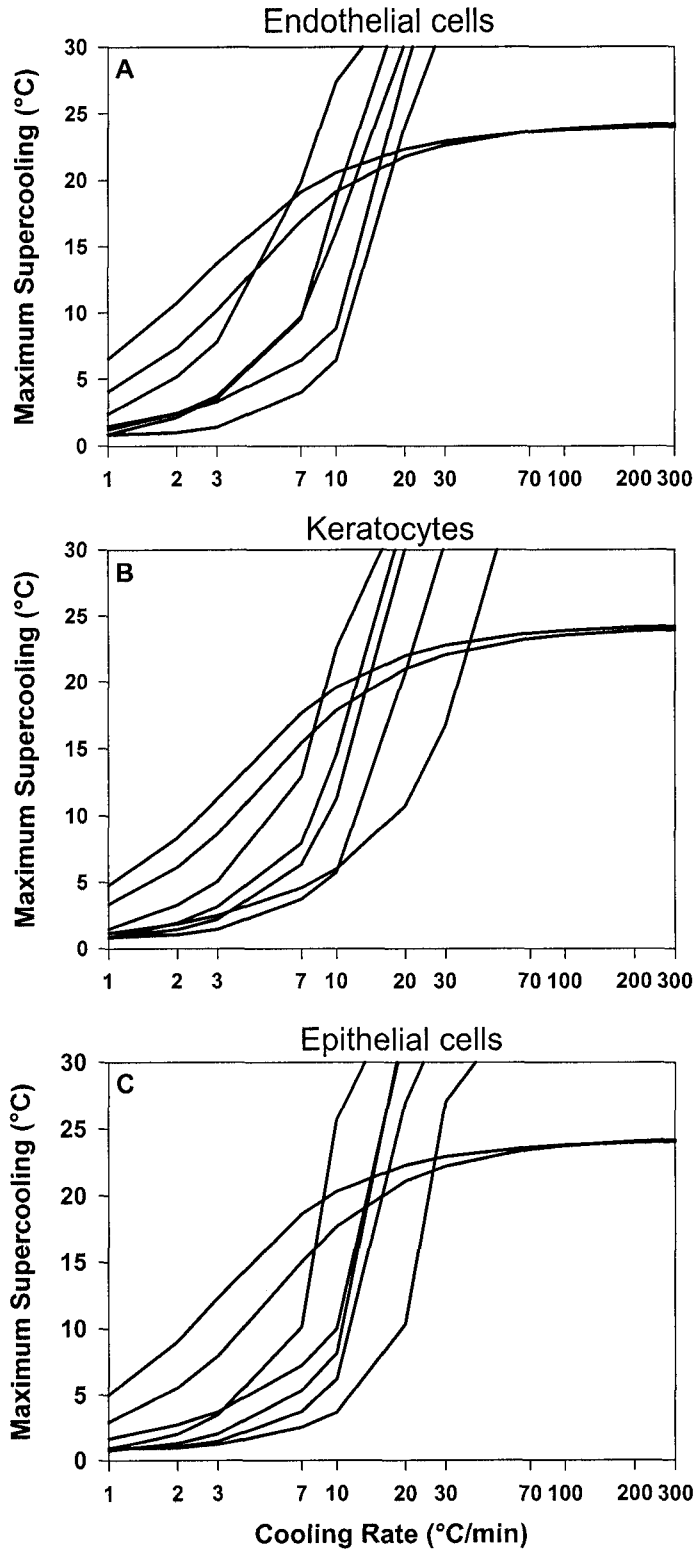


Fig. 6. Maximum supercooling calculated at various cooling rates for human corneal endothelial (A), keratocyte (B), and epithelial (C) cells in the presence of no cryoprotectant, 1M DMSO, 1M PG, 4M DMSO, 4M PG, 1M DMSO + 0.3M sucrose, and 1M PG + 0.3M sucrose.

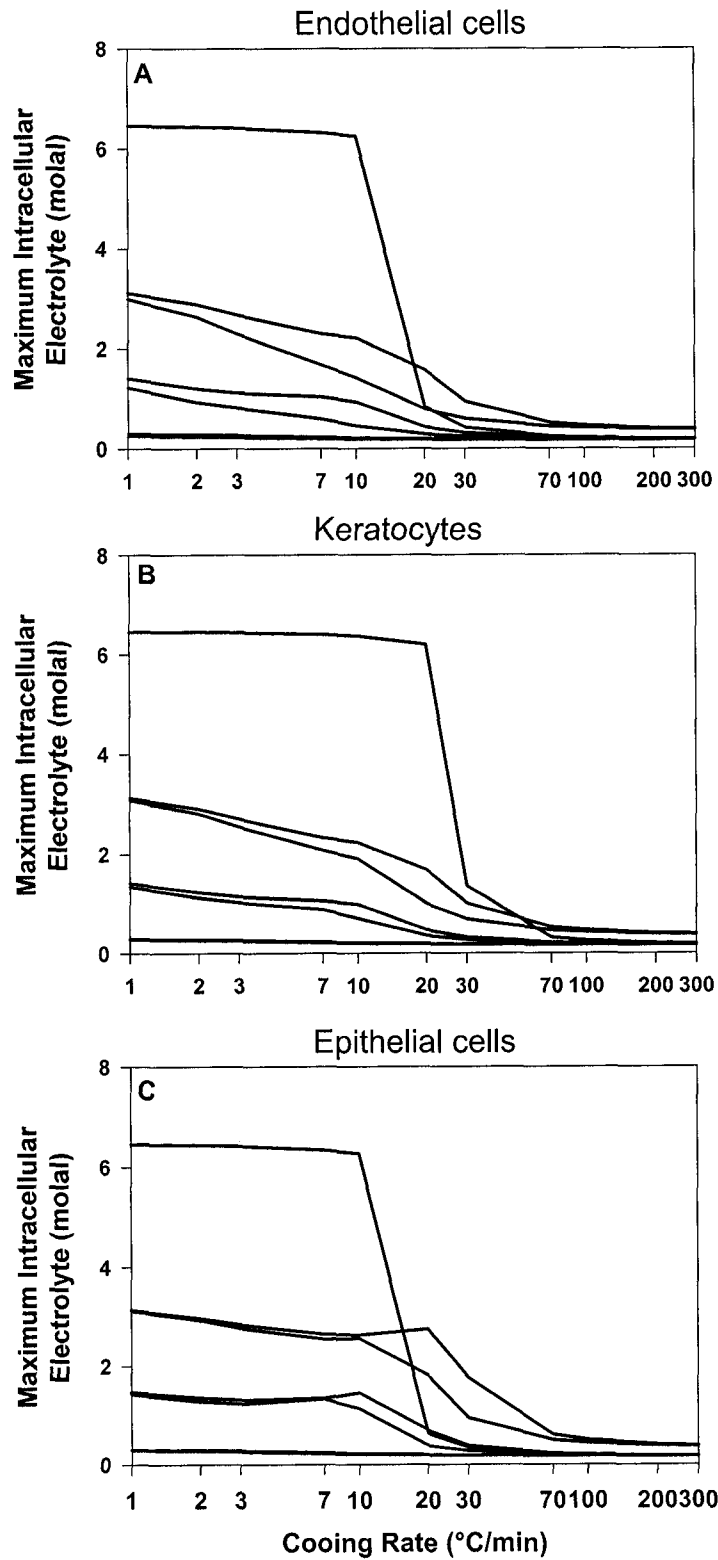


Fig. 7. Maximum intracellular electrolyte concentration calculated at various cooling rates for human corneal endothelial (A), keratocyte (B), and epithelial (C) cells in the presence of no cryoprotectant, 1M DMSO, 1M PG, 4M DMSO, 4M PG, 1M DMSO + 0.3M sucrose, and 1M PG + 0.3M sucrose.

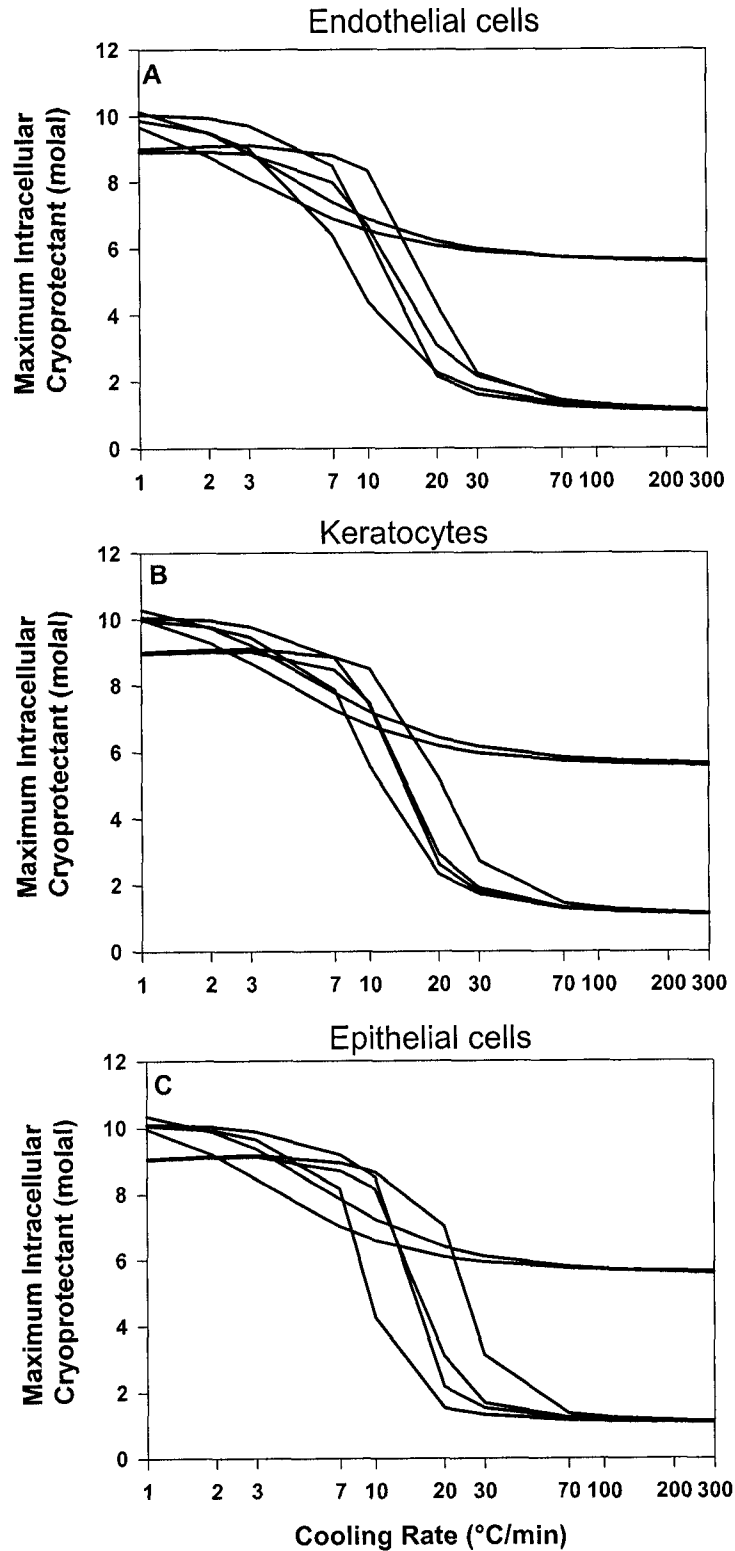


Fig. 8. Maximum intracellular cryoprotectant concentration calculated at various cooling rates for human corneal endothelial (A), keratocyte (B), and epithelial (C) cells in the presence of 1M DMSO, 1M PG, 4M DMSO, 4M PG, 1M DMSO + 0.3M sucrose, and 1M PG + 0.3M sucrose.

## Chapter 6: Conclusion

Successful cryopreservation of tissues has proven to be very difficult. Much of the work done to date has been largely based on empirical experimentation based on procedures successful for cell suspensions and this approach has met with limited success. It now seems that the ability to cryopreserve tissues will require a more methodical approach that addresses the individual components of the tissue separately, and subsequently bringing this knowledge together and applying it to the tissue in its entirety. This thesis describes such an approach and provides a rational, scientific method for developing a cryopreservation protocol for a bioengineered human corneal construct, a process that can be applied to any tissue or bioengineered tissue product.

The first study in this thesis describes the use of an *in vitro* cellular monolayer system designed to mimic the native tissue structure. This human corneal endothelial monolayer system was used in a graded freezing protocol to extend our knowledge of the basic cryobiological properties and mechanisms of cryoinjury. From this study we were able to conclude that solution effects damage is not a significant cause of injury during slow cooling of human corneal endothelial cell monolayers. However, rapid cooling and storage at  $-196^{\circ}\text{C}$  is detrimental to the endothelial cell monolayers. Improved recovery and decrease in detachment is seen with rapid cooling and storage at  $-80^{\circ}\text{C}$ , indicating the need to re-evaluate the final storage conditions for the long-term preservation of bioengineered human corneal constructs and human corneas. The differences in

recovery between storage at  $-80^{\circ}\text{C}$  and  $-196^{\circ}\text{C}$  cannot be explained on the basis of intracellular ice formation alone, therefore a novel hypothesis to explain this additional damage as storage temperatures are lowered has been suggested. The hypothesis identifies a phase transition, glass transformation of the intracellular contents upon rapid cooling to  $-196^{\circ}\text{C}$ , and upon subsequent warming, devitrification of the intracellular contents occurs resulting in increased loss of membrane integrity. Membrane integrity may have also been lost from mechanical damage due to complete freezing of the extracellular solution. Another important contribution is the identification of the ability of pluronic polyols to protect against detachment.

The second and third studies undertaken in this thesis were the determination of cellular osmotic and permeability parameters. These are the first reported values for osmotically inactive fraction, membrane hydraulic conductivity ( $L_p$ ), membrane permeability ( $P_s$ ) to DMSO and PG, and Arrhenius activation energies for  $L_p$  and  $P_s$  for human corneal endothelial, keratocyte, and epithelial cells. Determination of these values is important to show the existence of differences in the osmotic and low temperature responses of the constituent cells in the corneal construct, indicating significant physiological consequences during freezing and thawing of the corneal constructs and making clear the challenge in optimizing a cryopreservation strategy for tissues. Knowledge of these parameters allows the theoretical prediction and mathematical simulation of addition and removal of cryoprotectant, responses of cells to cooling at various rates in different cryoprotectants and combinations of cryoprotectants, which

enables us to optimize cryopreservation conditions that can be tested experimentally.

Mathematical models are powerful tools that can predict osmotic and low temperature responses of cells in tissues and are useful in reducing the scope of empirical experimentation required. In chapter 5 of this thesis mathematical models, which were previously developed and implemented by Dr. Locksley McGann, were used to predict volume changes, amount of supercooling, intracellular electrolyte concentrations, and intracellular cryoprotectant concentrations of human corneal cells during cooling. Simulations were performed to theoretically describe the graded freezing of human corneal endothelial cells and these predictions were used to understand the mechanisms of cryoinjury in the graded freezing experiments. Simulations of the responses of human corneal cells after the addition and removal of different cryoprotectants, and during the sucrose dilution technique for removal of cryoprotectants, were used to elucidate the mechanisms of cryoprotection. Simulations also predicted the increasing concentration of intracellular cryoprotectants during slow cooling to vitrifiable concentrations, which can be used to design a procedure for cryopreservation, using the recently suggested protocol for intracellular vitrification. The ability to simulate low temperature responses of cells in a tissue is critical in an attempt to theoretically describe osmotic and low temperature responses, from which a cryopreservation protocol can be developed and verified experimentally.

From this thesis, general recommendations for the cryopreservation of the bioengineered human corneal construct can be made: 1) further studies should use an appropriate carrier solution such as CP-tes or tissue culture medium, 2) low concentrations (1M) of DMSO and PG will not successfully cryopreserve the endothelial cells, keratocytes, and epithelial cells in the tissue construct as the predicted optimal cooling rates vary significantly, 3) attention needs to be focused on detachment which has been recognized as a major problem, and 4) storage at  $-196^{\circ}\text{C}$  is detrimental to all cells of the biosynthetic corneal construct and storage at  $-80^{\circ}\text{C}$  should be evaluated further with long term storage viability assessments. More specific recommendations for further experimentation on the bioengineered human corneal construct can also be made. Cryopreservation protocols to be verified experimentally are as follows: 1) Corneal constructs equilibrated in 3M PG, cooled at  $2^{\circ}\text{C}/\text{min}$  to  $-40^{\circ}\text{C}$ , plunged and stored at  $-80^{\circ}\text{C}$ . Stepwise addition and dilution of cryoprotectant is needed to avoid damaging osmotic stresses and volume changes. 2) Corneal constructs equilibrated in 2M DMSO + 0.3M sucrose, cooled at  $7^{\circ}\text{C}/\text{min}$  to  $-40^{\circ}\text{C}$ , plunged and stored at  $-80^{\circ}\text{C}$ . Addition of cryoprotectant should be stepwise and dilution can be done directly. 3) Corneal constructs equilibrated with 2M PG + 0.3M pluronic F68, cooled at  $3^{\circ}\text{C}/\text{min}$  to  $-40^{\circ}\text{C}$ , plunged and stored at  $-80^{\circ}\text{C}$ . Addition and dilution of cryoprotectant should be stepwise.

This thesis has described a systematic approach to tissue cryopreservation that can be used to identify mechanisms of cryoinjury through the use of in vitro models systems, and to optimize variables, such as cooling

rate, choice of cryoprotectant and concentrations, and addition and removal procedures for cryoprotectants through theoretical predictions. By combining the knowledge gained through experimentation and mathematical modelling, a cryopreservation protocol can be established. The theoretically-derived cryopreservation protocol can then be verified and optimized through experimentation. This type of approach to the cryopreservation of tissues establishes a scientific and theoretical basis for the development of tissue cryopreservation protocols and can be applied to any tissue or bioengineered human construct.

## **Appendix A: Low Temperature Responses of Human Corneal Keratocytes and Epithelial Cells**

### **A.1 Introduction**

Most of the research investigating cryopreservation of corneas has only taken into consideration the recovery of the endothelium (6). This is because the function of the cornea is to maintain transparency, which is a result of its hydration that is controlled by the barrier and pump functions of the endothelial monolayer (4,6). Also, in clinical transplantation, corneas are assessed for suitability by examination and cell count of the endothelium, without regard for the stroma and epithelium and current preservation procedures have been developed to maintain viability of the corneal endothelium. Therefore, loss of viability or loss of endothelial cells as a result of poor preservation will result in an edematous, cloudy cornea that cannot function in vivo.

However, when considering the cryopreservation of a bioengineered human corneal construct, it is important to be able to successfully preserve all the constituent cells, as the applications of the engineered corneal equivalents include transplantation, biomedical research, and as a replacement for animals for irritancy and drug efficacy testing (3).

A recent review on keratocytes and their function has identified the importance of these cells in maintaining corneal health and transparency by regulating corneal stroma constituents, forming a communicating network, and maintaining structural integrity of the collagen lamellar organization (5). Snyder et

al state that keratocyte health must also be considered when investigating any and all new procedures and treatments (5).

There have been a few studies looking at the cryopreservation of corneal keratocytes; unfortunately there have been no previous studies on the cryopreservation of corneal epithelium.

A previous study by Armitage and Juss found that rabbit corneal keratocytes frozen in suspension had different low temperature responses when frozen as a monolayer (1), reinforcing the inability to apply cryopreservation protocols designed for cells in suspension to tissues. They also found that keratocytes in a monolayer had better recovery if frozen at lower cooling rates (i.e.  $0.2^{\circ}\text{C}/\text{min}$ ) (1).

Another study looked at cryopreservation of human corneal keratocytes in suspension, where they achieved relatively high recovery using 10% DMSO and human albumin and direct transfer of the keratocytes from  $0^{\circ}\text{C}$  into a  $-80^{\circ}\text{C}$  freezer (2). The findings from this study will likely not be used for developing a cryopreservation protocol for intact corneas, because of the difference in low temperature responses of cells in suspension versus cells in a tissue matrix.

This study uses a primary human corneal keratocyte and epithelial cell line, that is morphologically, biochemically, and electrophysiologically similar to freshly isolated human corneal cells (3). The objective of the study is to extend our understanding of the basic low temperature responses through preliminary experiments using isolated human corneal keratocytes and epithelial cells cultured as confluent monolayers to model the native tissue structure.

## **A.2 Materials and Methods**

### *Human Corneal Cell Culture*

Human corneal keratocytes and epithelial cells (a gift from Dr. May Griffiths, University of Ottawa) were incubated at 37°C in 5% carbon dioxide in Medium 199 with 10% v/v fetal bovine serum (GIBCO BRL, Burlington, Canada), and supplemented with 1% v/v insulin transferrin selenium (Sigma, Mississauga, Canada). Cells were grown in 75cm<sup>2</sup> Falcon tissue culture flask (VWR, Edmonton, Canada) and harvested by exposure to 0.05% trypsin-EDTA (GIBCO BRL) solution at 37°C for 2-3 minutes. The cells were re-suspended in supplemented M199 to obtain cell suspensions, and plated on sterilized coverslips (12mm circle, Fisher Brand; Fisher Scientific, Edmonton, Canada) precoated with bovine collagen type I (sigma). The cells were allowed to grow into a confluent monolayer on the coverslips for use in freezing experiments.

### *Assessment of Monolayer Recovery*

A dual fluorescent stain, SYTO 13 (SYTO; Molecular Probes, Eugene, OR) and ethidium bromide (EB; Sigma) was used to assess membrane integrity of the human corneal keratocyte and epithelial cell monolayers. SYTO enters cells and stains the nucleic acids green. EB enters cells that have lost membrane integrity and stains the nucleic acids red. The final staining solution contained 12.5µM SYTO and 25µM EB in phosphate buffered saline (PBS; Gibco BRL). Cell monolayers were stained with 20µl of SYTO/EB solution for 5 min at 22°C and examined with a Zeiss fluorescent microscope. Representative images were captured with a Polaroid DMCIe camera and counted with in-house software. Cell

recovery is expressed as the percentage of cells with intact membranes in the monolayer after treatment.

The monolayers were also subjectively rated for cell detachment from the glass coverslips. Subjective measurements were assigned as 0 for no detachment, 1 for mild, 2 for moderate, 3 for severe and 4 for complete detachment.

### *Experimental Solutions*

The experimental solutions used in the freezing experiments were 2M DMSO, 2M PG or isotonic PBS. The final concentrations of cryoprotectants were 1M DMSO and 1M PG in the experimental samples.

### *Graded Freezing Experiments*

Coverslips with keratocyte and epithelial cell monolayers were placed in 10ml glass vials (Kimble; Fisher Scientific) containing 100 $\mu$ l of isotonic PBS with the monolayers facing up, then 100 $\mu$ l of experimental solution was added. Monolayers were equilibrated with the experimental solution for 5 min at 22°C, and then immersed in ice water for 5 min. The vials were then placed into a programmable rate freezer (FTS systems, Stoneridge, NY) at -5°C and held for 5 min for temperature equilibration. Ice was nucleated in the experimental solution using a cooled copper probe and the temperature maintained for 1 min to allow release of the latent heat of fusion. The vials were cooled at 1°C/min to various subzero temperatures (-5, -10, -15, -20, -30, -40°C) and either thawed directly at 480°C/min in a 37°C water bath or cooled at 325°C/min to -196°C or at 235°C/min to -80°C for storage before thawing. Control monolayers were not

placed into the programmable rate freezer, but were taken from the ice water and placed into the 37°C water bath for 1 min before assessment. Monolayers were assessed immediately after thawing for membrane integrity and detachment. Triplicate samples were used for each experimental condition, and experiments were repeated 3 times.

### **A.3. Results/Discussion**

#### *Control Monolayers*

The human corneal keratocyte and epithelial cell monolayers used as controls showed 98±2% membrane integrity and no detachment, indicating that 1M DMSO and 1M PG were not toxic and the addition protocol for the cryoprotectants did not damage the cells.

#### *Graded Freezing of Human Corneal Keratocyte Cell Monolayers*

Fig. 1A shows loss of membrane integrity and detachment of human corneal keratocytes after direct thaw from the experimental temperatures in the three experimental solutions. Monolayers frozen without cryoprotectant show an increasing loss of membrane integrity and increase in detachment as the experimental temperatures are lowered. The addition of 1M DMSO and 1M PG resulted in very high recovery of membrane integrity at all experimental temperatures. However, the presence of cryoprotectants did not decrease the detachment at any of the experimental temperatures. The results in Fig. 1A showed that human corneal keratocytes tolerate the increase in solute concentrations as cells are cooled slowly and damage caused by solution effects can be overcome by the addition of cryoprotectants.

Fig. 1B shows the results of rapid cooling keratocyte monolayers to  $-196^{\circ}\text{C}$  from the experimental temperatures. Cooling in all the experimental solutions resulted in virtually complete loss of keratocyte membrane integrity and moderate to severe cell detachment, especially in the presence of 1M PG. Human corneal keratocytes do not tolerate rapid cooling and storage to  $-196^{\circ}\text{C}$ .

Fig. 1C shows the results when keratocyte monolayers are rapidly cooled to  $-80^{\circ}\text{C}$  from the experimental temperatures. Without cryoprotectant there was no maintenance of membrane integrity and moderate to severe detachment, which was no different from the results seen after rapid cool to  $-196^{\circ}\text{C}$ . However, monolayers frozen in 1M DMSO or 1M PG and stored at  $-80^{\circ}\text{C}$  resulted in some recovery of membrane integrity, with maximum recovery of about 40% after slow cooling to  $-40^{\circ}\text{C}$ , before rapid cool to  $-80^{\circ}\text{C}$ . Storage at  $-80^{\circ}\text{C}$ , also decreased the detachment to slight after slow cooling to  $-40^{\circ}\text{C}$ , followed by rapid cooling to  $-80^{\circ}\text{C}$ . Storage at  $-80^{\circ}\text{C}$ , resulted in better recovery and decreased detachment of the human corneal keratocyte monolayers as compared to storage at  $-196^{\circ}\text{C}$ .

An important consideration when interpreting monolayer results for human corneal keratocytes is that detachment may not be as important a factor for the keratocytes as compared to the endothelial and epithelial cells that are the outermost layers of the cornea. Because the keratocytes are embedded within the extracellular matrix of the cornea, it is likely that detachment and loss of cells from the stromal matrix will not be a factor that has to be considered for cryopreservation of the bioengineered human corneal equivalent. Therefore, the

membrane integrity results are the most important outcome and not the amount of detachment from this study.

#### *Graded Freezing of Human Corneal Epithelial Cell Monolayers*

The results of slow cooling epithelial cell monolayers to experimental temperatures followed by direct thaw are shown in Fig. 2A. When the monolayers are cooled without cryoprotectant there is approximately 40% maintenance of membrane integrity and slight detachment at all experimental temperatures. When 1M DMSO or 1M PG is added, the membrane integrity is about 80% when frozen in the presence of PG and about 90% in the presence of DMSO, and there is only slight detachment in the presence of both DMSO and PG. During slow cooling of human corneal epithelial cells cryoprotectants effectively protect against solution effects damage and detachment is not a factor during slow cooling of the epithelial cell monolayers.

Fig. 2B shows the results after rapid cooling to  $-196^{\circ}\text{C}$  of the epithelial cell monolayers from the experimental temperatures, and in all experimental solutions used there was no recovery of membrane integrity under any condition tested. The presence of cryoprotectant also did not alter the amount of detachment and severe detachment was seen after rapid cooling from higher subzero temperatures, with a subsequent decrease in detachment to moderate when monolayers were rapidly cooled to  $-196^{\circ}\text{C}$  from lower subzero temperatures.

Fig. 2C shows the response of human corneal epithelial cell monolayers after rapid cooling to  $-80^{\circ}\text{C}$  from experimental temperatures. The monolayers

frozen without cryoprotectant show no maintenance of membrane integrity and severe detachment at the higher subzero temperatures with a subsequent decrease in detachment at the lower subzero temperatures, however these results are not different from the results seen after rapid cooling to  $-196^{\circ}\text{C}$ . With the addition of 1M DMSO or 1M PG there is about 25-30% maintenance of membrane integrity and the amount of detachment lessens from severe to slight as the experimental temperature is lowered. Therefore, there does seem to be some improvement in recovery, increase in membrane integrity and decrease in detachment, when human corneal epithelial cells are rapidly cooled and stored at  $-80^{\circ}\text{C}$  versus rapid cooling and storage at  $-196^{\circ}\text{C}$ .

The low temperature responses of human corneal keratocytes and epithelial cells are consistent with the results from graded freezing of human corneal endothelial cells in chapter 2, in that storage at  $-196^{\circ}\text{C}$  was detrimental to the recovery of the monolayers and storage at  $-80^{\circ}\text{C}$  improved recovery.

## A.5 References

1. Armitage, W.J., and Juss, B.K. The influence of cooling rate on survival of frozen cells differs in monolayers and in suspensions. *Cryo-Letters*. **17**, 213-218 (1996).
2. Borderie, V.M., Lopez, M., Lombet, A., Carvajal-Gonzalez, S., Cywiner, C., and Laroche, L. Cryopreservation and culture of human corneal keratocytes. *Invest Ophthalmol Vis Sci*. **40**, 1511-1519 (1998).
3. Griffith, M., Osborne, R., Munger, R., Xiong, X., Doillon, C.J. Laycock, N.L.C., Hakim, M., Song, Y., and Watsky, M.A. Functional human corneal equivalents constructed from cell lines. *Science*. **286**, 2169-2172 (1999).
4. Klyce, S.D., and Beuerman, R.W. Structure and function of the cornea. In "The Cornea" (H.E. Kaufman, B.A. Baron, M.B. McDonald, and S.R. Waltman, Eds.), pp. 3-54. Churchill Livingstone, New York, 1988.
5. Snyder, M.C., Bergmanson, J.P.G., and Doughty, M.J. Keratocytes: no more the quiet cells. *J Am Optom Assoc*. **69**, 180-187 (1998).
6. Taylor, M.J. Clinical cryobiology of tissues: preservation of corneas. *Cryobiology*. **23**, 323-353 (1986).

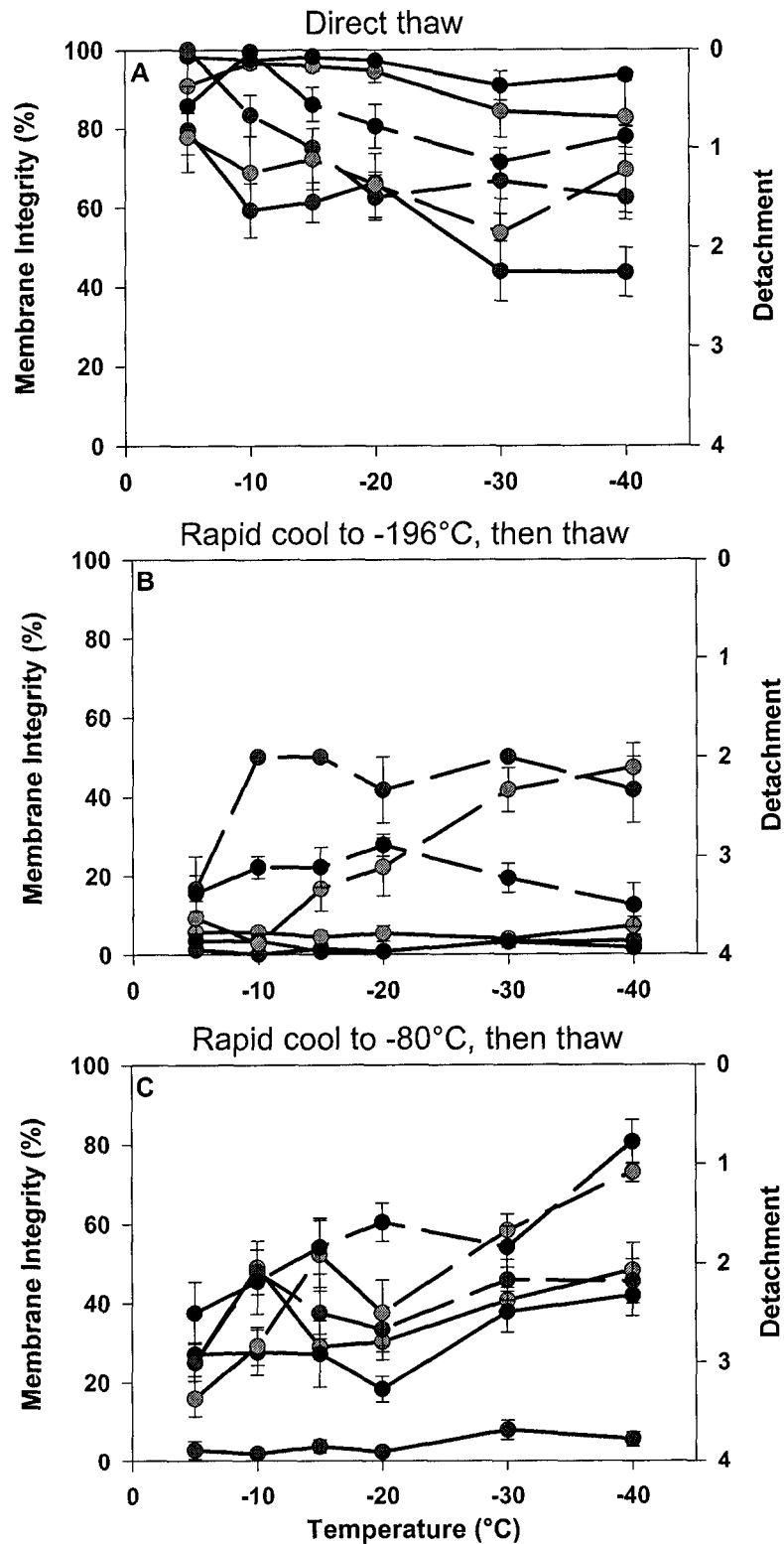


Fig. 1. Comparison of the membrane integrity (solid line) and detachment (dashed lines) of human corneal keratocytes frozen in isotonic PBS, 1M DMSO, or 1M PG following controlled cooling to experimental temperatures. A) direct thaw from experimental temperatures, B) rapid cooling to  $-196^{\circ}\text{C}$  before thawing, and C) rapid cooling to  $-80^{\circ}\text{C}$  before thawing.

Detachment: 0 = none, 1 = mild, 2 = moderate, 3 = severe, 4 = complete.

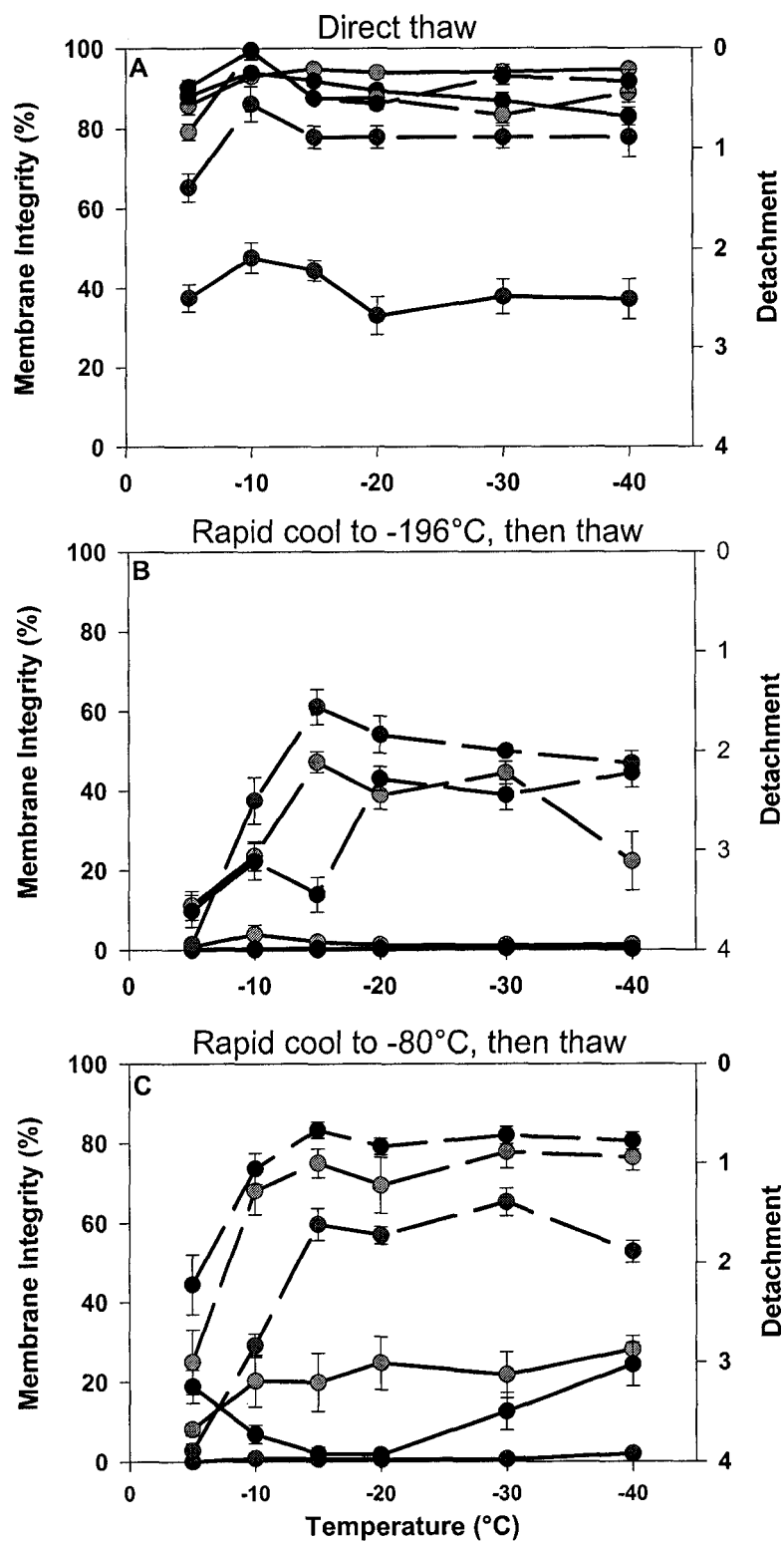


Fig. 2. Comparison of the membrane integrity (solid lines) and detachment (dashed lines) of human corneal epithelial cells frozen in isotonic PBS, 1M DMSO, or 1M PG following controlled cooling to experimental temperatures. A) direct thaw from experimental temperatures, B) rapid cooling to  $-196^{\circ}\text{C}$ , before thawing, and C) rapid cooling to  $-80^{\circ}\text{C}$  before thawing. Detachment: 0 = none, 1 = mild, 2 = moderate, 3 = severe, 4 = complete.

## **Appendix B: Determination of Appropriate Measure of Central Tendency for Analysis of Osmotic Parameters**

### **B.1 Introduction**

Determination of osmotic and permeability parameters (chapter 3 and 4) requires measurements of cell volume as a function of time upon exposure to anisosmotic conditions. Typically, the mean is used to determine the 'average' volume that represents the cell population. However, the measure of central tendency chosen to determine the average volumes affects the calculated parameters (i.e.  $L_p$ ,  $V_b$ ,  $P_s$ ) (3). Armitage and Juss showed that cell volume distributions for keratocytes were positively skewed, which is typical for mammalian cells, and suggested that using mode to determine 'averages' may be more applicable (1).

This study uses a primary human corneal endothelial cell line. The objective of the study is to determine which measure of central tendency is the most appropriate for analysis of cellular osmotic parameters, using the process reported by Elmoazzen et al. (2).

### **B.2 Materials and Methods**

#### *Human Corneal Cell Culture*

Human corneal endothelial cells (a gift from Dr. May Griffiths, University of Ottawa) were incubated at 37°C in 5% carbon dioxide in Medium 199 with 10% v/v fetal bovine serum (GIBCO BRL, Burlington, Canada), and supplemented with 1% v/v insulin transferrin selenium (Sigma, Mississauga, Canada). Cells were grown in 75cm<sup>2</sup> Falcon tissue culture flask (VWR, Edmonton, Canada) and

harvested by exposure to 0.05% trypsin-EDTA (GIBCO BRL) solution at 37°C for 2-3 minutes. The cells were re-suspended in supplemented M199 to obtain cell suspensions, which were used in determination of osmotic parameters.

#### *Measurement of Isotonic Volume Distribution*

Human corneal endothelial cells were added and mixed with supplemented M199 and cell volume measurements were taken at 22°C using a Coulter counter. The Coulter method is described in detail in chapter 3. Briefly, a Coulter counter (model ZB1; Coulter Inc, Hialeah, FL) was connected to a personal computer via a pulse-height analyzer (The Great Canadian Computer Company, Spruce Grove, Canada), with the accompanying cell size analyzer software, which recorded the time and relative volume of each cell passing through the aperture (5), resulting in a histogram of the relative raw volume distribution under isotonic conditions. The raw volume distributions were converted into a smoothed and log normal volume distributions, and all three of these volume distributions were used in the theoretical simulations of cellular volume response after exposure to anisotonic conditions. Fig. 1 shows the volume distributions of the human corneal endothelial cells.

#### *Simulating Volume Responses*

Simulations were performed using in-house software (Distributions; schematic shown in Fig. 2) designed by Dr. Locksley McGann. The Distributions program creates a population of  $10^4$  to  $10^6$  cells, all with specified osmotic permeability parameters, and with their isotonic volumes distributed to fit a selected volume distribution. The program then calculates the osmotic response

of each individual cell based on the membrane transport model by Jacobs and Stewart (4), and reports the volume distribution as a function of time after exposure to a hypertonic solution.

$$\frac{dV}{dt} = L_p A R T (\pi_i - \pi_e) \quad (1)$$

The simulations were performed using different cell counts (10 000 and 500 000 cells) to test the effect of population size on the determination of cellular osmotic parameters. The resulting volume distributions were averaged using the mean, median, mode, or D32 (the surface area moment mean or Sauter Mean Diameter, and is often used in applications where the active surface area is important) measures of central tendency, using in-house cell size analyzer software (Fig. 3).

#### *Determination of Osmotic Parameters*

These averaged cell volumes as a function of time were then fit for  $L_p$  and  $V_b$  using the procedure previously described in chapter 3. The % error between the fit  $L_p$  and  $V_b$  results and the specified parameters ( $L_p=0.09$  and  $V_b=0.3$ ) was calculated and these error values were used to choose the most appropriate measure of central tendency to calculate average cell volumes.

### **B.3. Results/Discussion**

Figs. 4, 5, and 6 show the volume as a function of time data averaged using different measures of central tendency from simulations using the raw, smoothed, and log normal population distributions for human corneal endothelial cells, respectively. These plots show that D32, mean, and median all result in very little scatter of the volume measurements. However, using mode to calculate

average volume results in very scattered volume measurements and requires smoothing of the data to decrease the scatter, which greatly affects the resulting  $L_p$  and  $V_b$  determinations.

Table 1 and 2 show the resulting  $L_p$  and  $V_b$  values and their corresponding errors from the simulated osmotic volume distributions. When considering cell numbers the amount of error is very similar when low cell numbers or high cell numbers are used to simulate volume distributions, therefore cell number probably does not play a significant role in the determination of osmotic parameters when using the Coulter method. Using median and mode, results in consistently higher values for  $L_p$  and lower values for  $V_b$  when compared to the fixed theoretical parameters. The opposite is true when using D32 and mean, where consistently lower values for  $L_p$  and higher values for  $V_b$  are obtained. In all the population distributions tested, the mean consistently resulted in the lowest error for determining  $L_p$  and  $V_b$ , and therefore was chosen as the measure of central tendency to average volume responses determined for human corneal cells in chapters 3 and 4.

## B.5 References

1. Armitage, W.J., and Juss, B.K. Osmotic response of mammalian cells: Effects of permeating cryoprotectants on nonsolvent volume. *J Cell Physiol.* **168**, 532-538 (1996).
2. Elmoazzen, H.Y., Chan, C.C.V., Acker, J.P., Elliott, J.A.W., and McGann, L.E. The effect of cell size distribution on the predicted responses of cell. *Submitted.* Feb. 2002.
3. Grover, N.B. Naaman, J., Ben-Sasson, S., Doljanski, F., and Nadav, E. Electric sizing of particles in suspensions. I. Theory. *Biophys J.* **9**, 1398-1414 (1969a).
4. Jacobs, M.H., and Stewart, D.R. A simple method for the quantitative measurement of cell permeability. *J Cell Comp Physiol.* **1**, 71-82 (1932).
5. McGann, L.E., Turner, A.R., and Turc, J.M. Microcomputer interface for rapid measurement of average volume using an electronic particle counter. *Med & Biol Eng & Compute.* **20**, 17-20 (1982).

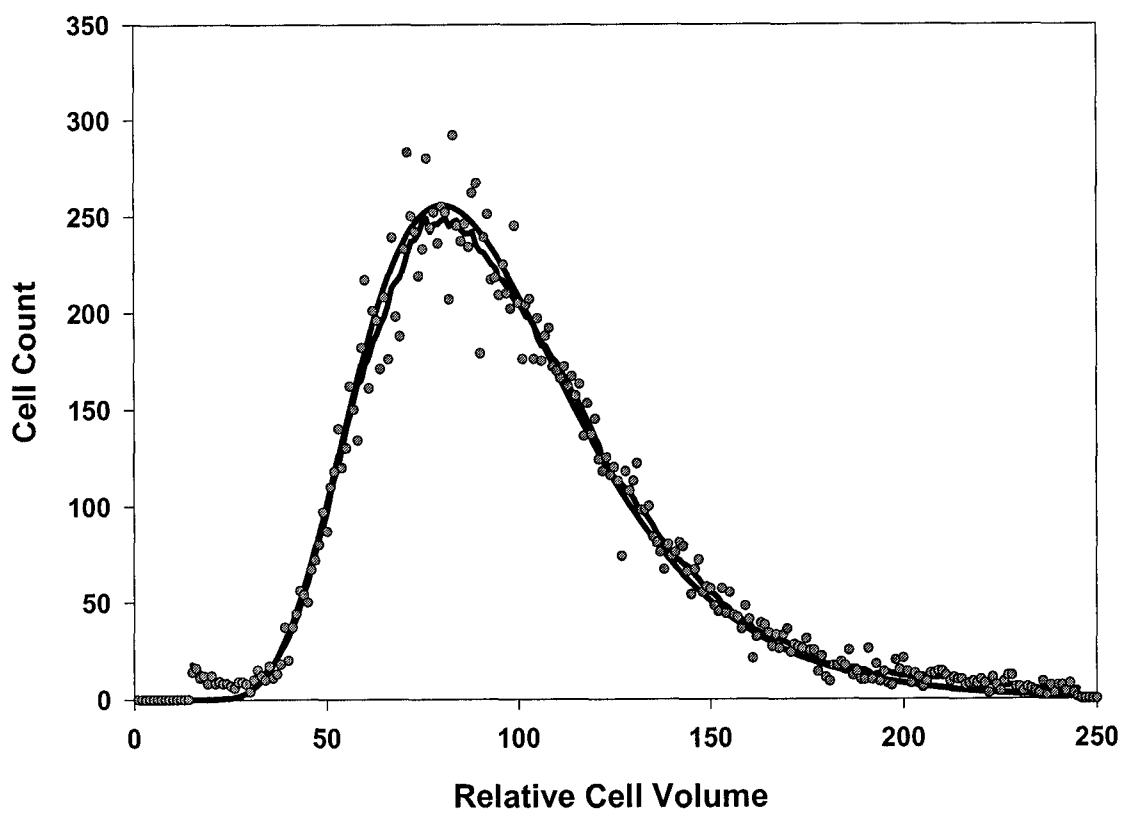


Fig. 1. Raw data, smoothed raw data, and a log normal volume distribution of human corneal endothelial cells at isotonic conditions.

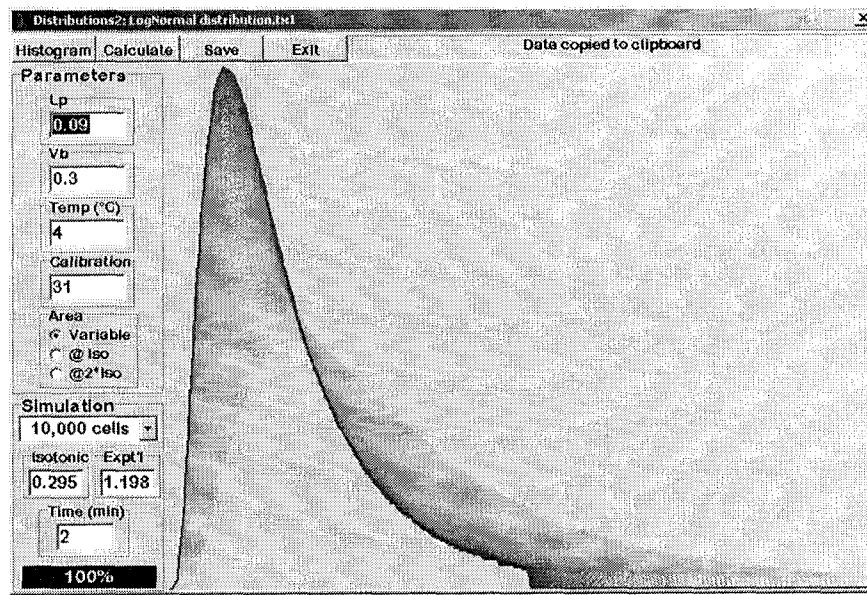


Fig. 2. Distribution program to simulate volume responses of a cell population as a function of time. Resulting data is a representative volume distribution using the user-defined variables as listed in the above figure.

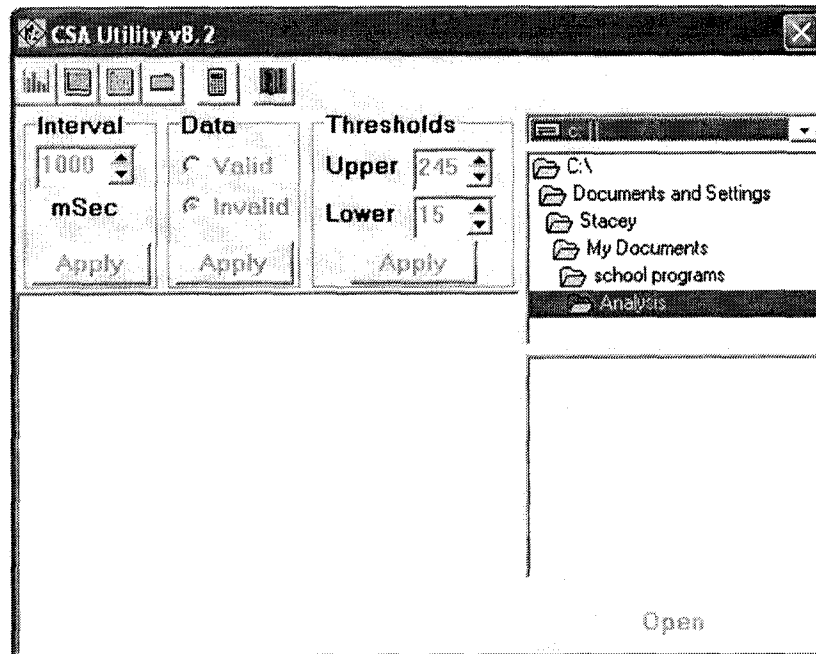


Fig. 3. Cell size analyzer utility program converts volume distributions into text files containing cell volume as a function of time. Cell volumes can be calculated using mean, median, mode or D32.

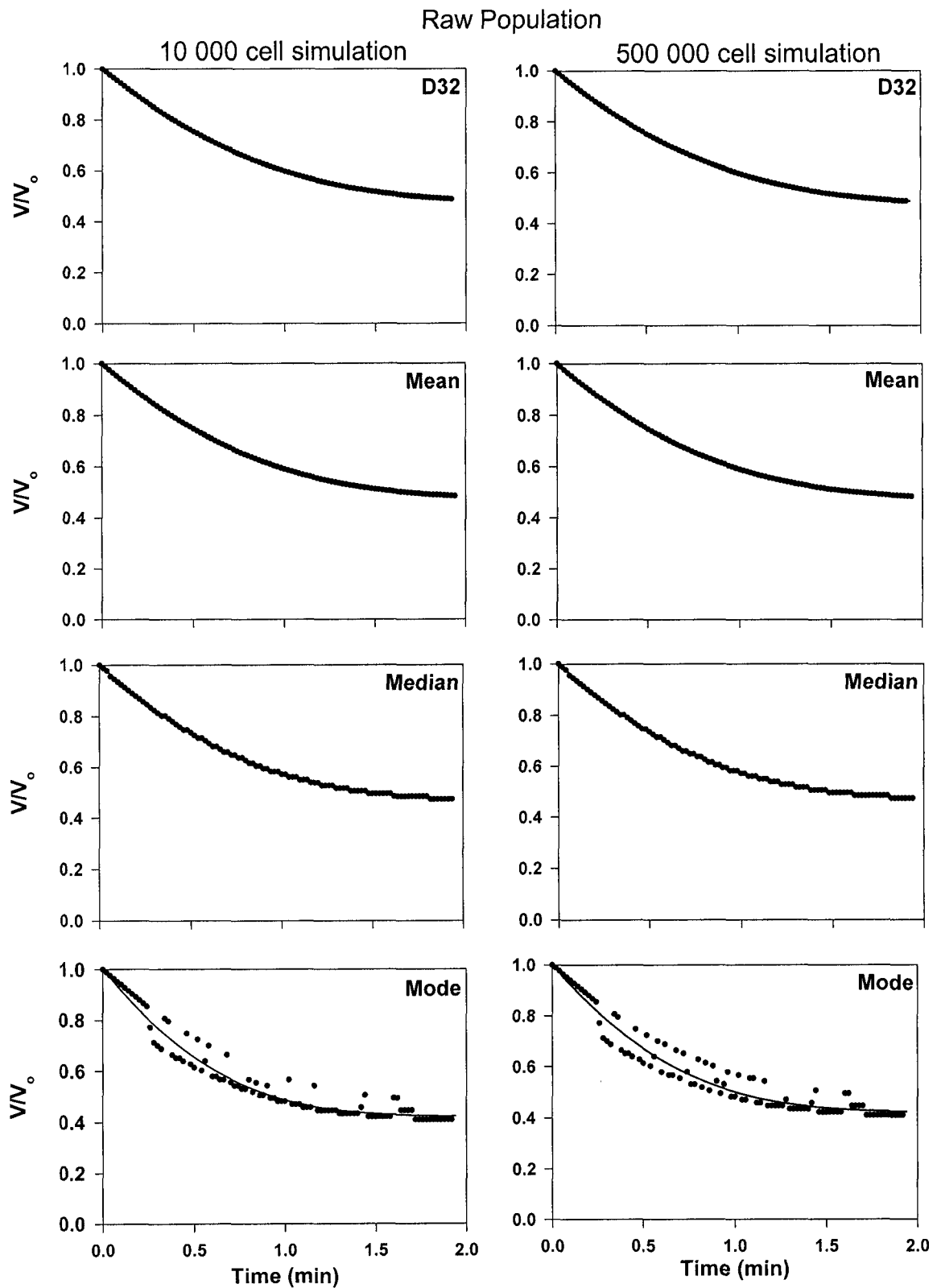


Fig. 4. A representative plot of volume versus time simulated by the distributions program from the raw population distribution of human corneal endothelial cells. The solid lines represent the best fit for  $L_p$  and  $V_b$  using the membrane mass transport model by Jacobs and Stewart (3).

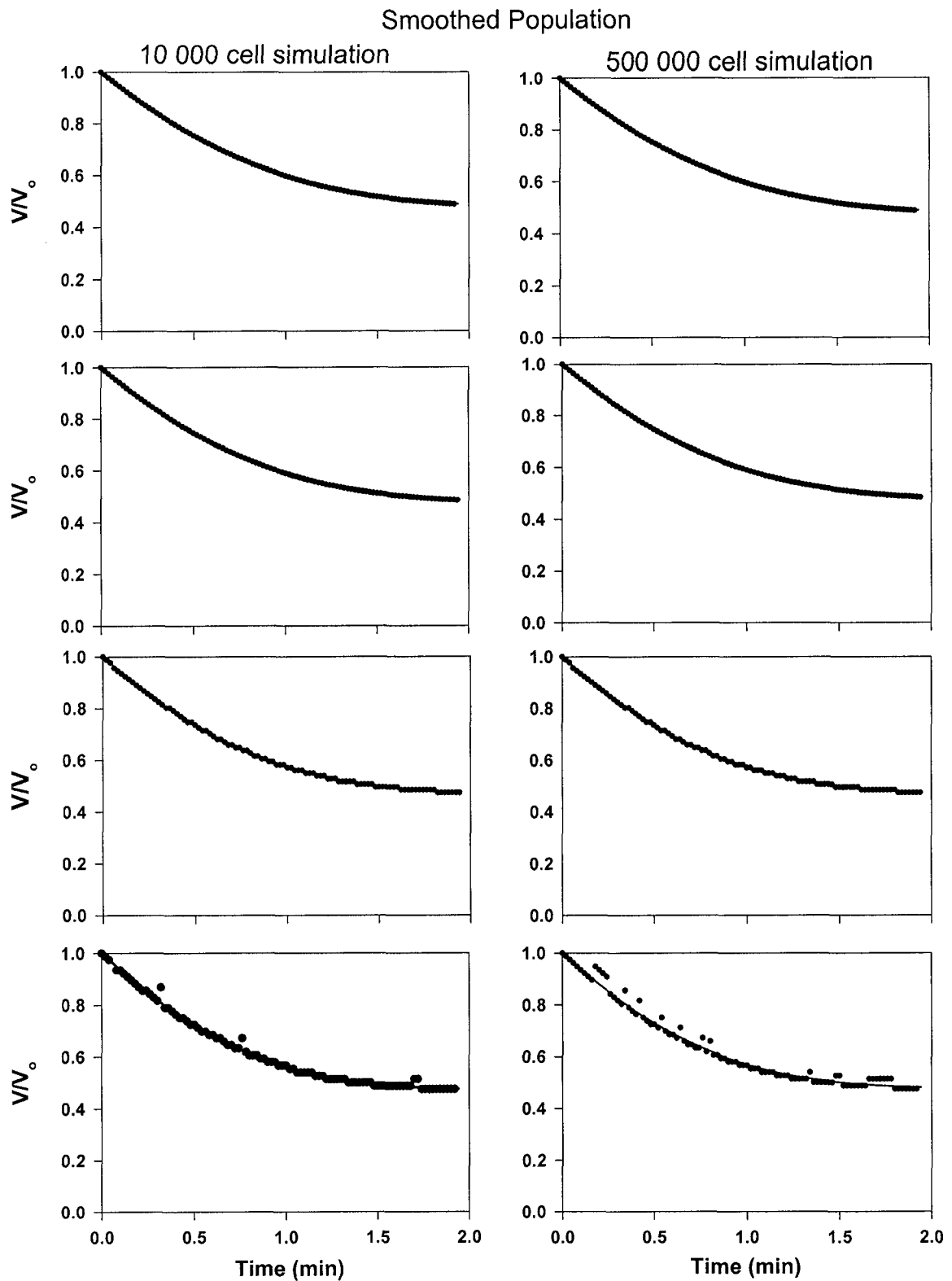


Fig. 5. A representative plot of volume versus time simulated by the distributions program from the smoothed raw population distribution of human corneal endothelial cells. The solid lines represent the best fit for  $L_p$  and  $V_b$  using the membrane mass transport model by Jacobs and Stewart (3).

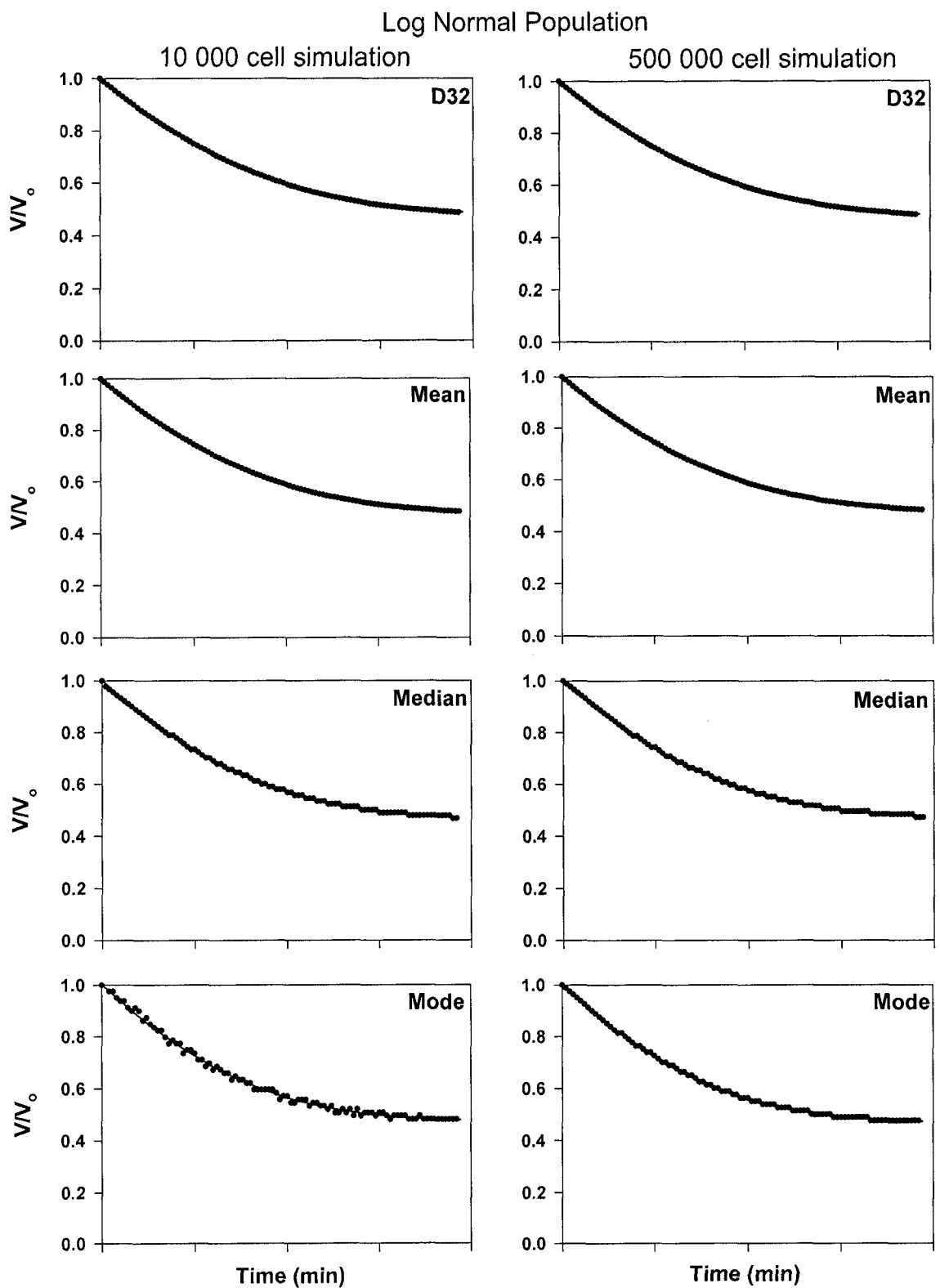


Fig. 6. A representative plot of volume versus time simulated by the distributions program from a log normal population distribution of human corneal endothelial cells. The solid lines represent the best fit for  $L_p$  and  $V_b$  using the membrane mass transport model by Jacobs and Stewart (3).

	$L_p$ ( $\mu\text{m}/\text{min}/\text{atm}$ )	Error (%)	$V_b$	Error (%)
Raw Data				
D32	0.0877	2.6	0.3034	1.1
Mean	0.0891	1.0	0.3032	1.1
Median	0.0922	2.4	0.2897	3.4
Mode	0.124	37.8	0.2315	22.8
Smooth Data				
D32	0.0877	2.6	0.3034	1.1
Mean	0.0891	1.0	0.3032	1.1
Median	0.0922	2.4	0.2894	3.5
Mode	0.0918	2.0	0.2945	1.8
Log Normal				
D32	0.088	2.2	0.3028	0.9
Mean	0.0893	0.8	0.3025	0.8
Median	0.0937	4.1	0.2885	3.8
Mode	0.0918	2.0	0.2993	0.2

Table 1. 10 000 cell simulations

Theoretical values for  $L_p=0.09$  and  $V_b=0.3$

	$L_p$ ( $\mu\text{m}/\text{min}/\text{atm}$ )	Error (%)	$V_b$	Error (%)
Raw Data				
D32	0.0876	2.7	0.3034	1.1
Mean	0.0891	1.0	0.3032	1.1
Median	0.0922	2.4	0.2897	3.4
Mode	0.1157	28.6	0.2289	23.7
Smooth Data				
D32	0.0876	2.7	0.3034	1.1
Mean	0.0891	1.0	0.3032	1.1
Median	0.0922	2.4	0.2894	3.5
Mode	0.0891	1.0	0.3021	0.7
Log Normal				
D32	0.0879	2.3	0.3028	0.9
Mean	0.0893	0.8	0.3025	0.8
Median	0.0903	0.3	0.2909	3.0
Mode	0.0936	4.0	0.2899	3.4

Table 2. 500 000 cell simulations